TECHNISCHE UNIVERSITÄT MÜNCHEN

Lehrstuhl für Molekulare Ernährungsmedizin

Metabolic Derangements in Pancreatic Cancer

Franziska Katharina Romrig

Vollständiger Abdruck der von der Fakultät Wissenschaftszentrum Weihenstephan für Ernährung, Landnutzung und Umwelt der Technischen Universität München zur Erlangung des akademischen Grades eines

Doktors der Naturwissenschaften

genehmigten Dissertation.

Vorsitzende: Univ.-Prof.Dr. H. Daniel

Prüfer der Dissertation: 1. Univ.-Prof. Dr. M. Klingenspor

2. Priv.-Doz. Dr. M. C. Arkan-Greten

3. Univ.-Prof. Dr. B. Küster

Die Dissertation wurde am 02.10.2012 bei der Technischen Universität München eingereicht und durch die Fakultät Wissenschaftszentrum Weihenstephan für Ernährung, Landnutzung und Umwelt am 18.02.2013 angenommen.

Index

1. Introduction

1.1 Obesity

1.1.1 Epidemiology

The prevalence of obesity increased dramatically over the past decades and reached epidemic proportions in many parts of the world (James 2008) (**Figure 1**). Excessive weight gain is one of the most serious health problem worldwide and can be seen in developed and especially in underdeveloped countries, which undergo economic changes (Chaput and Tremblay 2009). Mostly, lifestyle changes, which do not require too much physical activity and malnutrition are the main reasons for becoming obese.(Hezel, Kimmelman et al. 2006)

Another major contributing factor is the increased availability of cheaper food, which is rich in high calorie and poor in nutrients, and decreased physical activity to compensate increased food intake. The World Health Organisation (WHO) predicts that there will be approximately 2.3 billion overweight adults worldwide and more than 700 million of them will be obese by 2015 (WHO 2010). Over the last years an increased tendency towards obesity among not only predominantly adults but also children was observed (Aller, Abete et al. 2011), suggesting many more people will become overweight in the next decade.

1.1.2 Definition

Obesity is defined as abnormal or excessive fat accumulation in the body based on an imbalance between energy intake and physical activity over a long time period. Excessive consumption of calories leads to the storage of excessive fat in the visceral adipocytes. With the aid of the Body-Mass-Index (BMI) the body weight can be standardized and classified. The BMI is defined as a person's weight in kilograms divided by the square of his height in meters (kg/m^2). A healthy BMI is between 18,5 and 24,9 kg/m². Overweight is defined as BMI 25-29,9 kg/m², and obesity is referred to BMI ≥ 30 kg/m².
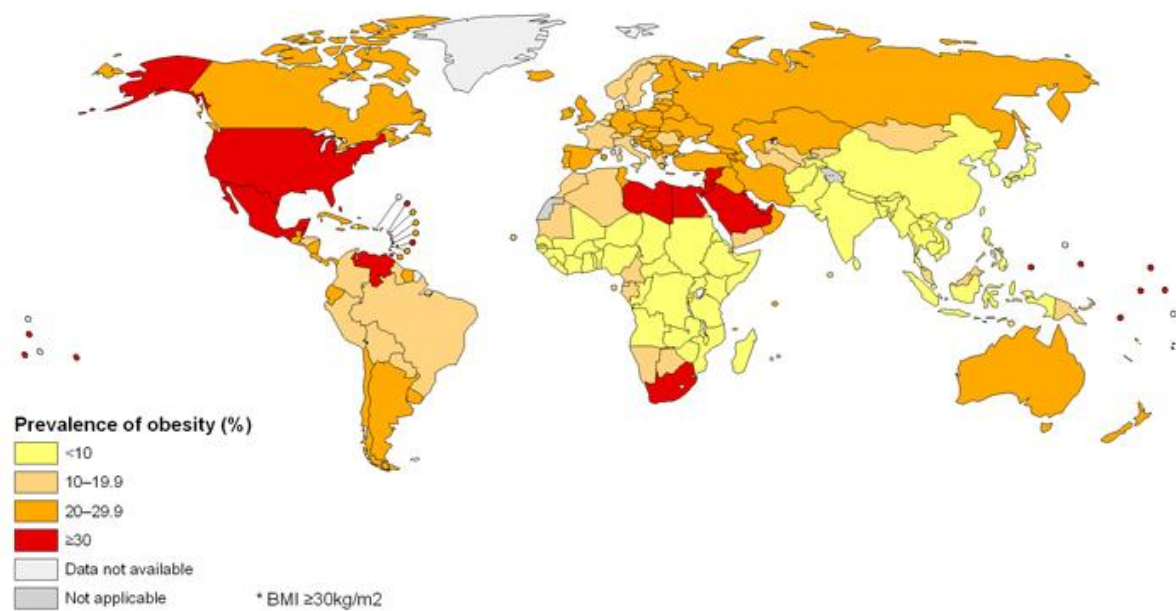
Figure 1: Prevalence of obesity worldwide in 2008 (Source: World Health Organisation).

1.2 Obesity as a risk factor for the development of disease

1.2.1 Diabetes

An excess increase in total body fat is directly associated with an increased risk of type 2 diabetes mellitus (T2DM) (Silverman, Swanson et al. 1998). Cohort studies suggest 10- to 20- fold increase in risk for developing diabetes in individuals with a BMI ≥ 35 kg/m^2 (Must, Spadano et al. 1999). The incidence of T2DM has reached epidemic proportions (Zimmet, Alberti et al. 2001) and the WHO estimates that by the year 2030 there will be around 366 million people affected by diabetes (Wild, Roglic et al. 2004). This epidemiological trend indicates that T2DM becomes an emerging disease even more in developing countries and will continue to increase in the future worldwide (Zimmet 1999; Wild, Roglic et al. 2004; Hossain, Kawar et al. 2007) (**Figure 2**). Besides peripheral insulin resistance, T2DM is characterized by an impaired insulin secretion. Insulin resistance impairs glucose utilization by insulin sensitive tissues and increases hepatic glucose production (HGP), both of which contribute to high levels of blood glucose in diabetics (Kahn 1998; Saltiel and Kahn 2001).
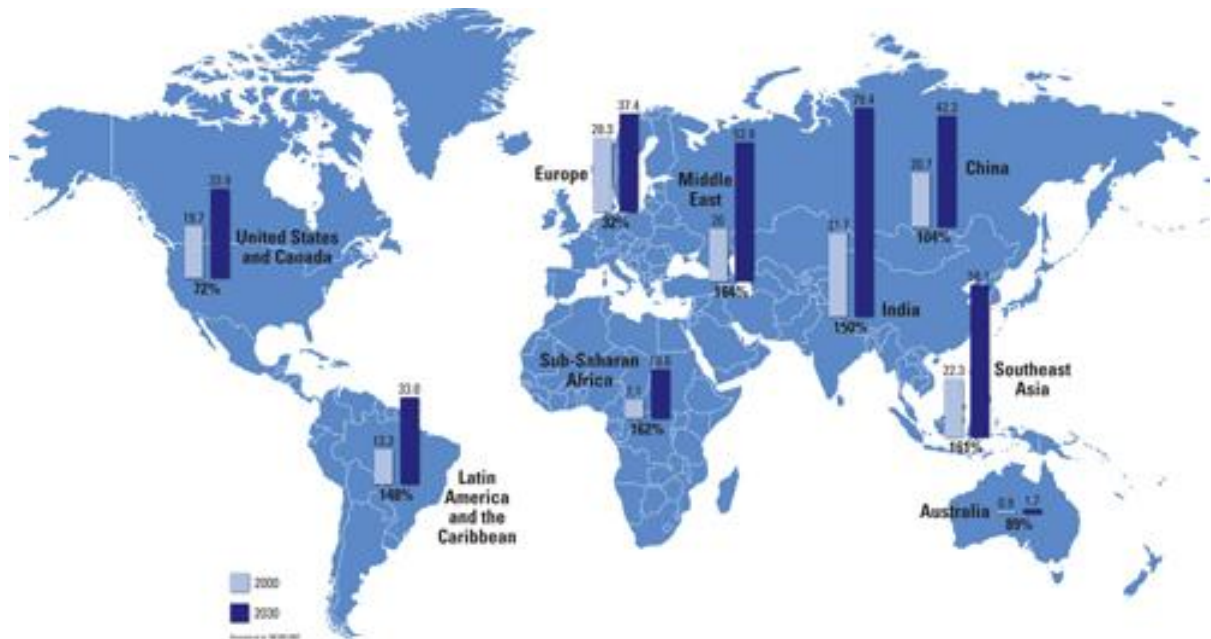
Figure 2: Diabetes incidence worldwide between year 2000 and 2030. (Wild, Roglic et al. 2004; Hossain, Kawar et al. 2007).

1.2.2 Cancer

Chronic hyperglycemia is associated with a very wide variety of serious health complications. It is suggested that there is a link between the history of type 2 diabetes and a higher risk of developing a variety of cancers such as non-Hodgkin's lymphoma, prostate, endometrial, liver, breast, and renal cell cancers (**Figure3**). Recent publications also report a strong correlation between T2DM and increased risk for pancreatic cancer (Everhart and Wright 1995). Indeed diabetic individuals for 5 or more years have a 2-fold increase in the risk of developing pancreatic cancer compared to those without diabetes history (Everhart and Wright 1995; Bonelli, Aste et al. 2003). Meanwhile, potential risk factors include obesity, hyperglycemia, hyperinsulinemia, and gradual impairment of beta cell function, decreased physical activity and dietary factors such as carbohydrate or sugar intake appear to be significantly involved (Michaud, Giovannucci et al. 2001; Michaud 2004). However the causal link remains unknown given that diabetes may be a consequence of pancreatic tumours.

Previous studies could not adequately address this question since the onset and the duration of diabetes prior to pancreatic cancer was not well defined. Nevertheless, whether diabetes is causally related to pancreatic cancer or is a consequence of it needs urgent insight since the prevalence and mortality rate for both diabetes and cancer, the two major diseases that threaten health care system worldwide, reached epidemic proportions (Parkin, Bray et al. 2005; Permutt, Wasson et al. 2005). Indeed epidemiological studies report elevated risk for pancreatic cancer among overweight and obese individuals (Calle, Rodriguez et al. 2003). People who had gained 12 kilos or more as adults, compared to those who only gained 2-5 kilos, displayed an increased risk of developing pancreatic cancer (Isaksson, Jonsson et al. 2002). Furthermore moderate physical exercise was associated with more than 50% reduction in disease incidence (Michaud, Giovannucci et al. 2001). Similarly, individuals with moderate to high occupational and leisure activity had a 58% lower risk compared to those with sedentary work and life style (Stolzenberg-Solomon, Pietinen et al. 2002). Moreover, cancer-associated death rates were significantly increased among men and women with BMI greater then 30 (Jaffee, Hruban et al. 2002). Although the intricate connection between obesity and cancer development is evident, the exact underlying molecular and cellular mechanisms remain largely unknown.
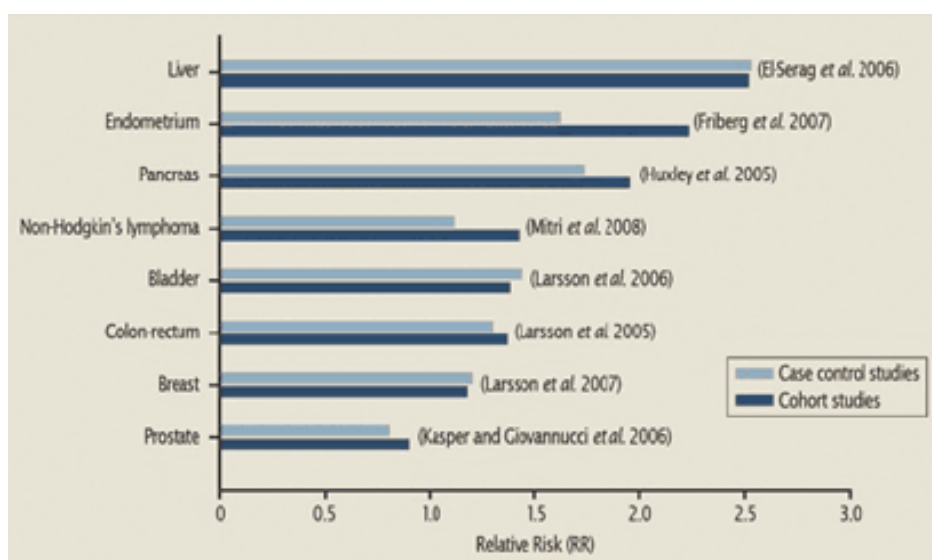
Figure 3: Meta analyses provide an insight into the relative risk of different cancers seen in patients with T2DM history (Mussig, Staiger et al. 2011).

1.3 Pancreatic Cancer

1.3.1 Epidemiology

Pancreatic ductal adenocarcinoma (PDAC) has quite poor prognosis (Xu, Zhang et al. 2010) and is the fourth most common cause of cancer-associated death (Bray, Sankila et al. 2002). This is the most frequent malignancy of pancreas and has a high mortality rate, which is almost comparable to the number of patients suffering from PDAC (Krejs 2010; Pandol, Gukovskaya et al. 2012). The median survival for patients with pancreatic cancer is 4 to 6 months and the 5-year survival rate is lower then 5% (Greenlee, Hill-Harmon et al. 2001; Pham, Schwock et al. 2008). Since the disease becomes clinically apparent at very late stages and that it is resistant to all forms of conventional chemotherapies, pancreas cancer is almost 100% lethal (Wray, Ahmad et al. 2005). PDAC rate in people under the age of 40 is rarely seen but rather appears mostly in later ages and the diagnosis is often around 60-65 years of age (Ahlgren 1996; Yeo, Hruban et al. 2002).

The high mortality rate is also due to the poor diagnosis of early precursor lesions as obscured by the retroperitoneal location of the pancreas as well as their small size, which makes it difficult to observe by the current imaging systems. Another factor contributing to this bad outcome is the high metastatic property of PDAC, which is already present in around 80% in all cases at the time of diagnosis (Yeo, Hruban et al. 2002).

1.3.2 Risk factors

Despite obesity and long term T2DM there are other risk factors, which promote the development of pancreatic cancer (**Figure 4**). An increased risk is associated with tobacco consumption (active or passive) (Lowenfels and Maisonneuve 2006) and it could be shown that smokers have a 2-fold increased risk to develop pancreatic cancer in comparison to non-smokers (Silverman, Dunn et al. 1994; Ahlgren 1996; Yeo, Hruban et al. 2002).
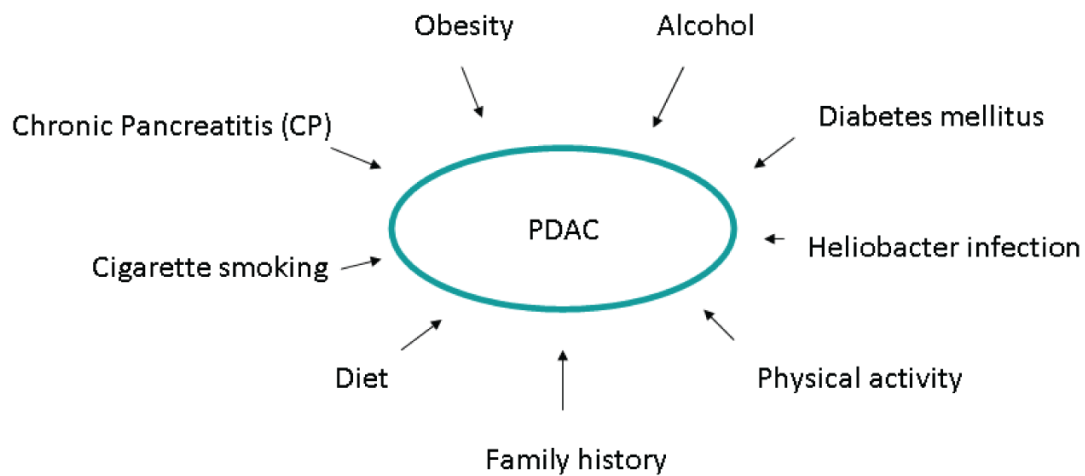
Figure 4: Risk factors for PDAC.

Silverman et al. suggested that if people quit smoking the risk of pancreatic cancer will decrease over the years after cessation (Silverman, Dunn et al. 1994). Generally it is assumed that smoking causes around one fifth of all pancreatic cancers (Raimondi, Maisonneuve et al. 2009)

Another risk factor for pancreatic cancer that is well established is chronic pancreatitis (CP) (Maisonneuve and Lowenfels 2002; Greer and Whitcomb 2009). Patients with CP have significantly increased risk for developing pancreatic cancer in comparison to healthy individuals suggesting sustained inflammation observed in these patients is actually what triggers the progression of pancreatic tumors (Lowenfels, Maisonneuve et al. 1993; Maisonneuve and Lowenfels 2010). Hereditary pancreatitis, a rare disease that is caused by a mutation in the trypsinogen gene, leads to acinar autodigestion and subsequent pancreatitis. It could be demonstrated that in hereditary pancreatitis the risk to develop PDAC is much higher compared to non-hereditary patients (Krejs 2010). Frequent recurrence of acute inflammation leads to tissue damage, fibrosis and eventually chronic inflammation in affected patients, which at advanced ages leads to pancreatic cancer incidence (Lowenfels, Maisonneuve et al. 1997).

On the other hand, increased pancreatic cancer risk in patients with sporadic chronic pancreatitis is correlated with the persistence of inflammation (Lowenfels, Maisonneuve et al. 1993). Although this disease constitutes only a small proportion of the cancer cases, they suggest that malignant transformation in the pancreas is more likely to happen in the presence of a chronically inflamed stroma.

Furthermore the inherited predisposition of pancreatic cancer is a potential risk factor for PDAC and it is proposed that 10% of all PDAC cases are related to a positive familial history (Hruban, Petersen et al. 1998; Schenk, Schwartz et al. 2001). Based on proband studies the risk for developing pancreatic cancer is 2-fold higher in patients with a positive family history of pancreatic cancer. Another study supported these findings and reported that patients with a familial predisposition have even a threefold increased incidence of pancreatic cancer compared to those with a negative family history (Fernandez, La Vecchia et al. 1994).

Also germline mutations in BRCA genes are associated with an elevated predisposition to PDAC (Murphy, Brune et al. 2002; Hahn, Greenhalf et al. 2003). Furthermore it is suggested that a familial predisposition with diseases containing mutations in BRCA2 such as that seen in breast and/or ovarian cancer increases as well the risk for pancreatic cancer (Thompson and Easton 2002). Germline mutations in BRCA2 increases the risk for pancreatic cancer around 3.5- to 10-fold (1999; Yeo, Hruban et al. 2002). Another family predisposition for PDAC is the Peutz-Jeghers Syndrome (PJS), which has mutations in the tumor suppressor LBK1 (or STK11) and is associated with many cancer types (Chu, Kohlmann et al. 2010). Giardiello et al. could show that the mutations in LBK1 lead to a significantly increased risk in developing pancreatic cancer (Giardiello, Brensinger et al. 2000).

Further it seems that the gender difference plays also an important role in PDAC development. Although it is suggested that men are more susceptible to develop pancreatic cancer in comparison to women (Gold and Goldin 1998; Krejs 2010) the gap between men and women decreases over the last years. This decrease might be due to the fact that the number of women smoking in these decades is almost equal to those of men.

The contribution of other risk factors for pancreatic cancer like bacterial infection, alcohol and coffee consumption are controversially discussed. But more and more evidence arises for an existing link between an infection with Helicobacter pylori and development of pancreatic cancer. De Martel et al. suggested that infection with Helicobacter pylori appeared to be a high risk factor for the development of pancreatic cancer (de Martel, Llosa et al. 2008) whereas Genkinger et al. could not identify alcohol as a risk factor for PDAC (Genkinger, Spiegelman et al. 2009). The results vary among the studies but it is suggested that excessive alcohol consumption can lead to chronic pancreatitis, which is already known to be an important risk factor for pancreatic cancer development.

1.3.3 Tumor Initiation, Promotion & Progression

PDAC arises from proliferative premalignant lesions of the ductal epithelium, named as pancreatic intraepithelial neoplasms (PanINs), via a series of genetic alterations, which include activating mutations in the *Kras* oncogene and the loss of the tumor suppressor genes *p16, p53*, and *DPC4* (Hruban, Goggins et al. 2000; Jaffee, Hruban et al. 2002; Hruban, Adsay et al. 2006) (**Figure 5 + 6**).
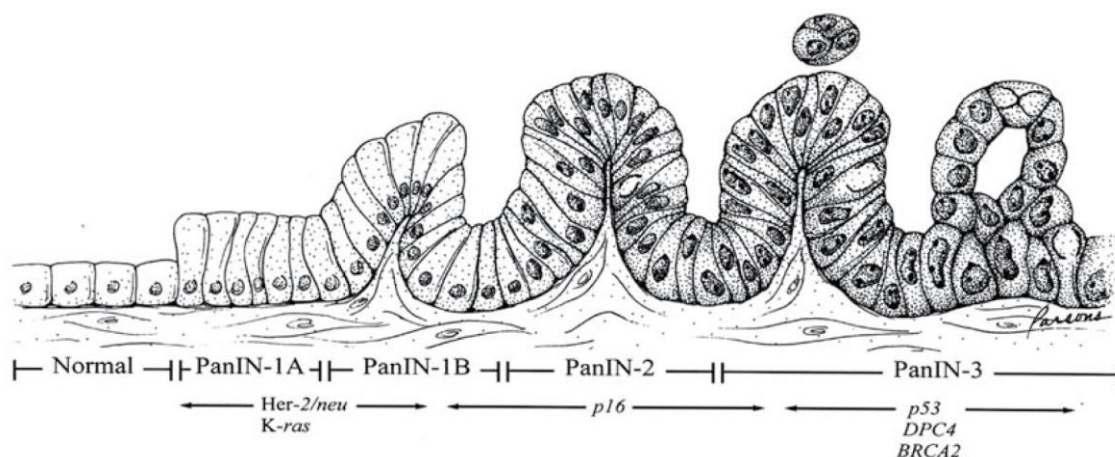
Figure 5: Progression Model of Pancreatic Cancer: Histological abnormalities in different stages of PanIN lesions and early and late genetic events during tumor progression (Wilentz, Iacobuzio-Donahue et al. 2000; Klein, Hruban et al. 2002).

Kras mutations are the very first genetic alterations to be detected within PanIN lesions thus they most likely represent the essential step during tumor initiation. PanINs are characterized according to their morphological features (Brembeck, Schreiber et al. 2003; Hingorani, Petricoin et al. 2003). The earliest precursor lesions display elongation of ductal cells with abundant mucin production whereas progressive stages show papillary structures. Eventually, these lesions progress and display nuclear abnormalities with abnormal mitosis and budding of cells into the lumen, which are known to be precursors of invasive pancreatic cancer
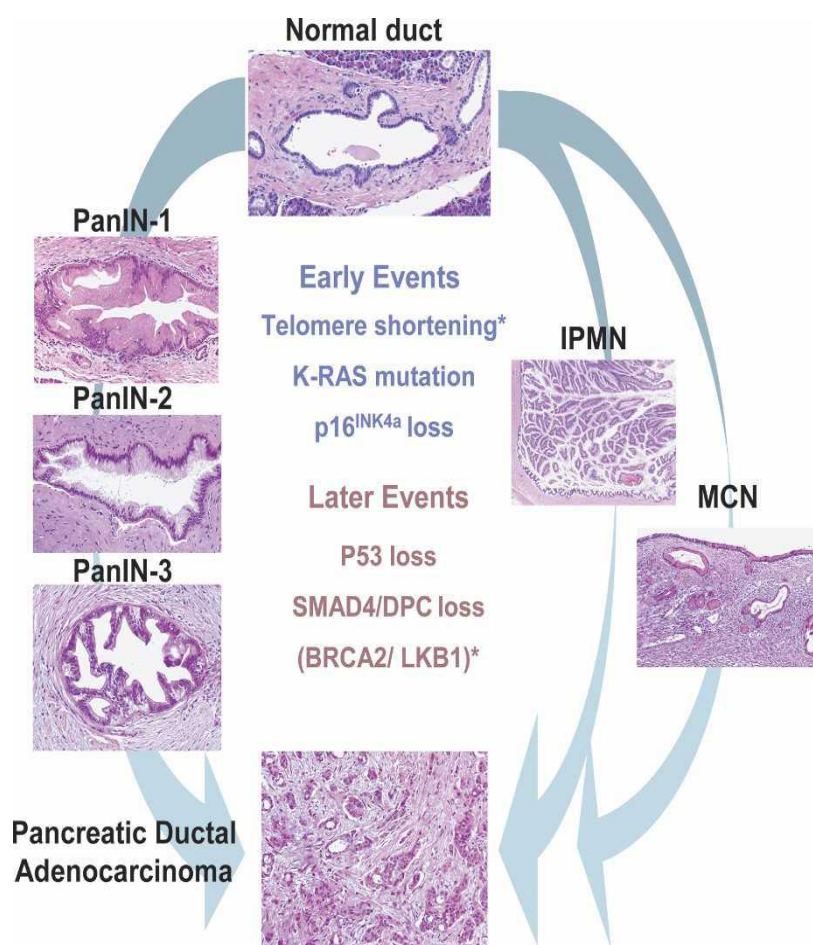
Figure 6: Three identified pancreatic non-invasive precursor lesions of pancreatic cancer include pancreatic intraepithelial neoplasm (PanIN`s), mucinous cystic neoplasm (MCN`s), and intraductal papillary mucinous neoplasm (IPMN`s) with series of genetic alterations, which are involved at different stages in tumor progression (Hezel, Kimmelman et al. 2006).

1.3.4   Animal Models

Mouse models of PDAC have served as great tools for determining the molecular and genetic mechanisms underlying the carcinogenic process in the pancreas. Although these studies await to be confirmed in patients, still animal models with oncogenic $Kras^{G12D}$ activation continues to provide great insight into the signaling events meanwhile recapitulating the human disease very closely (Tuveson, Shaw et al. 2004). These mice were generated by targeted mutation of oncogenic $Kras^{G12D}$ to pancreatic progenitor cells by crossing to mice that express Cre recombinase under the control of pancreatic-specific promoter *p48* (*Ptf1*) (**Figure 7**). In *p48-Kras*^{G12D} mice exon 1 contains a G to A transition in codon 12 that results in a glycine to aspartic acid substitution in the expressed protein that is the most common form of mutation seen in human malignancies comprising both its intrinsic and extrinsic GTPase activity and resulting in constitutive downstream signaling of RAS effector pathways.

As *Kras* activating mutations are one of the very initial events during the formation of premalignant lesions and that they display PanINs at various stages during the pathogenesis of the disease and resemble many aspects of human malignancy, *p48-Kras*^{G12D} mice are considered as one of the best model for studying the molecular mechanisms of pancreatic tumor development.
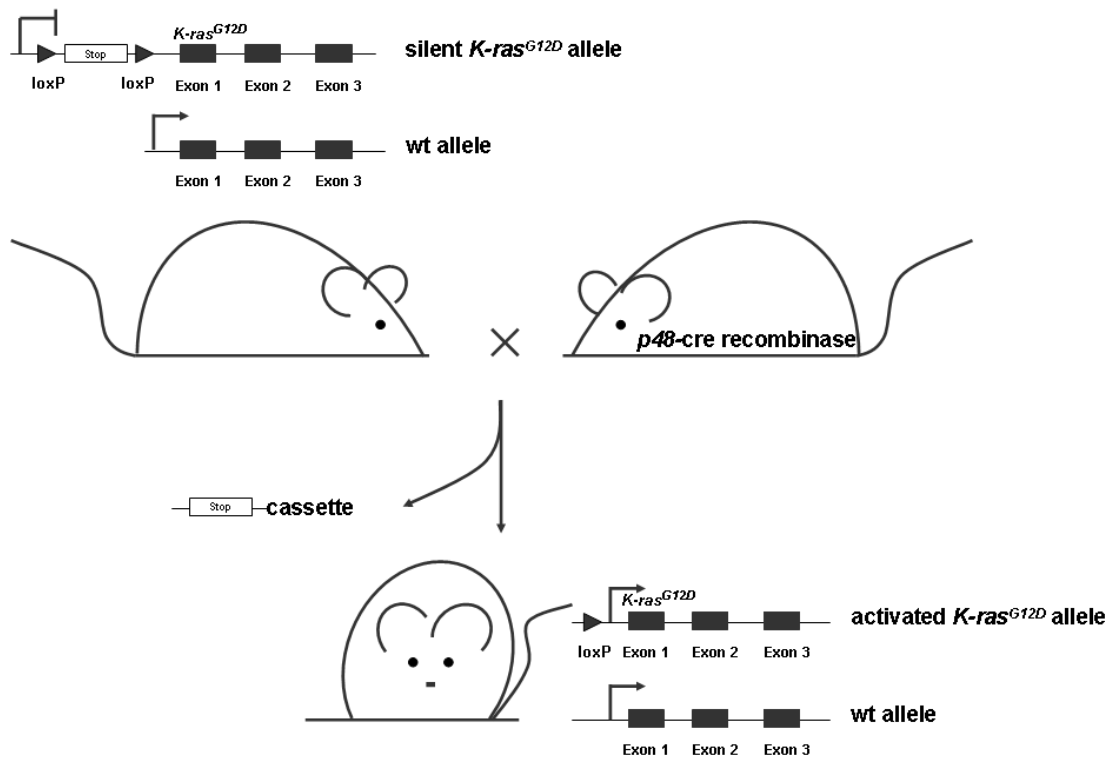
Figure 7: Oncogenic *Kras*^{G12D} activation. Mice with silent oncogenic *Kras*^{G12D} mutation crossed to animals expressing cre recombinase under the control of pancreatic-specific promoter *p48 (Ptf1)*.

Pioneering work suggested that although *Kras*^{G12D} activation is sufficient to lead cell transformation still it requires additional events in order to induce carcinogenesis, such as chronic inflammation suggesting inflammation to be an essential component of tumor promotion and progression in this model (Guerra, Schuhmacher et al. 2007). It has been long shown that *Kras*^{G12D} model displays an active inflammatory stroma probably due to the destruction of the normal architecture of the acini that elicits infiltration of myeloid cells and lymphocytes majorly (Clark, Hingorani et al. 2007). However, the exact function of these cell types, neither in the development/progression of lesions nor in the anti-tumor immunity has yet been fully understood. Further studies using diet models of obesity clearly showed that chronic low-grade inflammation in addition to the pre-existing inflammatory stroma skews tumor promotion earlier in *Kras* mice clearly suggesting pro-inflammatory cytokine expression to play a crucial role in disease development (Khasawneh, Schulz et al. 2009)

1.4 Macrophage polarization and their involvement in tumor development

Since inflammation is one the hallmarks of cancer development, macrophages, which are cells of the immune system that differentiate from monocytes, are important key players. These immune cells take part in the immune response and phagocyte foreign proteins, glycoproteins and injured tissue. Followed by antigen presentation on their surface to activate T-lymphocytes several cytokines are released to attract other immune cells and promote tissue infiltration. Macrophages can be classified into M1 and M2 phenotype. According to polarisation, the cells are differently activated and show distinct phenotypes (Mantovani, Sica et al. 2004; Mantovani, Sica et al. 2005) (**Figure 8 + 9**).
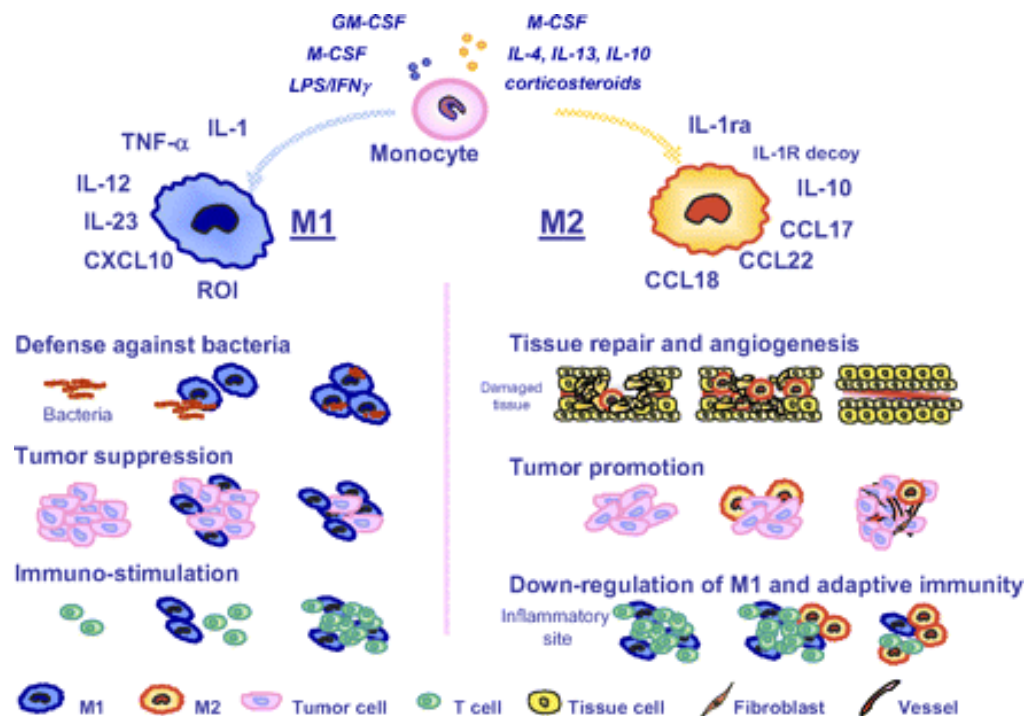
Figure 8: M1 and M2 macrophage polarisation and their distinct phenotypes and functions (Solinas, Germano et al. 2009)

M1 macrophages are classically activated by IFNγ, TNFα, GM-CSF or microbial stimuli such as LPS and have a phenotype with high IL-12, high IL-23 and low IL-10 levels (Taylor and Gordon 2003; Mantovani, Sica et al. 2005). Furthermore M1 cells produce a high amount of inflammatory cytokines, e.g. TNFα, IL-6, IL-1β, produce increased reactive oxygen species and defend the host against viral and microbial infections (Mantovani, Sica et al. 2007; Martinez, Helming et al. 2009; Solinas, Germano et al. 2009). It is proposed that M1

macrophages show a higher utilization of glycolysis through the transcription factor HIF-1a and thus via the enhanced expression of glycolytic genes and decreased oxygen consumption (Solinas, Germano et al. 2009; Biswas and Mantovani 2012; Escribese, Casas et al. 2012) (**Figure 9**). However M2 cells are alternatively activated via IL-13 or IL-14 and show low IL-12, low IL-23 and high IL-10 levels (Mantovani, Sica et al. 2005). M2 macrophages are mainly involved in tissue repair and remodelling, controlling inflammatory response through repressing M1 mediated features and are suggested to be tumor promoting (Martinez, Helming et al. 2009; Solinas, Germano et al. 2009). Another characteristic of M2 cells is their metabolic phenotype with an increased FA oxidation (Solinas, Germano et al. 2009; Biswas and Mantovani 2012; Blagih and Jones 2012) (**Figure 9**).
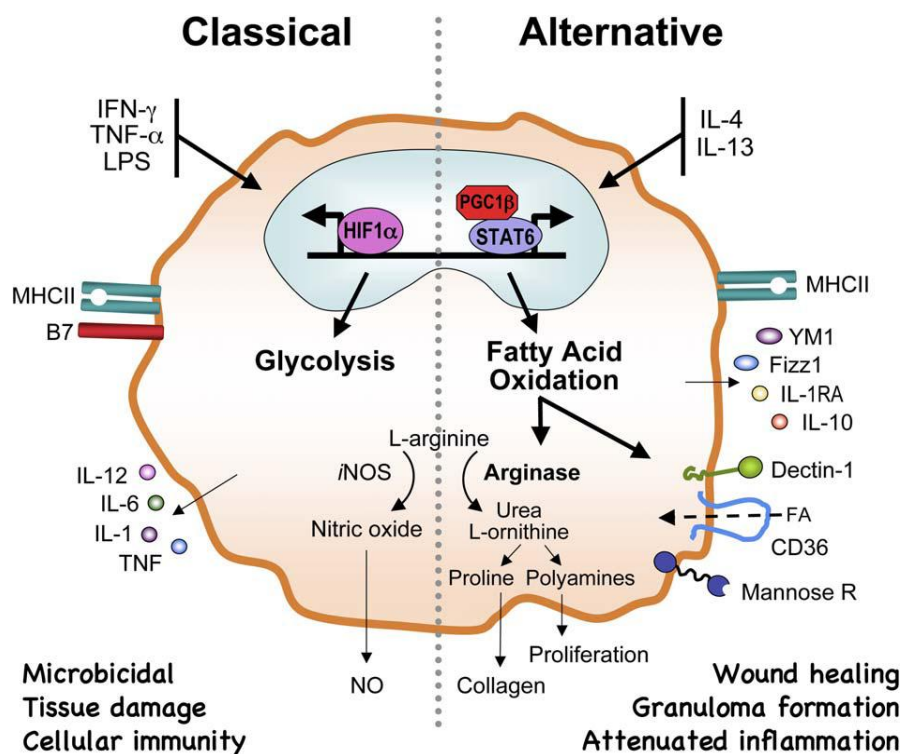
Figure 9: Classical and alternative macrophage activation and their metabolic profiles (Lacy-Hulbert and Moore 2006).

In the last years more and more evidence arises that macrophages play an important in tumor development. It is suggested that tumor associated macrophages (TAM) are M2 polarized and show tumor promoting features such as the release of growth factors, which promote angiogenesis (Leek, Lewis et al. 1996; Bingle, Lewis et al. 2006). Further increased TAM levels can be found in many tumor types, (e.g. pancreatic, ovarian and

breast cancer) and are often associated with a poor prognosis in different cancer types (An, Sood et al. 1987; Balkwill 2004; Solinas, Germano et al. 2009). However it is still poorly understood what is responsible for the macrophage polarisation during tumor development. It is suggested that macrophages can adapt to their surrounding tissue environment such as low oxygen (Chang, Shih et al. 2004; Murdoch and Lewis 2005; Escribese, Casas et al. 2012). Further investigations have to be done to get more insight in the tumor associated macrophage polarization and changes in bioenergetic pathways during tumorigenesis to define whether these two identities are interconnected.

1.5   Metabolic changes during carcinogenesis

In addition to chronic inflammation that plays an important role in supporting tumor promotion and progression, oncogenic driven alterations in tumor energy metabolism seem to be a hallmark of cancer (**Figure 10**).
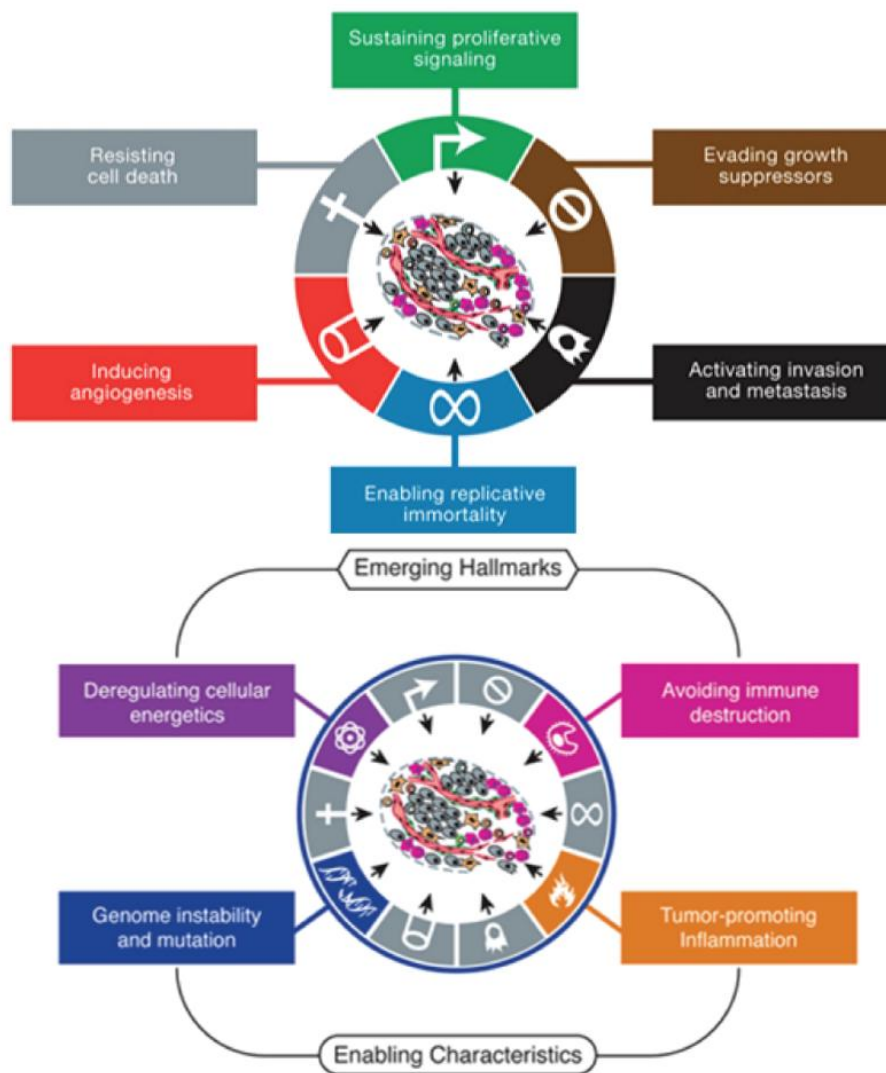
Figure 10: Hallmarks of Cancer (Hanahan and Weinberg 2011).

Highly proliferating cells like tumor cells have an increased energy demand and building blocks to support their excessive growth. Therefore it is suggested that metabolic shifts in bioenergetic pathways fulfill the needs of these fast growing cells and also increase the invasive potential of cancer cells (Pedersen 2007; DeBerardinis, Lum et al. 2008; Vander Heiden, Cantley et al. 2009)**.** Whether these changes are in any means linked to macrophage polarization needs further emphasis.

1.5.1 Bioenergetic Pathways

1.5.1.1 Glycolysis and Oxidative Phosphorylation

Biogenetic pathways use different sources to provide cells with energy in the form of ATP, which is required for all energy dependent processes in normal proliferating cells. The two major bioenergetic pathways, which provide cells with ATP are glycolysis and oxidative phosphorylation (OXPHOS) (Kaelin and Thompson 2010).

1.5.1.2 Glycolysis

Glycolysis is the catabolic process to metabolize glucose and generate energy in the form of ATP and reduction equivalents, which are additionally used for energy production and different anabolic processes. After glucose enters the cells via glucose transporters located on the cell surface, the key enzyme hexokinase phosphorylates glucose and converts it to glucose-6-phosphate. Following further multiple conversion steps in the cytoplasm, one molecule of glucose is catabolized into 2 molecules of pyruvate. Depending on oxygen status at the cell level pyruvate is utilized differently. In the absence of oxygen pyruvate is reduced to lactate in the cytoplasm via lactate dehydrogenase and will be carried out of the cell via lactate transporters (Kim and Dang 2006). This so called anaerobic glycolysis leads to an energy outcome for the conversion of one molecule glucose into two molecules of lactate and two ATP (Vander Heiden, Cantley et al. 2009). With the availability of oxygen, pyruvate is actively transported into the mitochondria and through the pyruvate dehydrogenase complex it is converted into acetyl-CoA. This metabolite enters subsequently the tricarboxylic acid (TCA) cycle and leads to the production of reduction equivalents NADH and $FADH_2$, which will be further used for the ATP production via the oxidative phosphorylation (OXPHOS) (Kim and Dang 2006; Kaelin and Thompson 2010).

1.5.1.3 Oxidative Phosphorylation (OXPHOS)

The oxidative phosphorylation is the main energy producing part of the glucose and long chain fatty acids degradation, which takes part in the inner mitochondrial membrane. After the catabolism to acetyl-CoA and its entrance into the TCA cycle, the produced

reduction equivalents are used in the respiratory chain for the ATP generation. The respiratory chain consists of five serial-connected protein complexes, which function as a redox system (Trifunovic and Larsson 2008). This system is based on electron transfer to create an electrochemical proton gradient and use these protons for the conversion of ADP (adenosine bisphosphate) into ATP via the ATP synthase (complex V) (Stock, Gibbons et al. 2000).

Due to OXPHOS, the anaerobic catabolism of glucose is much less efficient then the aerobic glycolysis (Fogg, Lanning et al. 2011). The rate of yield for one molecule glucose from glucose uptake and conversion to lactate provides the cell with 2-4 molecules of ATP, whereas the glucose degradation via TCA and oxidative OXPHOS to 36 ATP **(Figure 11)** (Vander Heiden, Cantley et al. 2009; Marie and Shinjo 2011).

Despite from ATP generation in the mitochondria also reactive oxygen species (ROS) such as superoxide, hydrogen peroxide and nitric oxide are produced as toxic by-products of oxidative phosphorylation (Singh and Kulawiec 2009; Fogg, Lanning et al. 2011). Under normal oxidative conditions, these ROS are used to assist normal cellular functions and also rendered harmless by the mitochondrial antioxidant defense system (Giles 2006; Galaris, Skiada et al. 2008; Acharya, Das et al. 2010). The system consists of enzymatic and non-enzymatic antioxidants such as superoxide dismutases (SOD), catalase (CAT), and glutathione peroxidases (GPx) (Thannickal and Fanburg 2000; Acharya, Das et al. 2010).

The imbalance between excess ROS production and impaired mitochondrial antioxidant defense system leads to increased oxidative stress, which further causes increased DNA mutation rate, mitochondrial DNA damage, apoptosis, cell proliferation and also affects lipid and protein metabolism (Fogg, Lanning et al. 2011).
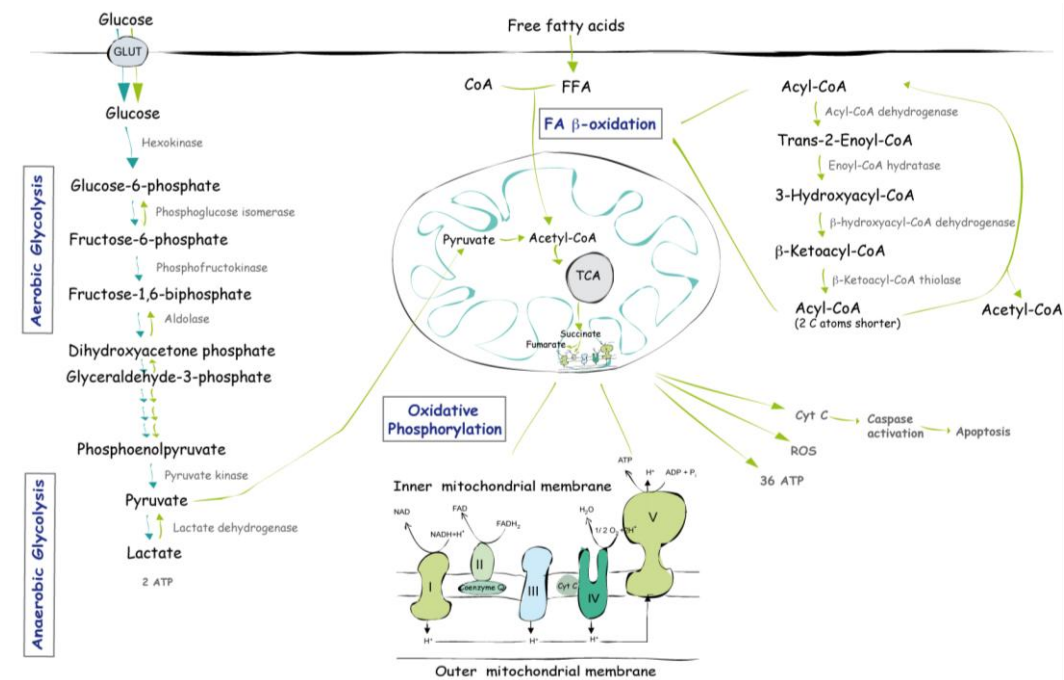
Figure 11: Glucose decomposition via different bioenergetic pathways and the ATP yield for one molecule of glucose.

1.5.1.4 Mitochondrial Fatty Acid (FA) ß-Oxidation

Besides glucose the breakdown of fatty acids also supports the energy production in cells. Long chain fatty acids have to be activated in the cytosol and followed by the transport into the mitochondrial matrix via the Carnitin Acyl-Transferase Systems (CATs). The further catabolism is called mitochondrial fatty acid (FA) ß-oxidation, where the fatty acids are degraded into acetyl-CoA, which also enters the TCA cycle and leads to the production of reduction equivalents, which will be as well used for ATP production via OXPHOS (Pike, Smift et al. 2011).

1.5.2 Dependency of different tumour entities on different bioenergetics pathways

Cancer cells use different bioenergetic pathways to generate energy in order to achieve their increased energetic and biosynthetic needs. One of the most predominant metabolic changes in malignant cells is their increased preference to metabolize glucose through glycolysis, which is in accordance with increased glycolytic rates, increased expression of glycolytic key enzymes and elevated lactate secretion (Argiles and Lopezsoriano 1990; Altenberg and Greulich 2004; Fogg, Lanning et al. 2011).

Key enzymes such as hexokinase II (HK2), phosphofructokinase (PFK), glyceraldehyde-3-phosphate dehydrogenase (GAPDH), pyruvate kinase (PK) and lactate dehydrogenase (LDH) are upregulated in different tumour entities (Schek, Hall et al. 1988; Ko, Pedersen et al. 2001; Pelicano, Martin et al. 2006; Moreno-Sanchez, Rodriguez-Enriquez et al. 2007). Further increased expression of glucose transporters (GLUTs) especially GLUT1 and GLUT 3 are demonstrated in various cancer types that correlate well with a poor diagnosis (Dang and Semenza 1999; Shaw, Evans et al. 2010; Piatkiewicz and Czech 2011).

In the early 1920s Otto Warburg observed that cancer cells show significantly higher glycolytic rates compared to normal cells even in the presence of oxygen, a phenomenon known as 'Warburg effect' or 'aerobic glycolysis' (Warburg 1956) **(Figure 12).**
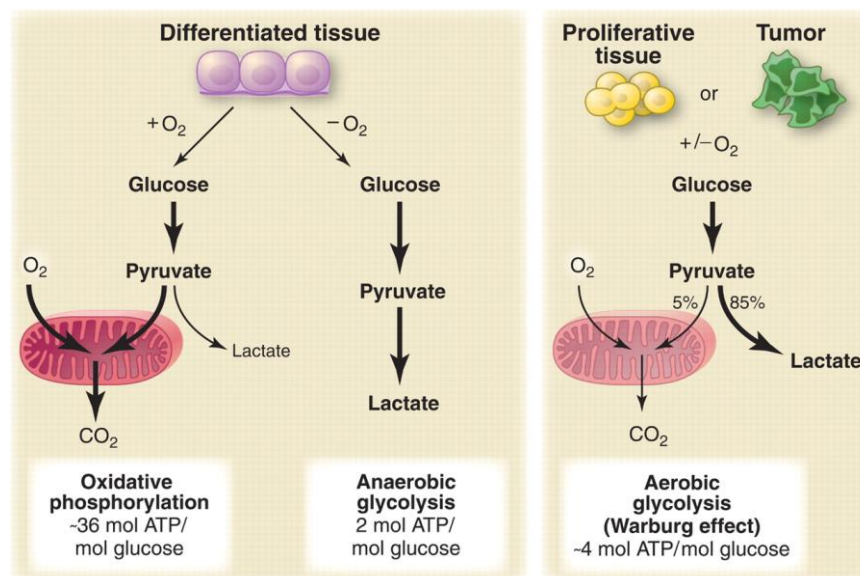
Figure 12: Warburg effect in highly proliferating cells (Vander Heiden, Cantley et al. 2009).

Indeed the shift from oxidative phosphorylation to glycolysis is a common feature of cancer cells and serves for the detection of various cancer types (Gatenby and Gillies 2004). Therefore the radioactive labelled glucose analogue 2-deoxy-2-[^{18}F]fluoro-d-glucose (FDG) is applied to patients and monitored by positron emission tomography (PET). The analogue is carried into the cell through glucose transporters, converted to 2-deoxy-glucose-6-phosphate via hexokinase II but can not be further metabolized in the cells and accumulates in the cytoplasm.

Although increased glycolysis in tumor cells serves the basis for ^{18}F-fluorodeoxyglucose (FDG) positron emission tomography (PET) analysis in cancer patients, however, not all cancer types can be clearly detected by FDG-PET. Bensinger et al. just recently gave an

overview on possible cancer types that can be detected via FDG-PET (Bensinger and Christofk 2012). A high ^{18}F-FDG phenotype can be seen for breast, lung and in some extent for colorectal cancer, whereas this imaging tool is not secure to detect primary prostate cancer and as well the detection of pancreatic cancer can lead to false positive results (Liu 2006; Bensinger and Christofk 2012; Herrmann, Erkan et al. 2012). This is based on the fact that through the FDG uptake in inflammatory lesions the specificity of this detection method is diminished but Herrmann et al. demonstrated further in their clinical study that the FDG-PET method is able to detect malignant pancreatic disease with high sensitivity (Herrmann, Erkan et al. 2012). However the diagnostic features still remain to be improved. Furthermore not all cancer types prefer the glycolytic pathway as their main energy source. These findings suggest a preferential use of bioenergetic pathways in cancer cells. Indeed some cancer types have preference for oxidative phosphorylation as the main energy pathway then aerobic glycolysis (Liu 2006; Moreno-Sanchez, Rodriguez-Enriquez et al. 2007).

Warburg suggested that increased glycolysis in tumor cells is the consequence of irreversible defects in the mitochondrial function, which contributes to the switch to glycolysis as the main energy source (Warburg 1956). In different cancer types dependency on oxidative metabolism is indeed lower whereas other malignant cells show a clear upregulation in glycolysis although they do not exhibit diminished mitochondrial metabolism (Moreno-Sanchez, Rodriguez-Enriquez et al. 2007; DeBerardinis, Lum et al. 2008; Yeung, Pan et al. 2008).

Since Warburg several mechanisms have been suggested to be responsible for the glycolytic phenotype of malignant cells. These mechanisms include malfunction of mitochondria, hypoxic conditions, changes in metabolic enzymes and activation of oncogenes (Rempel, Mathupala et al. 1996; Yeo, Hruban et al. 2002; Gatenby and Gillies 2004; Ramanathan, Wang et al. 2005; Pelicano, Martin et al. 2006).

A bulk of evidence suggested that the increased glycolytic rates in cancer is mostly due to the oncogenic reprogramming (Levine and Puzio-Kuter 2010). Oncogenes are involved in regulating cell metabolism due to their downstream targets and therefore support cancer growth by the ability to take up excess nutrients in an autonomous fashion. In combination with the loss of tumor suppressor genes the activation of oncogenes builds a perfect platform for cancer development. Different oncogenes including Kras, c-Myc,

tumor suppressors like p53, LKB1 and the hypoxia-inducible factor 1 (HIF-1) as well are known to be directly related to the metabolic changes in several cancers types (Bos, Fearon et al. 1987; Bos 1989; Aguirre, Bardeesy et al. 2003; Prenen, Tejpar et al. 2010; Shaw, Evans et al. 2010).

1.5.2.1 Transcription factor c-Myc

In many types of human cancer, including pancreatic cancer an altered expression of the c-myc gene is detected and an overexpression is observed in more then 40 % of all human cancers (Adhikary and Eilers 2005; Buchholz, Schatz et al. 2006; Wokolorczyk, Gliniewicz et al. 2008; Dang, Le et al. 2009). c-Myc acts as a transcription factor activated by growth factor stimulation and is a master regulator of cell proliferation, cell growth, apoptosis and energy metabolism (Levens 2003; Eilers and Eisenman 2008; Wise and Thompson 2010). Many genes which are involved in these processes are under the direct control of c-Myc. Through gene expression analysis it was shown that c-Myc regulates genes involved in nucleotide biosynthesis including key enzymes like thymidylate synthase (TS), inosine monophosphate dehydrogenase 1 and 2 (IMPDH1/2) and phosphoribosyl pyrophosphate synthetase 2 (PRPS2) (Liu, Li et al. 2008; Mannava, Grachtchouk et al. 2008; Tong, Zhao et al. 2009). In highly proliferating cells an enormous demand of building blocks is required to support their fast growth behaviour. Other target genes of c-Myc are involved in the glucose metabolism including GLUT1, HK2 and PFK (Dang, Le et al. 2009) as well as lactate dehydrogenase A (LDH-A), which converts pyruvate into lactate and therefore drives aerobic glycolysis (Lewis, Shim et al. 1997; Shim, Dolde et al. 1997; Dang 2010). Considering the direct influence of c-Myc on these different metabolic processes, especially nucleotide biosynthesis and glycolysis, oncogenic activation can enhance the glycolytic phenotype observed in most cancer types. However, the complete mechanism is not fully understood yet.

1.5.2.2 Hypoxia-inducible factor 1 (HIF-1)

Besides c-Myc, hypoxia-inducible factor 1 (HIF-1) is also known to regulate genes, which are involved in metabolic pathways. HIF-1 is a transcription factor that show higher expression under low oxygen conditions (hypoxia), which mostly occur in malignant cells. It is demonstrated that HIF-1 is often significantly upregulated in different cancer types

including pancreatic cancer (Sun, Qiu et al. 2007; Semenza 2009) and together with c-Myc it induces expression of various glycolytic enzymes including hexokinase II, glyceraldehyde 3-phosphate dehydrogenase, pyruvate dehydrogenase, phosphofructokinase 1 and lactate dehydrogenase (Yeung, Pan et al. 2008). Despite increased expression of glycolytic enzymes, HIF-1 additionally downregulates mitochondrial metabolism by decreasing the oxidation of pyruvate through activation of pyruvate dehydrogenase kinase (Simon 2006). This inactivation of the mitochondrial pyruvate dehydrogenase complex I leads to a reduced entry of pyruvate into the TCA cycle and thus enhances the glycolytic phenotype seen in cancer cells.

1.5.2.3 Tumor suppressor p53

Another central node in regulating cell metabolism is played by the tumor suppressor protein p53, which suppresses glycolysis and increases mitochondrial metabolism in normal cells through p53-inducible gene TIGAR (TP53-induced glycolysis and apoptosis regulator) (Green and Chipuk 2006). TIGAR lowers the glycolytic enzyme fructose-2,6-bisphosphate that decreases conversion of fructose-6-phosphate to fructose-1,6-bisphosphate and leads to diminished glycolysis in cells (Bensaad, Tsuruta et al. 2006; Yeung, Pan et al. 2008). In addition to the regulatory function of p53 on the synthesis of cytochrome c oxidase 2 (SCO2), which participates in the assembly of cytochrome c oxidase (COX), it contributes to the upregulation of oxidative phosphorylation. Considering the regulatory functions of p53, loss of the p53 gene often seen in cancer cells can thus contribute to the glycolytic phenotype in malignant cells.

Therefore, it seems that c-Myc, HIF-1 and p53 and their loss of function mutations are essential for the shift from oxidative phosphorylation in normal cells to aerobic glycolysis in cancer cells (**Figure 13**).
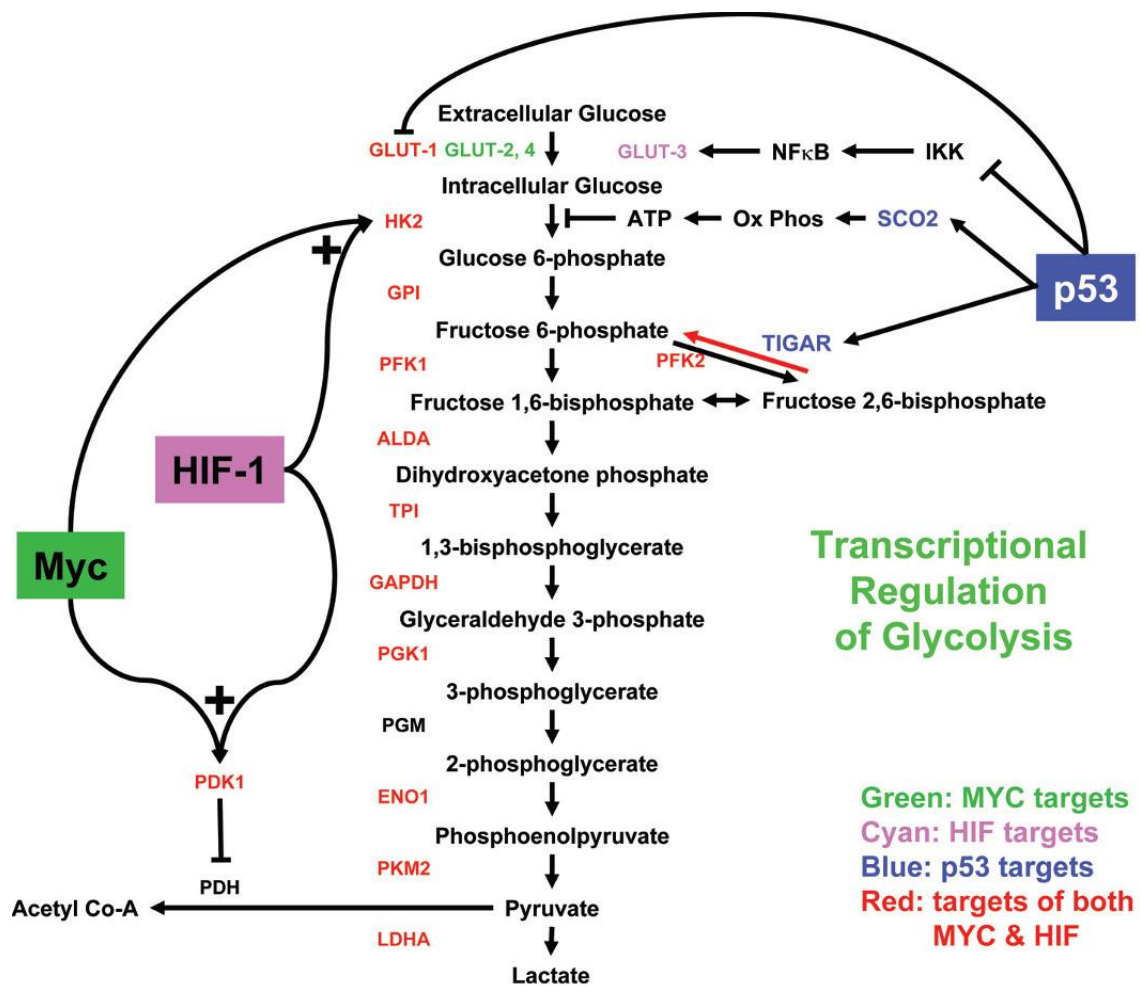
Figure 13: Regulatory effects of Myc, HIF-1 and p53 on the glycolytic metabolism (Yeung, Pan et al. 2008).

1.5.2.4 Oncogenic K-ras

Recently Ying et al. suggested that oncogenic reprogramming in PDAC seems to be more and more considered as one of the major events in promoting shift in energy metabolism (Ying, Kimmelman et al. 2012). Especially the mutation in oncogenic $Kras^{G12D}$ is the main candidate. Based on different transcriptome and metabolomic analyses it was shown that $Kras^{G12D}$ mutation enhances glycolytic flux and feed the non-oxidative branch of the pentose phosphate pathway (PPP) with glycolytic intermediates (Ying, Kimmelman et al. 2012). Several groups already suggested that $Kras^{G12D}$ mutation is supporting the glycolytic phenotype seen in many cancer types (Racker, Resnick et al. 1985; Fantin, St-Pierre et al. 2006; Yun, Rago et al. 2009). Weinberg et al proposed that the main role of glucose metabolism for cell growth is not the ATP production but is to support Pentose-Phosphate-Pathway (PPP), which mainly generates NADPH for biosynthetic reactions and

produces ribose-5-phosphate for the *de novo* nucleotide biosynthesis in proliferating cells (Weinberg, Hamanaka et al. 2010) (**Figure 14**).
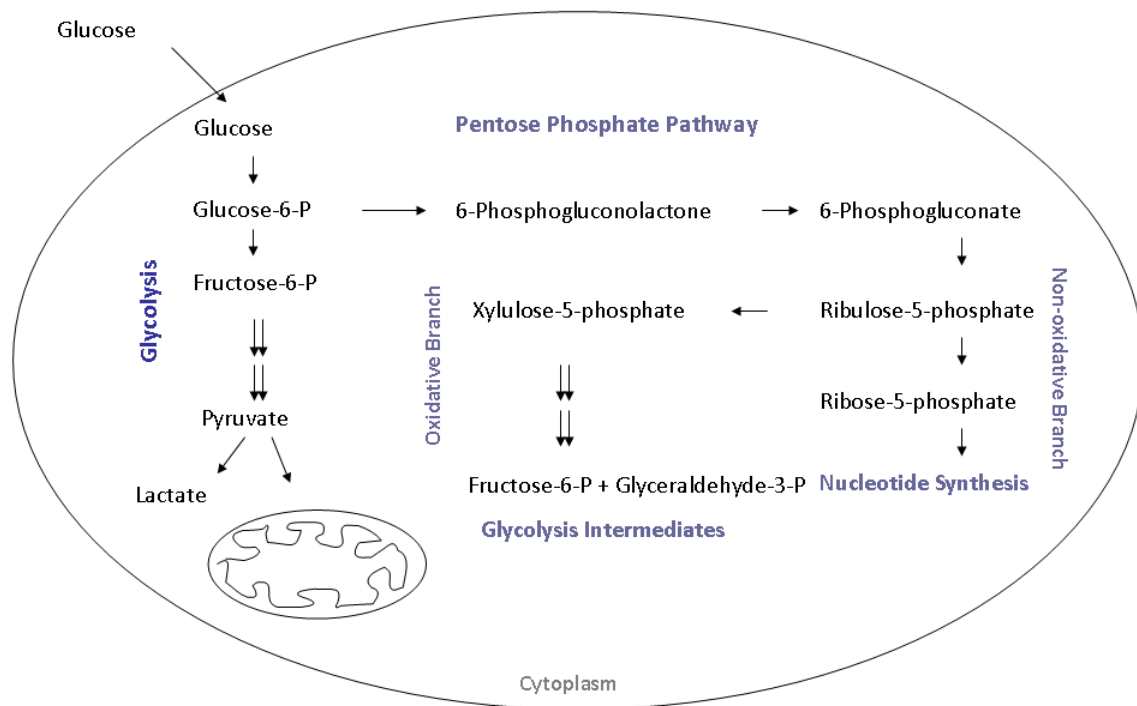
Figure 14: Oxidative and Non-oxidative branches of the Pentose Phosphate Pathway.

In recent studies it was shown that oncogenic *Kras*[G12D] inactivation in PDAC leads to a significant decrease in glycolytic flux, whereas no significant alterations in the TCA cycle could be observed (Ying, Kimmelman et al. 2012). Vander Heiden et al. already suggested that glycolytic metabolites were shifted into anabolic processes like nucleotide and phospholipid synthesis whereas alternative carbon sources are utilised to stabilize the TCA cycle (Vander Heiden, Cantley et al. 2009). One carbon source which is predominately considered to fulfill this function in *Kras*[G12D] driven PDAC is glutamine (Gao, Tchernyshyov et al. 2009). Beside glucose, glutamine is the most abundant nutrient used by mammalian cells as the bioenergetic substrate. It is also necessary for the generation of energy, macromolecules and cell survival. Non-transformed cells seem to use only a small amount of glutamine for macromolecular biosynthesis and energy production. In contrast, glutamine is consumed in large amounts in tumor cells and provides biosynthetic precursors instead of breaking it down completely for energy use

(DeBerardinis, Mancuso et al. 2007). Following glutamine uptake, it is transformed into α-ketoglutarate, which enters the TCA to maintain the mitochondrial integrity and provide TCA anaplerosis because different intermediates of the TCA such as citrate and oxalacetate will be used in high rate for the biosynthesis of macromolecules (DeBerardinis, Lum et al. 2008). Taken together it seems that glycolysis is the most commonly used energy source in PDAC driven by oncogenic $Kras^{G12D}$ activation. Metabolic changes and oncogenic reprogramming during pancreatic tumorgenesis play extremely important role but nevertheless the exact mechanism is poorly understood.

1.5.2.5 Nuclear receptors

Over the last years more and more evidence arised suggesting nuclear receptors take part in metabolic changes during cancer development. These receptors are known to act as multi-functional ligand activated transcriptions factors that regulate the expression of a wide range of target genes involved in metabolic pathways. (Shaw, Evans et al. 2010; Haemmerle, Moustafa et al. 2011). Peroxisome proliferator-activated receptors (PPAR`s) are nuclear receptors, which are members of the nuclear receptor gene superfamily and regulate genes in metabolic homeostasis, inflammation and cell differentiation (**Figure 15**) (Bishop-Bailey 2011; Haemmerle, Moustafa et al. 2011).
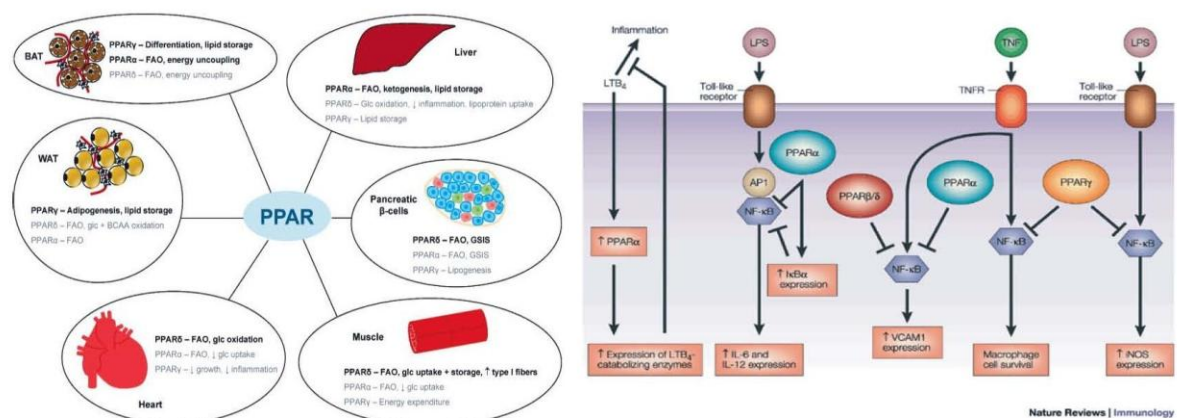
Figure 15: Function of the peroxisome proliferator-activated receptors in metabolic homeostasis and inflammatory response (Daynes and Jones 2002).

Furthermore PPARs also take part in the regulation of inflammatory response by regulating proliferation, differentiation and survival of macrophages and lymphocytes (Kostadinova, Wahli et al. 2005). The PPAR family consists of three members: PPARα, PPARβ/δ and PPARγ. In response to endogenous and exogenous ligands these receptors can modulate the expression of their target genes (Michalik, Desvergne et al. 2004; Michalik, Auwerx et al. 2006). PPARs serve as molecular targets for lipid lowering drugs, whereas fibrates including fenofibrate target PPARα and compounds like thiazolidinedione (TZD) activates PPARγ. The expression levels of the PPARs are highly tissue specific. PPARα is mainly present in tissue that shows high beta-oxidation activity including liver, intestinal absorptive, skeletal and cardiac muscle cells (Guan, Zhang et al. 2002; Mandard, Muller et al. 2004; Burns and Vanden Heuvel 2007). PPARβ/δ is found in broad spectrum of tissues and regulates the transcription of genes involved in glucose and fat metabolism (Dressel, Allen et al. 2003). PPARγ is more expressed in adipose tissue where it regulates the generation and differentiation of adipocytes and it also is included in inflammatory response (Imai, Takakuwa et al. 2004).

In-vitro studies showed that ligand activation of PPARγ leads to decreased cell growth in pancreatic cells due to cell cycle arrest (Kawa, Nikaido et al. 2002) and also a diminished cell invasion (Sawai, Liu et al. 2006). On the other hand Kristiansen et al. demonstrated a strong correlation between overexpression of PPARγ in pancreatic ductal adenocarcinoma and decreased survival in patients (Kristiansen, Jacob et al. 2006). Although not much is known about the role of PPARγ in pancreatic tumorgenesis however further evidence suggest PPARγ activation could promote tumor development (Eibl 2008). Except the lipid lowering function of fibrates, sustained activation of PPARα through different agonists causes hepatocarcinogenesis in mice and rodents (Peters, Cattley et al. 1997; Peters, Cheung et al. 2005). Although however the underlying mechanism for liver carcinogenesis is not completely understood, it is highly unlikely that it will occur in humans based on species difference and different response to agonists between humans and rodents (Klaunig, Babich et al. 2003; Tachibana, Yamasaki et al. 2008).

Long term studies of 30 different tested agonists showed that they also induce non-hepatic tumours including the Leydig cell or the pancreatic acinar cell tumour, however they appeared always in combination with liver tumors (Klaunig, Babich et al. 2003).

PPARβ/δ plays an important role in colon tumorgenesis. The mRNA levels are clearly upregulated in colorectal cancer in humans and this is associated with an increase in cell proliferation (Gupta, Tan et al. 2000). Indeed oncogenic activation of k-*ras* was found in colorectal cancer, which supports cell proliferation and tumour growth through activation of the mitogen-activated protein kinase (MAPK) pathway (Fearon and Vogelstein 1990; Kinzler and Vogelstein 1996). Additionally PPARβ/δ is known to be a downstream target of the Ras/Raf/MAPK pathway (Shao, Sheng et al. 2002). Park et al. showed that through genetic disruption of PPARβ/δ tumorgenesis in human colon could be decreased (Park, Vogelstein et al. 2001). Further Pedchenko et al. demonstrated that PPARβ/δ protein is expressed in the majority of primary lung cancers and they indicated an important role for PPARβ/δ in lung tumor progression (Pedchenko, Gonzalez et al. 2008). Although the role of PPARs in tumor development and lipid lowering drug is clear, the exact molecular mechanisms need further investigation.

1.5.2.6 Sirtuin 1 (SIRT1)

Sirtuin1 is the most studied sirtuin in mammals and encodes for a multifaceted NAD(+)-dependent protein deacetylase (Liang, Kume et al. 2009). SIRT1 is activated by caloric restriction and modulates gene expression according to the energy status of the cell. It regulates fatty acid oxidation, gluconeogenesis, mitochondrial activity and inflammatory response (**Figure 16**). Recent studies suggested that a decreased SIRT1 level is associated with an increased insulin resistance *in vivo* and *in vitro* (Sommer, Poliak et al. 2006; Sun, Zhang et al. 2007; Liang, Kume et al. 2009). Indeed an improvement of insulin resistance could be shown by the administration of SIRT1 activators (Milne, Lambert et al. 2007; Sun, Zhang et al. 2007; Feige, Lagouge et al. 2008). Besides improving insulin sensitivity another interesting feature of SIRT1 is its reducing function on the inflammatory response mediated by TNF (Yoshizaki, Milne et al. 2009). However its role in tumorgenesis is controversial.

In a number of tumor types such as human prostate cancer, SIRT1 is overexpressed, which occur mostly in combination with the loss of p53 whereas it is reduced in several other tumor types including breast cancer and hepatic carcinoma (Nemoto, Fergusson et al. 2004; Huffman, Grizzle et al. 2007; Wang, Sengupta et al. 2008). Zhao et al. showed that SIRT1 is overexpressed in pancreatic cancer cells and chemosensitivity is enhanced

through RNAi knockdown of SIRT1 (Zhao, Cui et al. 2011). Due to its involvement in multiple cellular and metabolic processes, SIRT1 is an interesting target for further studies.
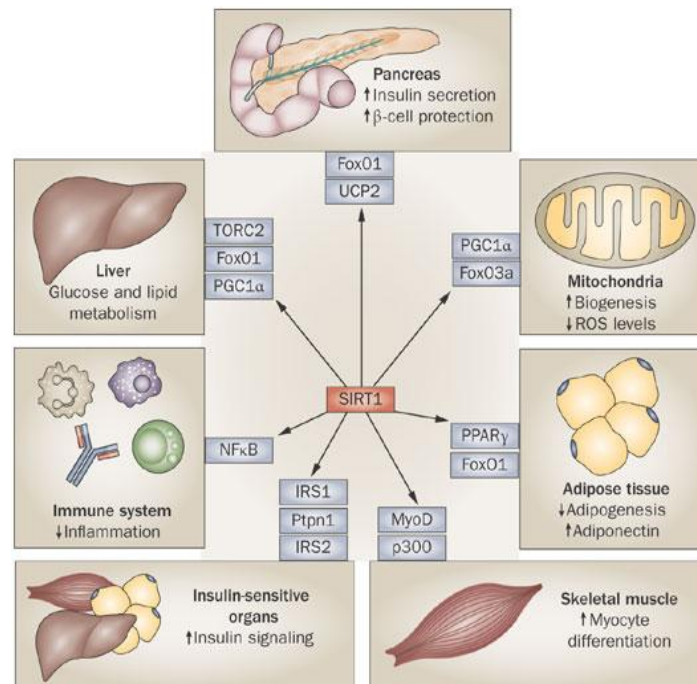
Figure 16: Regulatory functions of SIRT1 on different cellular and metabolic processes (Liang, Kume et al. 2009).

1.5.3 Why most cancer cells are dependent on glycolysis and whether switching bioenergetic pathways could provide therapeutic approach against PDAC?

Why do most tumor cells rely on aerobic glycolysis although the ATP outcome is much lower compared to glucose oxidization during mitochondrial metabolism? A couple of hypothesis addresses this phenomenon seen in malignant cells.

Several researchers suggested that glycolytic intermediates from the aerobic glycolysis serve mainly as building blocks to feed the Pentose-Phosphate-Pathway to support extensive tumor growth (DeBerardinis, Lum et al. 2008; Weinberg, Hamanaka et al. 2010). Another reason might be that energy supply in form of ATP is much faster then using the mitochondrial metabolism and due to the high glycolytic rate, the yield of ATP can be even higher compared to oxidative phosphorylation (Guppy, Greiner et al. 1993; Pfeiffer, Schuster et al. 2001). Yet another feature of the fast energy supply is that tumor cells can use more nutrients in shorter time and so starve their neighboring cells and gain space to proliferate (Kaelin and Thompson 2010). Kaelin et al. also reviewed that the increased

ROS production may support cancer cell proliferation through the inhibition of growth inhibitory phosphatases (Kaelin and Thompson 2010). Further it is assumed that high ROS generation can damage mitochondrial DNA and the respiratory chain and thus promote the glycolytic phenotype (Pelicano, Carney et al. 2004). Hypoxic environment contribute most likely also to an increased glycolysis because of the reduced oxygen in tumor tissue (Xu, Pelicano et al. 2005).

Still very little is known about the underlying mechanisms responsible for the switch from oxidative phosphorylation to aerobic glycolysis. However, detailed analysis of genes involved in the regulation of energy metabolism as well as modulation of the switch between bioenergetic pathways using drugs will unravel important insights that can be used for therapeutic intervention in PDAC.

2. Aim of the Study

The "Western or Secondary lifestyle" implies an enhanced availability of cheaper food, less physical activity and leads often to obesity in both adults and children. Excessive intake of high caloric food correlates with increased risk for several diseases including type 2 diabetes mellitus (TDM2) and gastrointestinal cancer (GI) such as pancreatic ductal adenocarcinoma (PDAC). Among all, PDAC is the 4th leading cancer in the United States with almost 100% lethality and a survival rate with less then 5%. Despite a high chemoresistance and aggressive tumor behaviour, the early diagnostic is still a limiting factor related to the decreased survival in patients. Therefore one of the most important aim is to improve diagnostic properties to provide patients with therapy in time to increase the healing prospects in PDAC patients.

Since Warburg's findings in the early 1920's regarding the preference of cancer cells to supply their energy mainly from glycolysis rather then oxidative phosphorylation independent of oxygen availability, the diverse preference of host and tumor energy metabolism are considered as a promising detection tool. The ^{18}F-fluorodeoxyglucose positron emission tomography (FDG-PET) is a commonly used imaging tool that detects several cancer types as well as metastasis by their increased glucose uptake however this method is less successful in the early detection of pancreatic cancer.

To gain deeper insight into the connection between obesity, the development of pancreatic cancer and bioenergetic shifts, we use a well-established pancreatic cancer mouse model with $Kras^{G12D}$ activation in the exocrine part of the pancreas and keep these mice on special diet containing 60% fat. Previous work suggested an increased dependence of pancreatic cancer on glycolysis and further several studies proposed that cancers cells require the increased amount of glycolytic intermediates to fulfill their needs, therefore different pharmacological therapeutics as well as mouse models with additional gene knockouts are used to modulate the cancer cell metabolism.

We aim to asses the different preferences of pancreatic tumor cells compared to host cells on bioenergetic pathways and investigate the modulation of energy metabolism on tumor incidence in the $p48$-$Kras^{G12D}$ mouse model during HFD-induced obesity and elucidate whether changes in metabolism could be used during therapeutic imaging purposes for the early detection of lesions in PDAC.

3. Material and Methods

Mice were kept at specific pathogen free (SPF) animal facility and fed with either normal diet (ND) (Altromin, #1314 forty) or high fat diet food (HFD) (Research Diet, #D12492).

3.1 Mouse Models

a) $Kras^{G12D}$ and p48 mice (Tuveson, Shaw et al. 2004; Nakhai, Sel et al. 2007)

b) $PPAR\alpha^{-/-}$ mice (Lee, Pineau et al. 1995)

c) $PPAR\gamma^{fl/fl}$ mice (He, Barak et al. 2003)

d) $SIRT1^{fl/fl}$ mice (Li, Rajendran et al. 2007)

$Kras^{G12D}$ and p48 mice were kindly provided by Dr. David Tuveson and Dr. Hassan Nakhai, respectively (a). $PPAR\alpha^{-/-}$ (b), $PPAR\gamma^{fl/fl}$ (c) and $SIRT1f^{l/fl}$ (d) mice were obtained from Charles River.

3.2 Genotyping of the mice

For genotyping mice tail biopsies were collected under anesthesia and lysed in 180 µl tail lysis buffer supplemented with 20 µl Proteinase K (Qiagen, #1017738) and incubated over night at 60°C. On the following day Proteinase K was heat inactivated by incubating at 95°C for 5 min. Afterwards the samples were centrifuged at 13.200 rpm for 10 min, 1:10 dilutions prepared using dH_2O were used for the polymerase chain reaction (PCR). Finally PCR products were loaded on 2 % agarose gel containing ethidium bromide (Invitrogen, #15585) to visualise the expected bands.

Tail lysis buffer:
- 1,5 M Tris/HCl (Roth, #4855.2)
- 200 mM NaCl (Fluka, #71376)
- 0,2% SDS (Roth, #2326.2)
- 5 mM EDTA (Fluka, #03609)
- 500 ml dH_2O

Kras PCR condition:

- 12,5 µl Mastermix (Qiagen, #201445)

- 0,5 µl Forward Primer

- 0,5 µl Reverse Primer

- 7,5 µl dH$_2$O

- 3 µl DNA

Total volume: 24 µl

Kras 5' → 5'-CCA TGG CTT GAG TAA GTC TGC G-3'

Kras 3' → 5'-CGC AGA CTG TAG AGC AGC G-3'

94°C   5 min

94°C   30 sec; 60°C 1 min; 72°C 1 min (35 cycles)

72°C   7 min

4°C   ∞

Size: 520 bp

Cre PCR condition:

- 12,5 µl Mastermix

- 0,5 µl Forward Primer

- 0,5 µl Reverse Primer

- 9 µl dH$_2$O

- 1,5 µl DNA

Total volume: 24 µl

Cre 370 FP → 5'-CAC AGT GCC CAC ATT ATT TAG ATA-3'

Cre 370 RP → 5'-ACC GTC AGT ACG TGA GAT ATC TT-3'

94°C   5 min

94°C   30 sec; 58°C 30 sec; 72°C 30 sec (35 cycles)

72°C   7 min

10°C   ∞

Size: 520 bp

PPARγ PCR condition:

- 12,5 µl Mastermix
- 0,5 µl Forward Primer
- 0,5 µl Reverse Primer
- 8,5 µl dH$_2$O
- 2 µl DNA

Total volume: 24 µl

oIMR1934 FP → 5'-TGT AAT GGA AGG GCA AAA GG-3'

oIMR1935 RP → 5'-TGG CTT CCA GTG CAT AAG TT-3'

94°C   3 min

94°C   30 sec; 60°C 1 min; 72°C 1 min (35 cycles)

72°C   2 min

10°C   ∞

Mutant = 250 bp

Heterozygote = 250 bp and 214 bp

Wild type = 214 bp

<u>PPARα PCR condition:</u>

- 12,5 µl Mastermix
- 0,5 µl Primer 1
- 0,5 µl Primer 2
- 0,5 µl Primer 3
- 8 µl dH$_2$O
- 3 µl DNA

Total volume: 25 µl

Primer 1: PPARa-wt RP → 5'-CCC ATT TCG GTA GCA GGT AGT CTT-3'

Primer 2: PPARa-wt FP → 5'-GAG AAG TTG CAG GAG GGG ATT GTG-3'

Primer 3: PPARa-mut RP → 5'-GGT TGA CTT AGG TCT TGT CTG-3'

94°C   3 min

94°C   30 sec; 60°C 1 min; 72°C 1 min (35 cycles)

72°C   2 min

10°C   ∞

Mutant = 650 bp

Heterozygote = 412 bp and 650 bp

Wild type = 412 bp

<u>SIRT1 PCR condition:</u>

- 12,5 µl Mastermix
- 0,5 µl Forward Primer
- 0,5 µl Reverse Primer
- 8,5 µl dH$_2$O
- 3 µl DNA

Total volume: 25 µl

Forward Primer: oIMR7909 → 5'-GGT TGA CTT AGG TCT TGT CTG-3'

Reverse Primer: oIMR7912 → 5'-CGT CCC TTG TAA TGT TTC CC-3'

94°C   3 min

94°C   30 sec; 56°C 1 min; 72°C 1 min (35 cycles)

72°C   2 min

10°C   ∞

Mutant = 750 bp

Heterozygote = 750 bp and 550 bp

Wild type = 550 bp

3.3   Glucose Tolerance Test (GTT)

The Glucose Tolerance Test (GTT) performed to check insulin resistance in mice. Therefore mice were fasted for 8 hrs, separated into single cages 3 hrs prior to the experiment to acclimatize and their weights were recorded. Blood glucose levels of the mice were measured at the time points 0, 15, 30, 60, 90 and 120 min with a glucometer (Roche, #6114986) and plasma samples were collected 0, 15, 30, 60 and 90 min. Glucose solution administrated by intraperitoneal (i.p.) injection, was prepared freshly before use and stored on ice.

Glucose solution

- 1 ml 50 % Glucose (Fresenius Kabi, # 6178495)
- 2ml 0,9 % NaCl (Diaco, #43-500)

At the beginning of the experiment first plasma samples were taken and the basal blood glucose level measured. According to the basal blood glucose level and the weight of the mouse the amount of the glucose solution for injection was calculated. Then the mice were i.p. injected with 1.5 or 2.0 g/kg bodyweight using glucose solution and the blood glucose levels were taken at the time points as described above. The same approach was accomplished for the collection of the plasma samples in parallel.

3.4 Mouse treatment

3.4.1 Etomoxir Administration

The animals were i.p. injected with 4 µl etomoxir per gram body weight once every second week over a time period of 20 weeks. To prepare the solution 5 mg etomoxir was dissolved in 1 ml dH_2O.

3.4.2 Fenofibrate administration

The animals were gavaged once a week with 7 µl fenofibrate per gram body weight over a time period of 20 weeks. 82 mg fenofibrate was dissolved in 1 ml DMSO and finally a 1:10 dilution with dH_2O was used.

3.4.3 3-Bromopyruvate (3-BP) administration

The animals were i.p. injected in every 2 weeks with 6 µl 3-BP per gram body weight over a time period of 20 weeks. 8 mg 3-BP was dissolved in 1 ml dH_2O and the pH was adjusted to 7,4 using sterile filtered 1M NaOH. Finally a 1:10 dilution was prepared with dH_2O.

3.4.4 2-Deoxyglucose (2-DG) administration

The animals were i.p. injected once a week with 6 µl 2-DG per gram body weight over a time period of 20 weeks. 83 mg 2-DG was dissolved in 1 ml dH_2O and the pH was adjusted to 7,4 using sterile filtered 1M NaOH.

3.5 Sacrificing of the mice

Prior to sacrificing, animals were fasted over night and the fasting glucose levels (FBG) were measured using a glucometer (Roche, #7306736). The mice received a dose of bromodeoxyuridine (BrdU) (Sigma, #B5002) (75mg/kg body weight) via intraperitoneal injection 1.5 hrs before euthanasia. BrdU is a thymidine analogue and incorporates into the cellular DNA during cell proliferation. Thus via immunohistochemistry (IHC) staining proliferating cells can be detected. After sacrifice, the tissues were harvested and cut two into halves. One part was directly transferred in freezing tubes (Brand, #780714) and snap

frozen in liquid nitrogen and further stored at -80°C. The other half was fixed in 4 % Paraformaldehyde (PFA) (Electron Microscopy Sciences, #15710) in PBS at 4°C overnight.

3.6   Histology

Tissue samples stored at 4°C overnight were transferred into a dehydration machine (Leica, APS3005) and processed. Afterwards the tissues were put into special embedding cassettes (Medite, #46-1100-00) and embedded in paraffin. For the stainings 3 μm thick sections were prepared by using a microtome (Leica, RM2235), smoothed in a warm water bath at 45°C and mounted on glass slides (Thermo Scientific, #J1800AMNZ). To ensure that the sections are dry enough before staining, they were kept at 37°C for at least 1-2 hrs.

3.6.1   Haematoxylin & Eosin staining (H&E)

H&E staining is a widely used histological method to make different cellular structures visible on paraffinized tissue sections. For differentiation haematoxylin stains the nuclei in blue/dark violet whereas eosin colours the cytoplasmic area of the cell in red.

Sections were prepared from paraffin embedded tissue, as described previously. After drying, the sections were deparaffinized for 10 min in Xylol (X-TRA Solv, Medite, #41-5213-00) and subsequently rehydrated by descending order of ethanol dilutions where they are incubated in each dilution for 2 min. Then the sections were transferred into phosphate buffered saline (PBS) (Gibco, #21600-069) for 5 min and stained with ready-to-use haematoxylin (Vector Laboratories, # H3401) for 1 min. They were then washed with distilled water repeatedly until the water was clear. The sections were counterstained with 1% eosin solution (Sigma–Aldrich, #E4382) for 10 seconds and then washed with again distilled water. They were then dehydrated by ascending order of ethanol dilutions, where the sections were incubated in each dilution for 2 min. To complete the dehydration, incubation in Xylol for 10 min was followed. Finally the dried sections were coated using mounting medium (Vector Laboratories, #H5000), covered with a cover slip and examined under the light microscopy.

Rehydration

- 10 min Xylol
- 2 min 100% Ethanol
- 2 min 96% Ethanol
- 2 min 80% Ethanol
- 2 min 70% Ethanol
- 2 min 50% Ethanol
- 5 min PBS

Dehydration

- 2 min 50% Ethanol
- 2 min 70% Ethanol
- 2 min 80% Ethanol
- 2 min 96% Ethanol
- 2 min 100% Ethanol
- 10 min Xylol

Eosin solution (1 %)

2,5 g Eosin Y Disodium Salt in 250 ml dH_2O and 15 drops of acetic acid (Sigma, #45726)

3.6.2   Alcian Blue staining

Alcian Blue staining is used for the detection of mucopolysaccharides and acetic mucins, which appears blue under the light microscope. The paraffin embedded tissue sections were prepared, deparaffinized and rehydrated as described before. Afterwards the sections were stained in 3% alcian blue solution for 30 min and followed by a washing step under running tap water until the water is clear. Then they were counterstained with Nuclear Fast Red (Vector Laboratories, #H3403) for 5 min and again the sections were washed under running tap water. Following dehydration and drying as described for the H&E staining before, finally the dried sections were coated using mounting medium, covered with a cover slip and examined under the light microscopy.

Alcian Blue solution (3 %)

- 100 ml 3 % acetic acid

- 1 g Alcian Blue (Sigma, #A5268)

→ Adjust pH 2.5 using acetic acid

3.6.3 Sirius Red staining

Sirius red staining is performed to visualize collagen fibres and to detect fibrotic areas. Sections were cut from paraffin embedded tissue, deparaffinized and rehydrated like described before. After 5 min incubation in PBS, sections were covered with Sirius red solution for 2 hrs in the dark. Then they were rinsed under running tap water until the water was clear. Finally dehydration and drying procedures were performed as described for the H&E staining previously. Then the dried sections were coated with mounting medium (Vector Laboratories, #H5000), covered with a cover slip and examined under the light microscopy.

Sirius Red Solution

- 0,1 g Direct Red 80 (Sigma-Aldrich , #365548)

- 0,1 g Fast Green FCF (Sigma-Aldrich, #7252)

- 100 ml Picric acid

3.6.4 Immunohistochemistry (IHC) staining

Immunohistochemistry is a method to detected specific antigens at tissue sections based on an immune reaction with mono- or polyclonal antibodies. Therefore tissue sections were prepared, deparaffinized and rehydrated as described before.

In order to block endogenous peroxidise activity the tissues were incubated with 3% hydrogen peroxide in PBS for 10 min, followed by washing in PBS 3 times for 5 min. Depending on the localization of the protein of interest, the next step of the protocol differs. For the nuclear staining the sections were boiled in sodium citrate solution (antigen unmasking solution; Vector Laboratories, #H3300) for 20 min in a microwave and cooled down for 30 min at room temperature (RT), whereas for proteins localized in

cytoplasm incubation of the slides in 0,03% Triton X-100 (Sigma, #T8787) for 10 min was sufficient for antigen retrieval. After the antigen unmasking the protocol for both techniques was the same. The slides were washed 3 times in PBS for 5 min and then treated with 3% Bovine serum albumin (BSA) (Sigma, #A3059) in PBS supplemented with 4 drops avidin solution per ml (Vector, #SP-2002) for 30 min to block nonspecific binding. This step was followed by incubation with the primary antibody (1:50-1:500) in 3 % BSA-PBS supplemented with 4 drops biotin per ml (Vector, #SP-2002) for 2 hrs RT or at 4°C overnight. Then slides were washed 3 times in PBS for 5 min and incubated with biotinylated secondary antibody (1:1000 dilution in 3 % BSA) for 30 min at RT. During the incubation time ABC solution (Vector Laboratories, #PK-6100) was prepared. 2 drops of solution A (avidin dehydrogenase) was added in 5 ml PBS and B (biotinylated horseradish peroxidase) was added and stored for 30 min at 4°C. The slides were washed 3 times in PBS for 5 min and afterwards treated with ABC solution for 30 min at RT and washed again 3 times in PBS for 5 min. Finally, the colour reaction was performed by using DAB solution (Vector Laboratories, #SK-4100), which consists of 2 drops DAB stock buffer, 4 drops DAB stock solution and 2 drops hydrogen peroxide solution dissolved in 5 ml distilled water. The colour reaction was observed under the light microscopy and incubation lasted until the specific staining could be seen. To stop the reaction the slides were transferred into distilled water, then counterstained with haematoxylin for 1 min and washed again in distilled water. The following dehydration and drying steps were as described for the H&E staining. Finally the dried sections were coated with mounting medium, covered with a cover slip and examined under the light microscopy.

3.7 Analysis of proteins

3.7.1 Protein isolation

Frozen tissue samples were crushed manually and then homogenized using a pellet pestle (Sigma-Aldrich, #Z359971-1EA) on ice in an adequate amount of freshly prepared protein lysis buffer (1x). After centrifugation at 13.200 rpm for 20 min at 4°C, the supernatant was directly transferred via a syringe into fresh tubes and stored at -80 °C.

10x Stock lysis buffer

- 50 mM Tris-HCl pH 7,5

- 250 mM NaCl

- 3 mM EDTA (Fluka, #3609

- 3 mM EGTA (Sigma, #E4378)

- 1 % Triton

- 0,5 % NP40 (Sigma, #T3021)

- 10 % Glycerol (Merck 1.04093)

- 25 mM Sodium pyrophosphate (Sigma, #231368)

Add 1 tablet of complete Protease Inhibitor Cocktail Tablets (Roche, #11697498001) in 50 ml stock lysis buffer.

1x Lysis buffer

- 8,0 ml stock lysis buffer including Protease Inhibitors

- 100 µl PMSF (Sigma, #7626)

- 500 µl 1M ß-Glycerolphosphat (Fluka, #50020)

- 500 µl 500 mM NaF (Sigma, #S7920)

- 500 µl 100 mM NaPyr (Sigma, #231368)

- 500 µl 100 mM Na Orthovanadat (Sigma, #S6508)

3.7.2 Determination of protein concentrations

Proteins were isolated as described before and their concentration was determined via Bradford Assay. Therefore 2 µl of protein extract was added to 1 ml of a 1:5 diluted Bio-Rad Protein Assay (Biorad, #500-0006) solution for 5 min and measured by Spectrometer (ThermoFisher, NanoDrop 2000c) at a wavelength of 595 nm.

3.7.3 Western Blot

For Western Blot analysis polyacrylamide gels (7-12%) were poured and afterwards transferred into electrophoresis tanks filled with running buffer (1x) by using Mini Protean Gel System® (Biorad). Accordingly the necessary protein amount (15 to 40 µg)

was calculated and protein lyses buffer (1x) was added to reach the end volume of 15 µl. Followed by an denaturation step where 9,5 µl Laemmli buffer and 0,5 µl mercaptoethanol were pipetted to each sample and incubated at 95℃ for 5 min, the protein samples were shortly centrifuged and loaded on the gel, which was running at a voltage of 80 mV.

Main Gel 7-12 %

- 6,75-8,62 ml dH$_2$O

- 3,75 ml Main Gel Buffer

- 2,63-4,5 ml 40 % polyacrylamide (Merck, #1.00638)

- 112,5 µl 10 % Ammoniumpersulfate (Sigma, #A3687)

- 11,25 µl TEMED (Sigma, #T9281)

Main gel buffer

- 181,65 g Tris pH 8.8

- 20 ml 20% SDS (Roth, #23.26.2)

→ Adjust to 500 ml with dH$_2$O

Stacking Gel

- 4,6 ml dH$_2$O

- 950 µl Stacking Gel

- 950 µl 40% Acrylamide

- 62,5 µl 10% Ammoniumpersulfate

- 12,5 µl TEMED

Stacking Gel Buffer

- 12,11 g Tris pH 7

- 5 ml 20 % SDS

- → Adjust to 100 ml with dH$_2$O

Laemmli Buffer

- 3,55 ml dH$_2$O

- 1,25 ml 0,5M Tris-HCL pH 6.8

- 2,5 ml Glycerol

- 1 ml 20 % SDS

- 0,2 ml 0,5% Bromphenol Blue (Sigma, #B5525)

10x Running Buffer

- 15,15 g Tris

- 72 g Glycine (Roth, #3908)

- 25 ml 20% SDS

- → Adjust to 500 ml with dH$_2$O

1x Running Buffer

- 100 ml 10x Running Buffer

- → Adjust to 1 lt with dH$_2$O

After running the gel, the proteins were transferred on a PDVF membrane (Zefa Laborservice, Immobilon-P, #Z.IPVH00010) at 250 mA for 2 hrs on ice. The membrane was first activated with methanol for 15 sec and then placed together with the gel into a sandwich construction consisting of one sponge followed by two layers of Whatmann paper on each side. For the transfer the Mini-Trans-Blot System® (Biorad) was used and filled with 1x transfer buffer.

10x Transfer Buffer

- 30 g Tris

- 144 g Glycine

→ Adjust to 1 lt with dH$_2$O

1x Transfer Buffer

- 100 ml 10x Transfer Buffer

- 200 ml Methanol (Merck, #1.06009)

→ Adjust to 1 lt with dH$_2$O

Afterwards the membrane was washed shortly in PBS-Tween (0,1% Tween 20, Sigma-Aldrich, #P1379) and then blocked for half an hour in 5 % slim milk powder (Fluka, #70166) in PBS-Tween (0,1%) to decrease unspecific binding at RT. For phosphorylated antibodies the membrane was blocked in 5 % BSA/PBS-Tween for 30 min at RT. A washing step 3 times for 5 min with PBS-Tween was followed by incubation with the primary antibody (1:200 to 1:1000) at 4°C overnight. The primary antibody was either diluted in Milk-PBS-Tween or in BSA/PBS-Tween. After 3 times washing with PBS-Tween for 5 min incubation with the secondary horseradish peroxidase conjugated antibody (1:1000) was performed for a half an hour at RT. Again the membrane was washed with PBS-Tween and then covered with chemiluminescence solution (Thermo, Super Signal West Pico, #1856135/36) for 5 min. Afterwards the membrane was exposed for 15 sec to 10 min to X-ray film (Thermo, #34089), which was developed that showed the proteins of interest.

3.8 RNA isolation

For total RNA isolation from the frozen tissue samples, the RNeasy Kit (Qiagen, RNeasy Kit, #74106) was used. The samples were first manually crushed and then disrupted in an adequate amount of Buffer RLT (enriched with 1 % ß-Mercaptoethanol) with a rotor-stator homogenizator (Kinematica, #PT1200E). After centrifugation at 13.200 rpm for 3 min, the supernatant was transferred to a new microcentrifuge tube and 1:1 volume of 70 % ethanol was added to each sample. The samples containing ethanol were

immediately mixed by pipetting and transferred to RNeasy spin column, which was placed in fresh 2 ml collection tube. After centrifugation at 10.000 rpm for 15 sec, the flow-trough was discarded and 700 µl Buffer RW1 was added to the spin column. Again the samples were centrifuged at 10.000 rpm for 15 sec and the flow-through was discarded. Then 500 µl RPE Buffer was added and centrifuged 10.000 rpm for 15 sec. Additionally 500 µl RPE Buffer was added and the sample were centrifuged at 10.000 rpm for 2 min. Afterwards the RNeasy spin was placed in a new 1,5 ml collection tube, 30-50 µl RNase-free water was added and then centrifuged 10.00 rpm for 1 min to elute the RNA. The RNA samples are stored at -80 °C.

3.8.1   cDNA synthesis

The RNA concentration was measured using a NanoDrop (ThermoFisher, NanoDrop 2000c) and 1µg of RNA was calculated for each sample accordingly. For the cDNA synthesis each sample received 1 µl Oligo's, 1 µl dNTP's, 1 µg RNA and then added up with RNase-free to 12 µl. The samples were transferred into a heating block and incubated at 65 °C for 5 min. During the incubation time a master-mix was prepared, which contained 5 µl RNase-free water, 1 µl DTT, 1 µl RNaseOut and 1 µl SuperSript III. After mixing through pipetting, each sample received 8 µl of the master-mix and was then incubated in a heating block at 42 °C for 50 min. For the inactivation the samples were incubated at 70 °C for 15 min and 80 µl of RNase-free water was added. The cDNA samples were stored at 4 °C.

3.8.2   Realtime (RT)-PCR

Specific primer dilutions containing reverse and forward primer were used in a master mix for the RT-PCR reactions.

Master-Mix

- 10 µl SYBR Green Master-Mix Rox (Roche, 14879600)

- 5 µl dH$_2$O

- 2 µl primer mix dilution

Then 17 µl of the master-mix were pipetted into the wells of a 96-well-plate and 3 µl cDNA (1:4 diluted with dH_2O) was added. StepOnePlus™ Real-Time PCR System (Applied Biosystems) was used with following PCR conditions:

<u>PCR conditions</u>

- 50°C 2 min
- 95°C 2 min
- 95°C 15 sec
- 60°C 30 sec
    - → Repeat for 40 cycles

For normalisation of the samples the housekeeping gene Cyclophilin D was used.

RT-PCR primers	Forward 5`-3	Reverse 5`-3
Cyclophilin	ATG GTCA ACC CCA CCG TGT	TTC TGC TGT CTT TGG AAC TTT GTC
11	ACT CCA GGC GGT GCC TAT G	GAG CGT GGT GGC CCC T
IL-6	ATG GTA CTC CAG AAG ACC AGA GGA	GTA TGA ACA ACG ATG ATG CAC TTG
IL-1β	GTG GCT GTG GAG AAG CTG TG	GAA GGT CCA CGG GAA AGA CAC
PEPCK	CCC AGG AGG TGA GGA AGT TTG	GGA GCC GTC GCA GAT GTG
GLUT1	ATC GTC GTT GGC ATC CT	CAA GTC TGC ATT GCC CA
GLUT2	GGT GTG ATC AAT GCA CCT	GTA TCT GGG GCT TTC TGG AC
G6Pase	GAA GGC CAA GAG ATG GTG TGA	TGC AGC TCT TGC GGT ACA TG
MCAD	ATG ACG GAG CAG CCA ATG ATG	TCG GCT TCC ACA TGA AT CGA
Cpt1α	CTC AGT GGG AGC GAC TCT TCA	GGC CTC TGT GTA CAC GAC AA
AOX	CGC CTA TGC CTT CCA CTT TCT C	CGC AAG CCA TCC GAC ATT CTT
ACC	GCC ATT GGT ATT GGG GCT TAC	CCC GAC CAA GGA CTT GTT TG

RT-PCR primers	Forward 5`-3	Reverse 5`-3
LPL	AAG GTC AGA GCC AAG AGA AGC A	CCA GAA AAG TGA ATC TTG ACT TGG T
FAS	GGC ATC ATT GGG CAC TCC TT	GCT GCA AGC ACA GCC TCT CT
SteCoA	GAG GCC TGT ACG GGA TCA TA	CCG AGC CTT GTA AGT TCT GTG
PGC-1α	TCT GGA ACT GCA GGC CTA ACT C	GCA AGA GGG CTT CAG CTT TG
Mttp	CAA GCT CAC GTA CTC CAC TGA	TCA TCA TCA CCA TCA GGA TTC T
SDHA	ATG CCA GGG AAG ATT ACA AAG TGC	GTA ACC TTG CCA GTC TTG ATG TCC
Ndufb9	CAG AAT CAG CAT CCT CAG CCG TAT ATC	AGG TCT GGT CAC AAT ATG CCA CA
Ndufb10	TGT GCC AAG GAA CTG GAG CA	GCC TCG CAG CCT TCC TTT CT
Cox7a2	CTT GCT CGA CGC GCG	AGC GCT AGG AGG GAG TTC CGT TTC C

Table 1: Primer sequences used for RT-PCR.

3.9   Fluorescence Activated Cell Sorting (FACS)

For the FACS analysis the whole pancreas harvested, placed into a petri dish containing 2 ml of digestion buffer and minced with a sterile scalpel on ice. The homogenizate was transferred into a 50 ml falcon, filled up to 5 ml digestion buffer and incubated at 37 °C for 40 min. To stop the enzyme activity 100 mM EDTA were added to the falcon, kept on RT for 5 min and further 10 ml PBS containing 2 % fetal calf serum (PBS-FCS) were added to wash the cells. After the homogenisation, the cell suspension was filtered first via a 70 µm filter cell strainer (BD Falcon™, #352350) and then via 40 µm cell strainer (BD Falcon™, #352340), a centrifuge step occurred at 1.500 rpm for 5 min at 4°C. The pellet was resuspended in 1 ml of red blood cell lysing buffer (Sigma, #R7757) via pipetting and incubated in this buffer for 5 min at RT. Again 10 ml PBS-FCS were added and centrifuged at 1.500 rpm for 5 min at 4°C. According to the pellet size, it was resuspended in 200-300 µl of PBS-FCS and then 100 µl of each sample was pipetted into a 96-well plate in a duplicate plus 2 controls. One control was EMA negative and EMA positive. After the 96-well plate was centrifuged at 1.500 rpm for 5 min 4°C and the SN was discarded, 100 µl of sample EMA solution was added to the samples except to the EMA negative control.

Followed by incubation on ice for 15 min with direct light irradiation, further the plate was washed with 100 µl PBS-FCS per well and then spinned down at 1.500 rpm for 5 min at 4°C. The supernatant was discarded, a blocking step took part with 100 µl of blocking solution for 10 min on ice covered with aluminum foil and again the plate was centrifuged under same conditions described previously. For the staining of the cell surface markers 100 µl of F4/80+, GR1+, CD11b+ and CD11C+ were added into each wells except to the controls which received 100 µl PBS-FCS. Again PBS-FCS was added to the wells and the plate was centrifuged at 1.500 rpm for 5 min at 4°C. After discarding the supernatant the cells were fixed via 100 µl of fixation buffer (eBioscience, #00-5223-56) added to each well and further incubated with aluminum foil covered on ice for 25-30 min. Next step was to wash the plate with 100 µl 1x permeabilization buffer (eBioscience, #00833-56) per well, to centrifuge it at 1.500 rpm for 5 min at 4°C and to discard the supernatant. For the intracellular staining for cytokines half of the samples received 100 µl of IL-4 and IL-13 in each well and on the other half 100 µl of TNFα, INFγ and IL-12 were added to each well. On the controls 100 µl PBS-FCS were pipetted and the plate was incubated on ice for 20 min. Afterwards the plate was washed again 100 µl PBS-FCS, the plate was centrifuged at 1.500 rpm for 5 min at 4°C and the supernatant discarded. Then 100 µl PBS-FCS + 0,5 mM EDTA were added to each well, subsequently the cell suspension was filtered and transferred into FACS tubes and further 100 µl PBS-FCS were added to each well.

EMA Solution for 1 sample:

- 1,5-2 µl EMA dye (Sigma, #E2028)

- 100 µl PBS-FCS

Blocking Solution

- Antibody CD16/32 (BD Pharmingen, #553142) 1:100 diluted in PBS containing 2% FCS

Antibody	Diluted in PBS + 2% FCS	Company	#
F4/80+	1:200	eBioscience	17-4801.80
GR1+	1:200	eBioscience	17-5931
CD11b+	1:200	eBioscience	47-0112
CD11c+	1:200	PD Pharmingen	557400
Antibody	Diluted in permeabilization buffer	Company	#
TNFa	1:200	eBioscience	25-7321-80
INFγ	1:200	PD Pharmingen	554412
IL-13	1:100	eBioscience	12-7133-81
IL-14	1:200	eBioscience	25-7042-42

Table 2: Primer used for Fluorescence Activated Cell Sorting.

3.10 Isolation of genomic DNA

For genomic DNA isolation ReliaPrep^{TM}gDNA Tissue Miniprep System (Promega, #A2051) was used. Frozen tissue samples were crushed manually, placed in 160 µl PBS and 20 µl of Proteinase K solution was added and vortexted. Afterwards 200 µl Cell Lysis Buffer was added to each sample and mixed by vortexing for at least 10 sec. For efficient lyses the samples were incubated in a heating block over night at 56°C. Then 250 µl Binding Buffer was added and the samples mixed by vortexing for 10 sec. Each sample was transferred into a ReliaPrepTMBinding Column placed in a collection tube and spinned down at 13.200 rpm for 1 min. The flow through was discarded, 500 µl Wash Solution was added to the sample and then centrifuged again at 13.200 rpm for 2 min.

The washing step was repeated in total 3 times. Afterwards the ReliaPrepTMBinding Column was placed in new 1,5 ml tube, 100 µl Nuclease-free water was added and the samples were spinned at 13.200 rpm for 1 min. The genomic DNA was stored at -20°C.

3.10.1 Quantification of mitochondrial genome

For the quantification of mitochondrial genome copy number relative to nuclear genome copy number special primer pairs were designed. The primer pairs were designed accordingly to sequences exclusively found either in the nuclear genome or in the mitochondrial genome. In each PCR a specific probe was used.

Mouse nuclear primer pair

Forward → 5'-TTT ACA GGA TCT CCA AGA TTC AGA-3`

Reverse → 5`-GAT ACA CCC ATG TGA ACA AA-3'

Probe No.26 (Roche, #04687574001)

Mouse mitochondrial primer pair

Forward → 5'-CAA ATT TAC CCG CTA CTC AAC TC -3`

Reverse → 5`-GCT ATA ATT TTT CGT ATT TGT GTT TGG-3'

Probe No.101 (Roche, #04692195001)

4 µl genomic DNA (25 ng/ µl) was used and a master-mix was prepared for the PCR. According to which sequence should be amplified the corresponding primer pairs and probe were included.

Master-Mix

- 0,2 µl forward primer

- 0,2 µl reverse primer

- 0,2 µl Probe

- 0,4 µl dH$_2$O

- 5 µl Mastermix (Roche, #04887301001)

6 µl of the master-mix and 4 µl genomic DNA was pipetted into a 96-well plate (Roche, #04729692001) for the PCR. Each sample was pipetted in duplicate. The PCR was runned in the LightCycler (Roche, LightCycler® 480 Real-Time PCR System) using the following PCR conditions.

PCR conditions

95°C 5 min

95°C 10 sec; 60°C 20 sec; 72°C 10 sec (45 cycles)

40°C 10 sec

For the quantification the ct values for mitochondrial and nuclear genome were raised by 2 and the reciprocal value was taken (1/(2^ct)). Based on the very low numbers the values were multiplied with a factor of 10^6. Then the mean mitochondrial DNA amount was divided by the mean nuclear DNA amount.

3.11 Citrate Synthase Assay

Citrate Synthase is used as an enzymatic marker for the content of intact mitochondria (Hood, Zak et al. 1989). Therefore snap frozen tissue was crushed and 10-26 mg of the crushed tissue was used for the assay. Further it was placed in 2 ml tube on ice containing 750 µl homogenisation buffer and two metal balls, which support the cell fraction. For further tissue homogenisation the tubes were placed in tissue lyser (Qiagen, Tissue Lyser II, #85300) and shaken at full speed for 2 min. After the elimination of the metal balls, the samples were centrifuged at 4°C at 13.200 rpm for 10 min and the supernatant was transferred into new 1,5 ml tubes. The next step was to determine the protein concentration via Biuret. For the Biuret assay 20 µl of 5 % (w/v) sodium deoxycholate was pipetted into a cuvette, followed by 20 µl of the supernatant and finally 1 ml Biuret reagent. The samples were incubated for 10 min and then measured at a wavelength of 540 nm using a BSA standard curve (0; 0,8; 1,6; 3,2; 6,4; 12,8, 25 mg/ml BSA). Finally the samples were diluted to a final concentration of 1 µg/ µl and pipetted in a triplicate on a 96-well plate (Fisher Scientific, Nunc C96 MicroWell™ Plates, #1019-4761). In each well 20 µl of the samples 205 µl Assay buffer and 25 µl Actely-CoA were loaded (Sigma, #A2056). Subsequently the plate was transferred to Tecan Reader (Tecan, Infinite M200,

#3001641103) and the absorbance was measured at 412 nm once in a minute for 6 min. Subsequently the injection of 3 mM oxalacetate (Sigma, #O4126) followed into the wells, the plate was shaked and again the absorbance at 412 nm was measured once a minute over a time period of 10 min.

<u>Homogensation Buffer</u>

- 50 mM Tris (Roth, #4855.2)

- 1 mM EDTA

- 0,1 % Triton (Roth, #3051.3)

→ Adjust to pH 7,4 with HCl

<u>Biuret-Reagent</u>

- 100 ml of 200 mM NaOH

- 8 mM sodium potassium tartrate (Roth, # 8087.1)

- 3 mM copper sulfate pentahydrate (Fluka, #61240)

- 4,5 mM potassium iodide(Roth, #6750.1)

→ Add up to 250 ml with dH_2O

<u>Assay Buffer</u>

- 100 mM Tris

- 1 mM EDTA

- 1 mM $MgCl_2$

- 0,1 mM DTNB (Sigma, #218200)

→ Adjust to pH 8,2 with HCl

3.12 Mitochondria Isolation

For the isolation of mitochondria from pancreas first the isolation and respiration buffer was prepared and stored at 4°C. The composition of the isolation buffer was adapted from (Hodarnau, Dancea et al. 1973) and only the original BSA concentration of 0,5 % was increased to 2,5 %. For avoiding pancreas autodigestion the isolation buffer additionally contained 100 µl of Halt[TM]Protease Inhibitor Single-Use Cocktail (TermoScientific, #78425) per 100 ml buffer. The respiration buffer was adapted from (Talbot, Hanuise et al. 2003) and modified. Instead of 1 mM $MgCl_2$ 2 mM $MgCl_2$ was used and the fatty acid free BSA concentration was increased from initial 0,3 % to 3 %.

Isolation Buffer

- 192 mM Mannitol (Roth, #4175.1)

- 58 mM Sucrose (Roth, #4621.1)

- 2 mM Tris-HCL

- 0,5 mM EDTA

- 500 µl Inhibitor Single-Use Cocktail

→ Adjust volume to 500 ml with dH_2O and adjust the pH to 7,2 with 10 M KOH at 4°C.

   Take 400 ml and add fatty acid free BSA (Sigma, #A3803) in a concentration of 2,5%.

Respiration Buffer

- 120 mM KCL (Roth, #6781)

- 5 mM KH_2PO_4 (Roth, # 3904)

- 3 mM HEPES (Roth, # 9105.4)

- 1 mM EGTA (Roth, # 3054.2)

- 5 % BSA

- 2 mM $MgCl_2$

→ Adjust volume to 500 ml with dH₂O and adjust the pH to 7,2 with 10 M KOH at RT

After euthanizing the mice the pancreas was taken out and directly stored in 5ml cold isolation buffer and manually disrupted on ice using scissors. Further the homogenate was transferred into 15 ml glass homogenizer (potter) (Sartorius, #BBI-854 2406), isolation buffer was filled up to 15 ml and the cells were fractured via moving the teflon plunger (Sartorius, #BBI-854 2805) 5 times up and down. The homogenate was transferred into a centrifuge tube and spinned down at 800 rpm at 4°C for 10 min to get rid of the cell fragments. Only the supernatant was used for the next centrifuge step at 9.000 rpm for 10 min. Afterwards the supernatant was discarded. The pellet was resuspended in isolation buffer free of BSA via a brush and transferred into a 1,5 ml tube trough a pipette. To ensure that the mitochondria are not disrupted through shear force the tip was cut. Subsequently the mitochondria concentration for each sample was measured via Bradford assay at 595 nm using a BSA standard curve with the concentrations from 0,04 to 0,2 µg/µl.

3.13 Clark Electrode

The Clark Electrode (Rank Brothers, #Digital model 10) was used for measuring the mitochondrial respiration in pancreas mitochondria at 37°C. The first step was to calibrate the Electrode with air-saturated assay medium (respiration buffer). Afterwards 1 ml of 37°C warm respiration buffer was pipetted into the chamber of the Clark electrode, 500 µg mitochondria suspension was added and mixed via a stirrer. For the basal mitochondrial respiration complex I (NADH dehydrogenase) was inhibited through administration of 4 mM rotenone (Sigma, #R8875) and 3 mM succinate (Sigma, #S3674) was added as substrate for complex II (Succinate dehydrogenase) to start state 2 respiration.

The state 3 respiration was started by providing adenosine diphosphate (ADP) in concentration of 3 mM (Sigma, #A2754) to the mitochondria. Through administration of 1 µM oligomycin the ATP-production was blocked via the inhibition of ATPase synthase (complex V) and so state 4 could be determined. Afterwards, the complex II driven maximum respiration was investigated by adding the mitochondrial uncoupler carbonylcyanide-p-trifluoromethoxyphenylhydrazone (FCCP). For each mitochondria sample the whole measurement was accomplished twice and finally the respiratory

control ratio (RCR), the ratio 3 to state 4, was calculated for each sample and the median

value was taken.

3.14 Appendices Methods

3.14.1 Antibodies

3.14.1.1 Immunblot Analysis

- Anti-ß-Actin (Sigma , #A4700)

- Anti-Total OXOHOS (MitoScience, #ab110411)

3.14.1.2 Immunohistochemistry

- Anti-BrdU (Amersham Bioscience, #RPN201)

3.14.1.3 Secondary Antibodies (Western Blot)

- Anti-mouse IgG HRP-linked (GE Healthcare, #NA9310V)

3.14.1.4 Secondary Antibodies (Immunohistochemistry)

- Anti-rat IgG biotinyliert (Vector Laboratories, #BA9400)

4. Results

4.1 Phenotype of *CO* and *p48-Kras*[G12D] mice during High Fat Diet-induced obesity

Kras mutations are one of the very initial events during the development of pancreatic ductal adenocarcinoma (PDAC) seen in nearly all patients suffering from advanced pancreatic cancer (Warshaw and Fernandez-del Castillo 1992; Klimstra and Longnecker 1994; Li, Xie et al. 2004). Already in one third of patients with chronic pancreatitis a mutation in GTPase is detectable and frequently increases during pancreatic tumorgenesis (Klimstra and Longnecker 1994; Rozenblum, Schutte et al. 1997; Johnson, Rosenblum-Vos et al. 2000; Lohr, Maisonneuve et al. 2000). Therefore *p48-Kras*[G12D] mice are considered as one of the best models for studying the molecular mechanisms of pancreatic tumor development as it mimics human disease very closely (Klimstra and Longnecker 1994; Tuveson, Shaw et al. 2004; Hezel, Kimmelman et al. 2006).

It is already known that HFD-induced obesity increases the risk of cancer and especially in the gastrointestinal tract. To investigate the effects of the metabolic changes triggered under high fat diet (HFD) condition, the mice carrying *LSL-Kras*[G12D] were crossed to animals containing a tissue specific Cre recombinase, which is under the control of the p48 promoter in the exocrine part of the pancreas. The *p48-Kras*[G12D] mice were born healthy and fertile. At the age of 5 weeks the control (*CO)* and *p48-Kras*[G12D] mice were fed a diet containing 60% fat to induce obesity and their weight curves were recorded over 20 weeks. Indeed, regardless of the gender, *CO* and *p48-Kras*[G12D] showed a significant difference in their weight gain under HFD condition. After 6 weeks on HFD, *p48-Kras*[G12D] mice lost significant weight in contrast to their *CO* littermates **(Figure 4.1 A and B).**

To investigate the effect of HFD-induced obesity on the insulin sensitivity in these mice, glucose tolerance test (GTT) was performed in previous studies (Khasawneh, Schulz et al. 2009). It was shown that *CO* mice had an impaired insulin response and this was supported by the highly elevated fasting blood glucose levels (FBG), which were taken 9 hrs after fasting. Taken together *CO* mice became hyperglycemic in response to HFD, whereas *p48-Kras*[G12D] animals showed enhanced glucose tolerance probably due to the significant weight loss observed in these mice. **(Figure 4.1 A, B and C).**
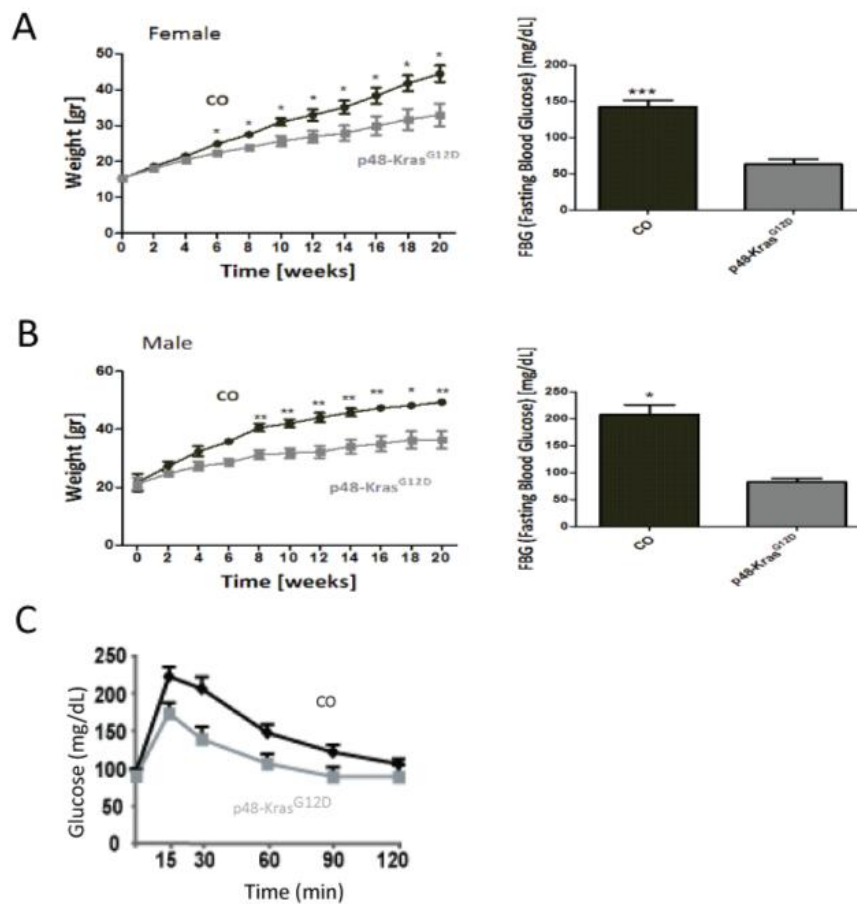
Figure 4.1: Weight curves and fasting blood glucose levels for *CO* and *p48-Kras*^{G12D} mice on HFD over a time period of 20 weeks. Weight curves of female *CO* (n=6) and *p48-Kras*^{G12D} (n=10) mice and their corresponding fasting blood glucose levels after 9 hrs fasting (A) and the according weight curves for male *CO* (n=4) and *p48-Kras*^{G12D} (n=5) mice and their fasting blood glucose levels (B). GTT results for female *CO* (n=5) and *p48-Kras*^{G12D} (n=5) mice after 20 weeks on HFD (C) (Khasawneh, Schulz et al. 2009). t-test: *p<0,05; ***p<0,001.

Despite impaired insulin resistance, obesity is known to induce low-grade inflammation. To see the effect of HFD on the inflammatory response blood count was checked for *CO* and *p48-Kras*^{G12D} animals. Although for the red blood cells, haemoglobin and hematocrit no significant differences were observed between *CO* and *p48-Kras*^{G12D} animals, the white blood cell counts in *p48-Kras*^{G12D} mice were significantly elevated suggesting increased inflammatory response in these animals **(Figure 4.2 A).** This was further supported by the RT-PCR results showing increased mRNA levels for pro-inflammatory cytokines IL-6, IL-1β and TNFα in *p48-Kras*^{G12D} mice compared to *CO* littermates **(Figure 4.2 B)** suggesting an increased inflammatory response in mutant animals.
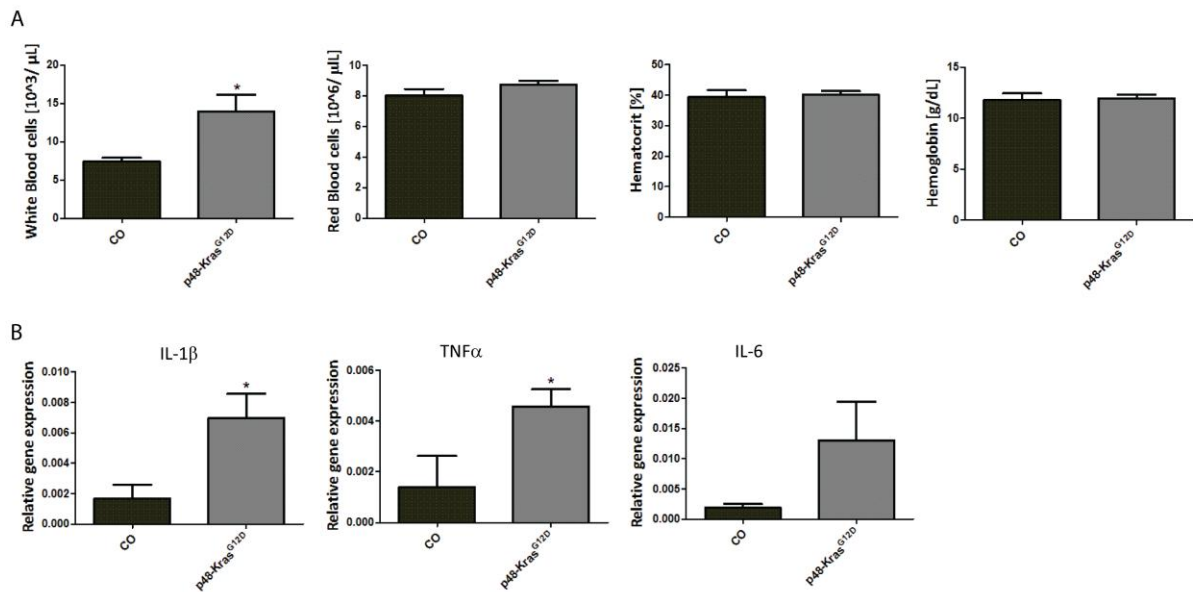
Figure 4.2: Blood count results for white blood cells, red blood cells, hematocrit and haemoglobin for *CO* (n=5) and *p48-Kras^{G12D}* mice (n=8) after 20 weeks on HFD (A). Taqman RT-PCR analysis of inflammatory genes in the pancreas from *CO* (n=5) and *p48-Kras^{G12D}* mice (n=8) (B). t-test: *p<0,05.

Further it is widely accepted that increased inflammation induced by HFD enhances tumor development. To investigate the influence of HFD on the pancreatic tumorigenesis histological analyses were performed. The whole pancreas from *p48-Kras^{G12D}* and *CO* mice were harvested right after sacrifice and embedded in paraffin blocks. H&E stained pancreas sections showed that all *p48-Kras^{G12D}* mice showed PanIN-1 lesions, 35% PanIN-2 lesions, whereas in only one pancreas PanIN-3 could be detected. The architectural tissue distortion in the pancreas of *p48-Kras^{G12D}* mice was between 95-100% and the tumor incidence in these animals was ~ 41**% (Figure 4.3 A and B)**. These results suggested increased tumor development in *p48-Kras^{G12D}* animals through HFD.

In accordance with increased tumor incidence, a higher proliferation rate especially in the pancreatic lesions was detected in *p48-Kras^{G12D}* mice compared to *CO*`s observed by immunohistochemistry (IHC) using an antibody against BrdU, a proliferation marker **(Figure 4.3 E-F)**. Further histological stainings demonstrated that *p48-Kras^{G12D}* mice showed more fibrotic areas in the pancreas as well as a higher production of acetic **(Figure 4.3 G-J)**. In accordance with the previous results, increased fibrosis and mucus secretion in *p48-Kras^{G12D}* animals was closely associated to enhanced cell proliferation and tumor incidence.
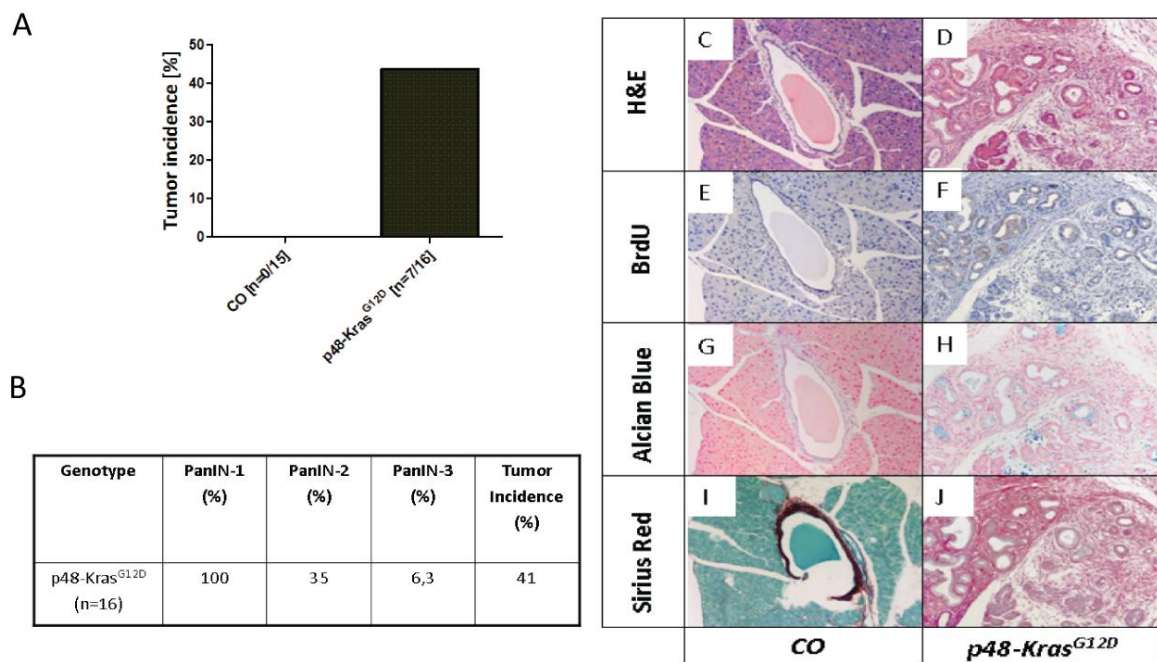
Figure 4.3: Percentage of PanIN lesions and tumor incidence in *p48-Kras*^{G12D} mice (A + B). H&E staining of *CO* (C) and *p48-Kras*^{G12D} (D) pancreata. Pancreas sections from *CO* and *p48-Kras*^{G12D} sections were stained with BrdU (E + F), Alcian Blue (G + H) and Sirius Red (I + J).

4.1.1 Obesity-induced metabolic changes in *p48-Kras*^{G12D} mice during pancreatic tumorigenesis

Metabolic shift that occurs during cancer development from OXPHOS to glycolysis indeed serves as basis for the FDG-PET analysis to detect tumor cells and metastasis in cancer patients. Although not all tumor types are detectable via this method however FDG-PET is the most useful imaging option in pancreatic cancer. Therefore the metabolic regulations and the changes that happen during pancreatic tumorgenesis under HFD conditions could provide a new tool for the early detection of precursor lesions.

Different approaches were used to investigate the metabolic alterations in *p48-Kras*^{G12D} mice and *CO* littermates. To get an idea about the aerobic glycolysis and mitochondrial OXPHOS in these mice, the Clark electrode was used to measure the respiratory capacity of isolated mitochondria from the pancreas of *p48-Kras*^{G12D} and *CO* animals **(Figure 4.4 A)**. It was shown that HFD significantly decreased the respiration capacity in *p48-Kras*^{G12D} mice compared to their control littermates and to *p48-Kras*^{G12D} group on ND **(Figure 4.4 A)**.

To test whether this decrease in RCR was associated with decreased mitochondria number and function we checked relative mitochondria copy numbers and citrate synthase activity, respectively. In accordance with diminished respiratory capacity in isolated mitochondria, we observed significant decrease in relative mitochondrial copy number in *p48-Kras*^{G12D} mice on HFD compared to *CO* littermates **(Figure 4.2 B).** Further we checked the citrate synthase activity, which is also a marker for mitochondrial viability and function that also showed a decrease in *p48-Kras*^{G12D} mice compared to *CO* animals **(Figure 4.4 C)**. In summary the data suggest that diminished dependency on oxidative phosphorylation in *p48-Kras*^{G12D} mice was based on a decreased mitochondria number and impaired mitochondrial function.
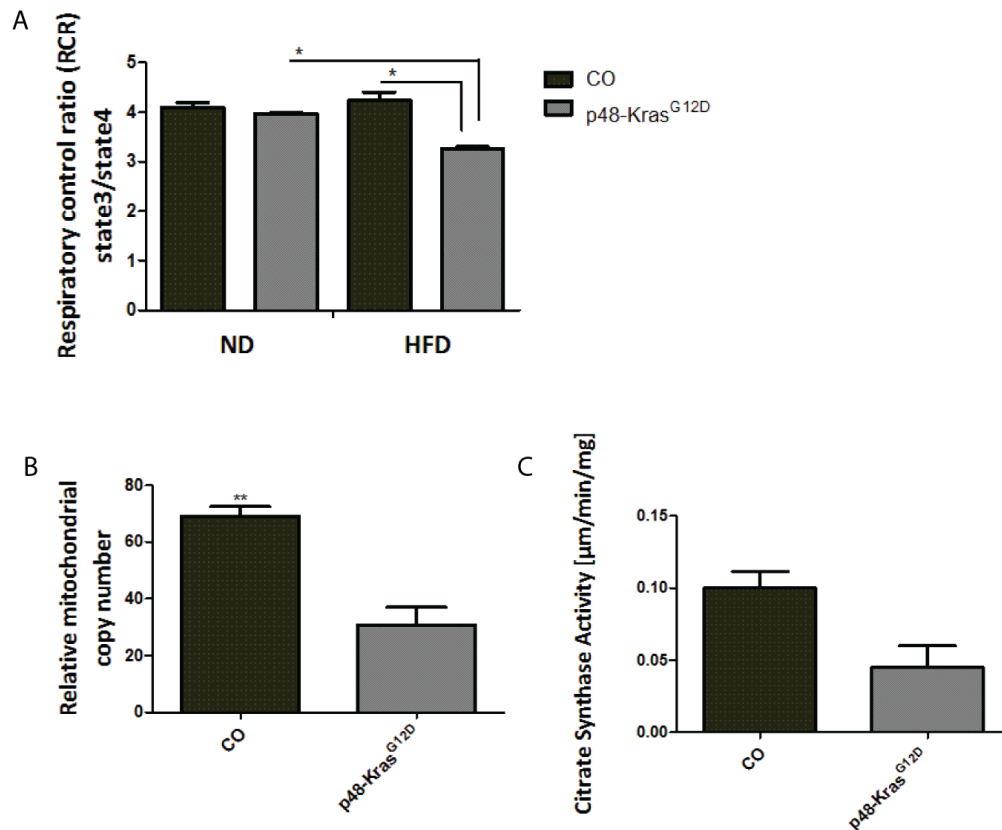
Figure 4.4: Following 20 weeks on normal diet (ND) and high fat diet (HFD) the pancreatic mitochondria of *CO* (n=3) and *p48-Kras^{G12D}* (n=2) mice were isolated and their respiratory control rates were measured via Clark electrode (A).The mitochondrial content of pancreata from *CO* (n=3) and *p48-Kras^{G12D}* (n=3) mice were investigated after 20 weeks on HFD (B). The viability of mitochondria was checked by citrate synthase activity in *CO* (n=3) and *p48-Kras^{G12D}* (n=3) mice after 20 weeks on HFD (C). t-test: *p<0,05; **p<0,01.

To check whether we could detect this decreased oxidative phosphorylation in *p48-Kras^{G12D}* mice at the protein and mRNA level as well we analyzed the different complexes of the respiratory chain using an antibody raised against one special subunit of each of the 5 different complexes of the respiratory chain **(Figure 4.5 A)**. Additionally four RT-PCR primer pairs were designed to see the gene expression profile for the subunits Ndufb9, Ndufb10 (complex I), SDHa (complex II) and Cox7a2 (complex IV) **(Figure 4.5 B)**.
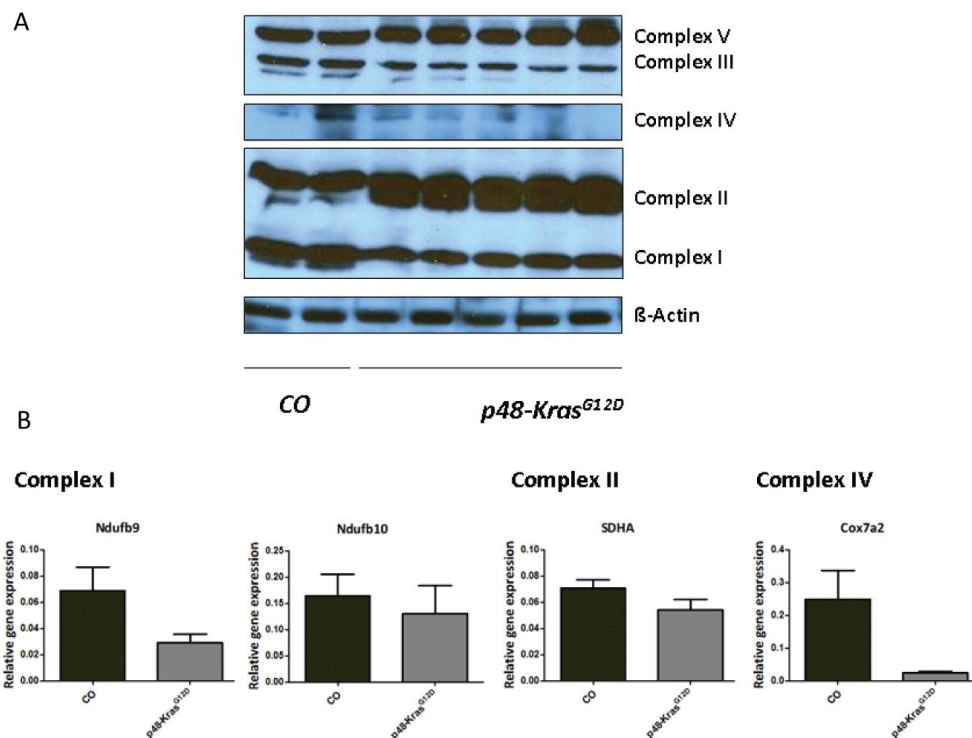
Figure 4.5: Western blot from *CO* and *p48-Kras^{G12D}* pancreata using an anti-OXPHOS antibody (A) and RT-PCR analysis for the subunits of complex I, II and IV (B). t-test: not significant (ns).

p48-Kras^{G12D} mice showed an upregulation in the subunit ATP5A of complex V compared to *CO* mice, whereas in complex III a clear decrease in subunit UQCRC2 was seen at the protein level. Also the subunit MTCO1 from complex IV was downregulated in *p48-Kras^{G12D}* mice and this tendency was as well reflected at the RT-PCR results for the subunit COX7A2. However complex II in *CO* mice showed less subunit SDHB, which was not in accordance with the RT-PCR results for the subunit SDHA. The subunit NDUFB8 from complex I was decreased in *p48-Kras^{G12D}* mice at the protein level and this tendency could also be seen for the subunits NDUFB9 and NDUFB10 as analyzed by RT-PCR.

Taken together we could not confirm the significantly reduced oxidative phosphorylation in *p48-Kras^{G12D}* mice at the protein and the mRNA level suggesting that the subunits, which were checked, may not be reflecting the complete subunits and the oxidative phosphorylation capacity in these animals. Else it is the enzymatic activity that is changed in these mice, which can not be detected at neither protein nor RNA level.
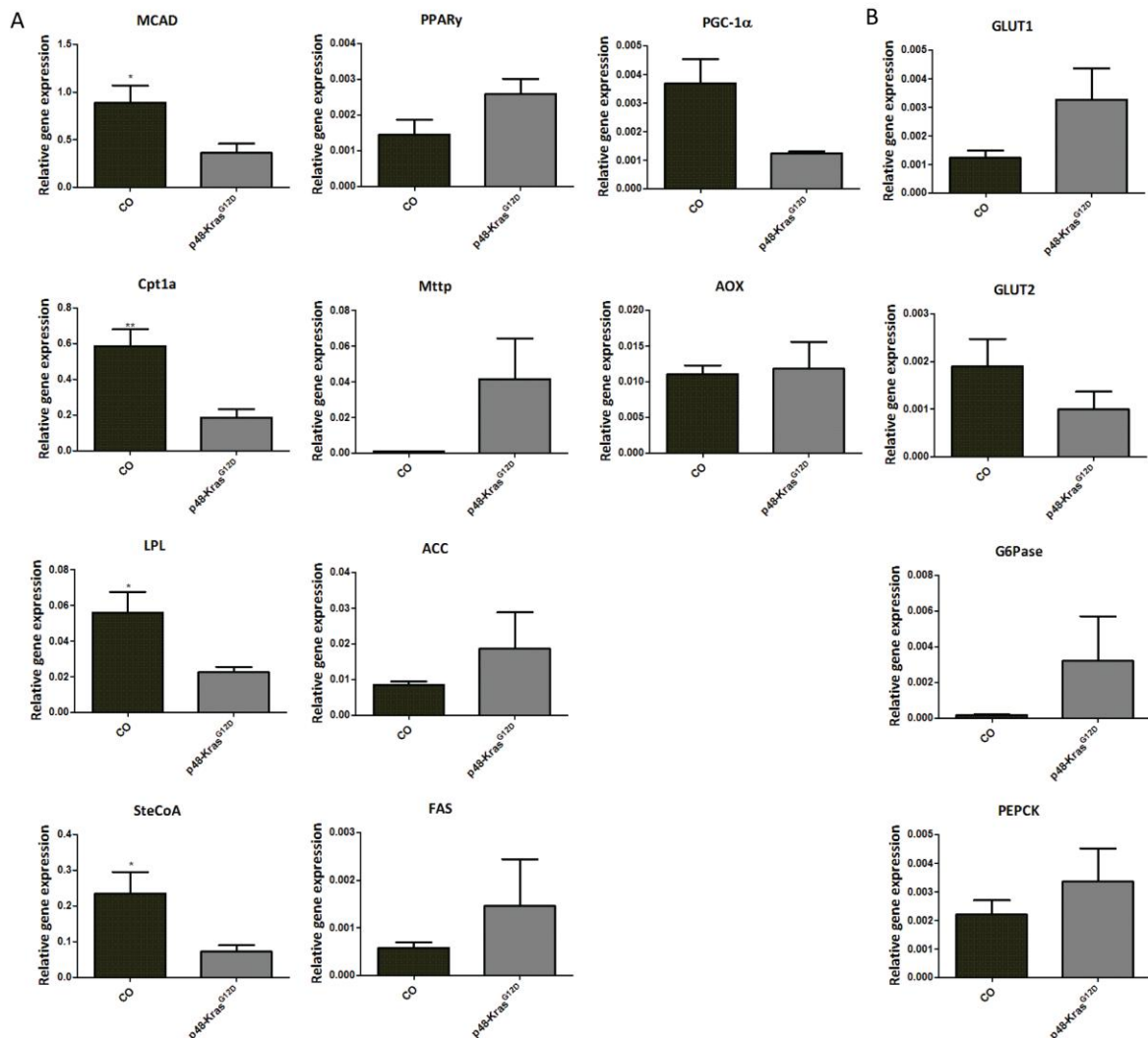
Figure 4.6: RT-PCR analysis from *CO* (n=5) and *p48-Kras*^G12D (n=8) pancreata for genes involved in fat (A) and glucose (B) metabolism. t-test: *p<0,05; **p<0,01.

To further investigate the expression of genes involved in glycolysis and fat metabolism, RT-PCR was performed **(Figure 4.6 A and B)**. Genes that were significantly downregulated in *p48-Kras*^G12D mice were medium chain acyl-CoA dehydrogenase (MCAD), which is essential for the fatty acid ß-oxidation as well as the carnitine palmitoyltransferase I (CPT1a), which is responsible for the transport of fatty acids into the mitochondrial matrix **(Figure 4.6 A)**, suggesting decreased fatty acid ß-oxidation in *p48-Kras*^G12D mice compared to *CO* littermates. Further, the lipoprotein lipase (LPL), which takes part in the lipogenesis, as well as the stearoyl CoA desaturase (SteCoA), an enzyme that is involved in the synthesis of unsaturated fatty acids were significantly decreased in *p48-Kras*^G12D mice **(Figure 4.6 A)** suggesting less triglycerides in the circulation of *p48-Kras*^G12D animals in

accordance with decreased weight gain in *p48-Kras*^{G12D} mice as well as decreased synthesis of unsaturated fatty acids. However no significant differences were seen for genes that are involved in glucose metabolism at mRNA level **(Figure 4.6 B)**.

4.2 Inhibition of Glycolysis in *p48-Kras*[G12D] mice by 2-Deoxyglucose-treatment

2-Deoxyglucose (2-DG), a glucose analogue, which enters the cell via the glucose transporters 1-5 (GLUT`s), is converted via hexokinase to 2-deoxyglucose-6-phosphate that inhibits the phosphoglucoisomerase. Glucose and 2-DG compete for the GLUT`s and the enzyme hexokinase already during the initial steps of the glycolysis. To verify whether inhibition of the majorly preferred metabolic pathway in tumor cells has any effect on insulin resistance and tumorgenesis, *CO* and *p48-Kras*[G12D] mice received weekly doses of 2-DG under HFD condition.

Around 12 weeks of 2-DG treatment, similar to untreated animals *p48-Kras*[G12D] mice lost significant weight compared to their *CO*`s **(Figure 4.7 A and B)**. However the weight loss started around 6 weeks later in 2-DG treated *p48-Kras*[G12D] mice then in untreated group **(Figure 4.7 C)** suggesting a protective effect of 2-DG in *p48-Kras*[G12D] mice.
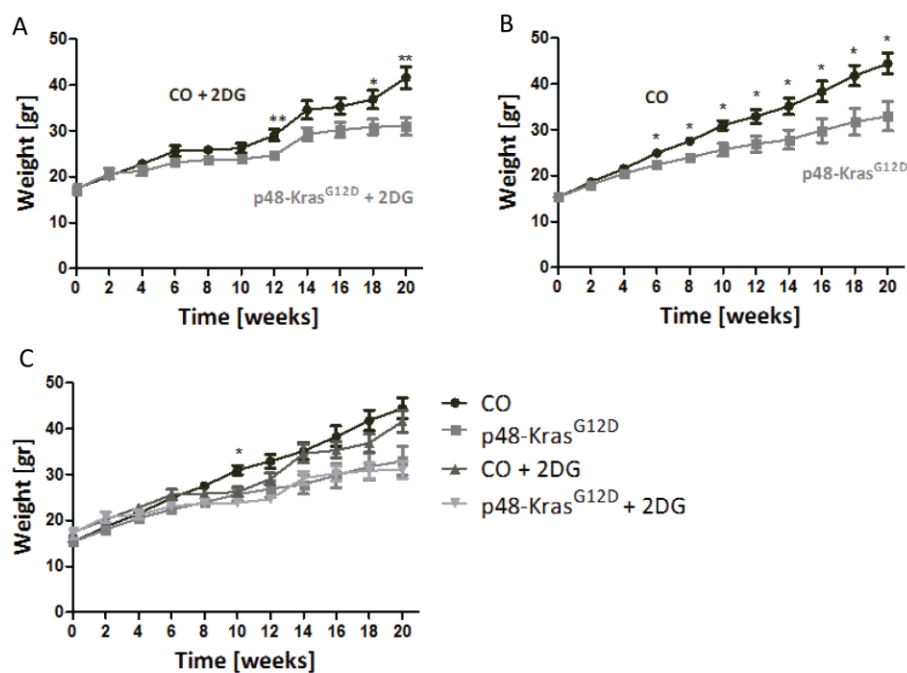
Figure 4.7: Weight curves recorded during 20 weeks 2-DG treatment in *CO* (n=5) and *p48-Kras*[G12D] mice (n=7) (A) and in untreated *CO* (n=6) and *p48-Kras*[G12D] (n=10) animals on HFD (B). 2-DG treated and untreated mice were compared to each other (C). t-test: *p<0,05; **p<0,01.

Based on the improved weight gain in 2-DG treated *p48-Kras*^{G12D} animals, we checked to see what effect this had on glucose tolerance. In order to investigate insulin sensitivity in 2-DG treated mice GTT was performed. Both *CO* and *K-ras*^{G12D} mice showed hyperglycemia but no difference in glucose clearance such as that described for untreated *p48-Kras*^{G12D} animals and *CO* littermates **(Figure 4.8 A).** The fasting blood glucose showed no difference in 2-DG treated mice although a significant increase in *p48-Kras*^{G12D} mice treated with 2-DG was observed compared to untreated *p48-Kras*^{G12D} group **(Figure 4.8 B)** suggesting impaired insulin sensitivity in both 2-DG treated animals.
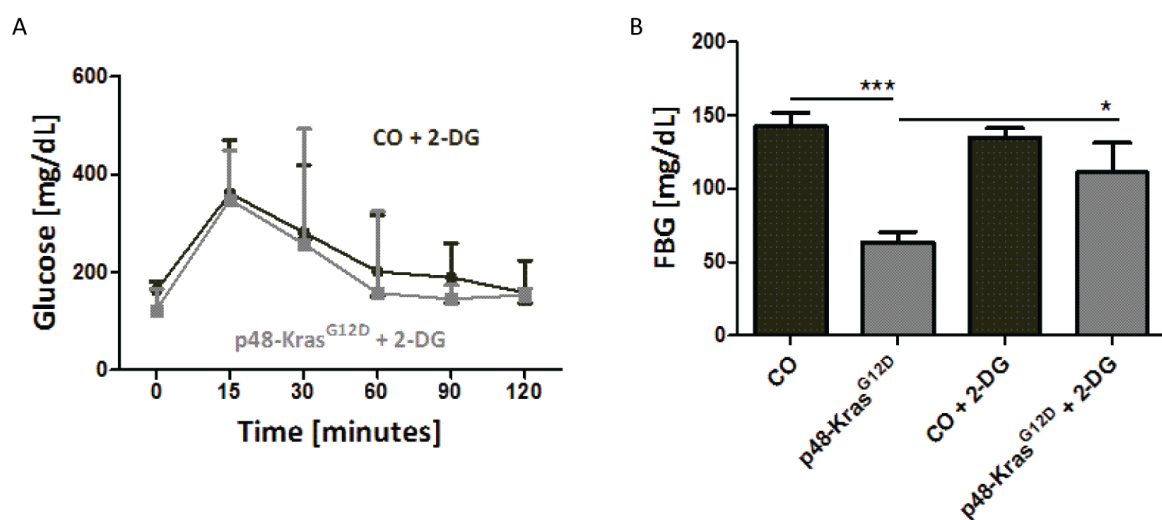
Figure 4.8: GTT results from 2-DG treated *CO* (n=5) and *p48-Kras*^{G12D} (n=7) animals (A). Fasting blood glucose levels after 20 weeks of HFD compared to untreated *CO* (n=5) and *p48-Kras*^{G12D} (n=7) mice (B). t-test: *p<0,05; ***p<0,001.

In order to check the effect of the 2-DG treatment on the tumor incidence histological analyses were performed. The whole pancreas from 2-DG treated *p48-Kras*^{G12D} and *CO* littermates were harvested right after sacrifice and embedded in paraffin blocks. H&E stained pancreas sections showed that all *p48-Kras*^{G12D} animals treated with 2-DG showed PanIN-1 lesions, 16,6% PanIN-2 lesions, whereas in only one pancreas PanIN-3 could be detected. The architectural tissue distortion in the pancreas was 82% and the tumor incidence in these animals was decreased down to ~ 17**% (Figure 4.9 A and B)**. Thus 2-DG treatment decreased the architectural disruption and most importantly the tumor incidence in *p48-Kras*^{G12D} animals compared to untreated *p48-Kras*^{G12D} mice.

Taken together the data suggest dependency on aerobic glycolysis during pancreatic tumorigenesis in untreated *p48-Kras*^{G12D} animals and thus reduced tumor development following 2-DG treatment due to inhibition of glycolysis.
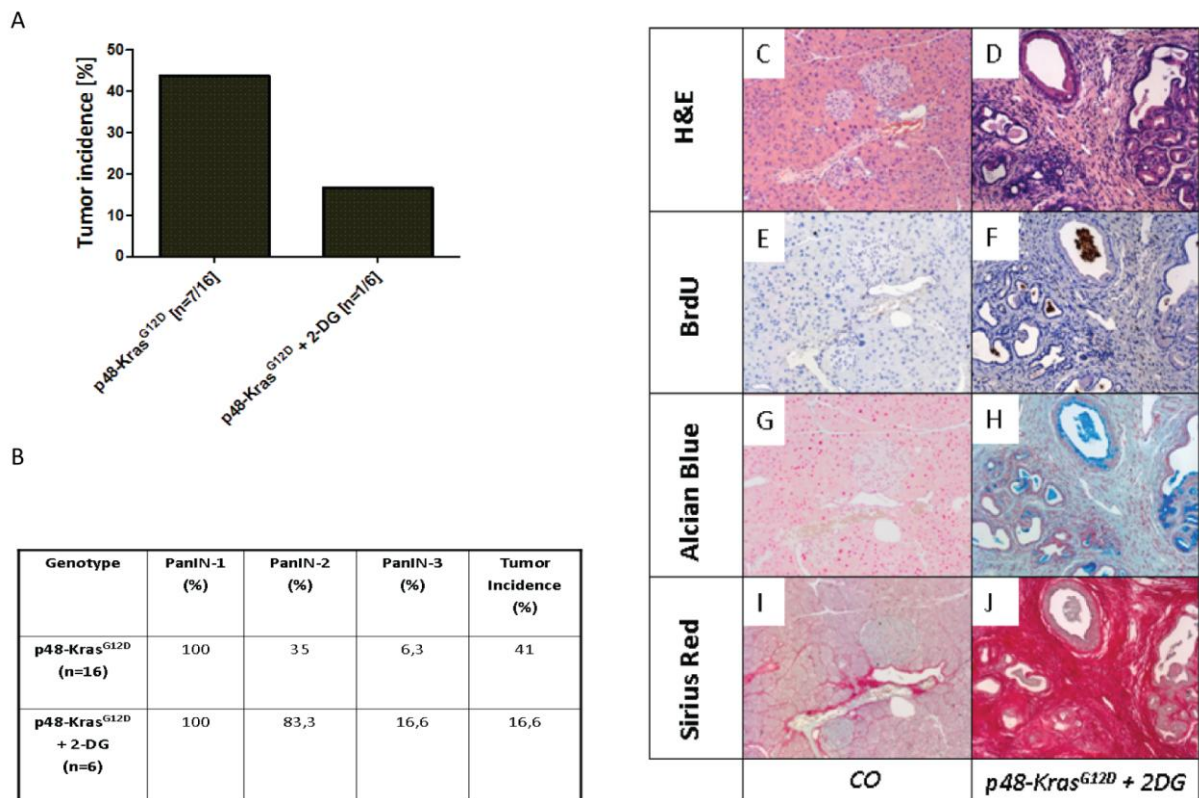
Figure 4.9: Tumor incidence and PanIN lesions in *p48-Kras*^{G12D} (n=17) mice and in 2-DG treated *p48-Kras*^{G12D} (n=6) animals after 20 weeks on HFD (A +B). H&E staining for *CO* (C) and *p48-Kras*^{G12D} (D) pancreas section from 2-DG treated animals and further stainings for BrdU (E + F), Alcian Blue (G + H) and Sirius Red (J + J).

To check the influence of 2-DG treatment on the oxidative phosphorylation the respiratory control rate was measured using the Clark electrode. As for the respiratory capacity in 2-DG treated animals, no significant difference was seen between CO´s and mutants. However when compared to untreated *p48-Kras*^{G12D} mice, 2-DG treated *p48-Kras*^{G12D} mice had a significant increase in RCR **(Figure 4.10 A)**. The mitochondria content as well the citrate synthase activity showed a significant increase in 2-DG treated *p48-Kras*^{G12D} mice compared to untreated *p48-Kras*^{G12D} animals, whereas no difference was seen between 2-DG treated *CO* and *p48-Kras*^{G12D} mice **(Figure 4.10 B and C)** suggesting

increased respiratory capacity due to 2-DG treatment and a switch from aerobic glycolysis to oxidative phosphorylation through administration of glucose analogue.
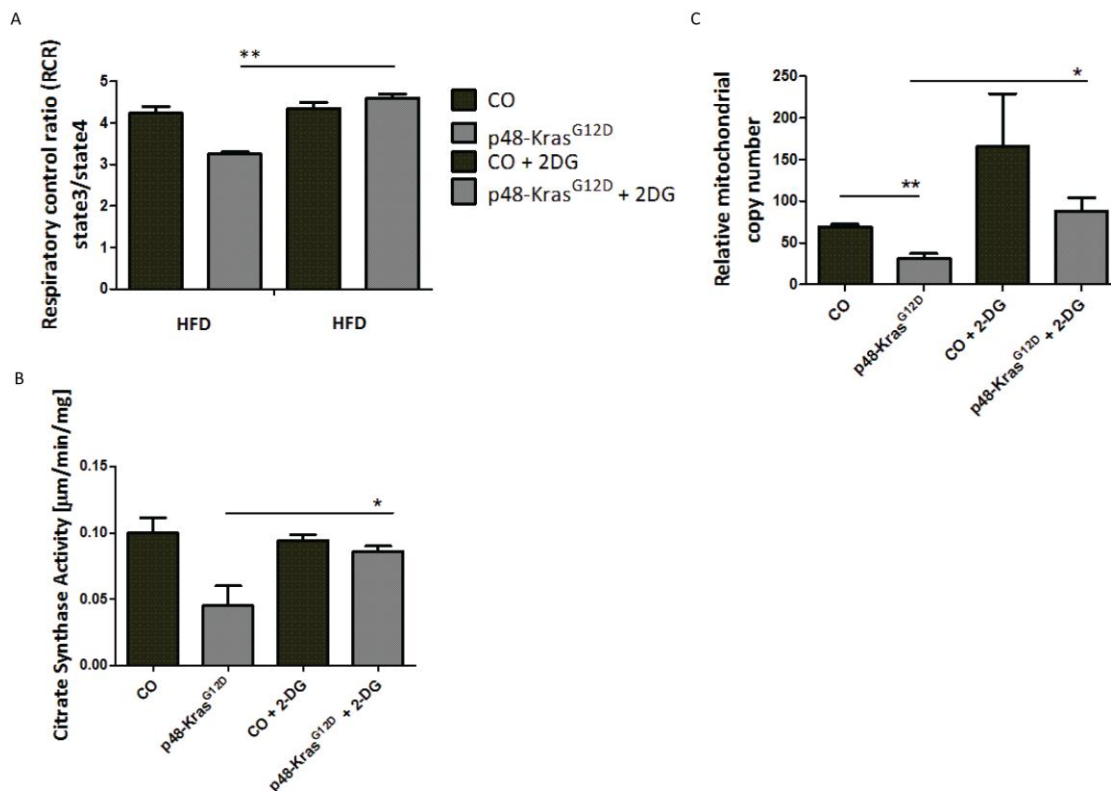
Figure 4.10: Following 20 weeks on high fat diet (HFD) the pancreatic mitochondria from 2-DG treated *CO* (n=2) and *p48-Kras^{G12D}* (n=2) mice as well as that of untreated *CO* (n=3) and *p48-Kras^{G12D}* (n=2) mice were isolated and the respiratory control rates were measured (A). The mitochondria content from 2-DG treated *CO* (n=3) and *p48-Kras^{G12D}* (n=3) mice as well as untreated *CO* (n=3) and *p48-Kras^{G12D}* (n=3) were investigated after 20 weeks on HFD (B). The citrate synthase activity was checked in 2-DG treated and untreated animals (n=3) (C). t-test: *p<0,05; **p<0,01.

In accordance with the RCR in 2-DG treated mice, the mitochondrial copy number and the citrate synthase activity were upregulated as well in *CO* and *p48-Kras^{G12D}* mice following 2-DG administration supporting the previous results for the RCR`s and suggesting increased dependency on oxidative phosphorylation in these animals.

4.3 Fenofibrate supplementation in *p48-Kras*^{G12D} mice under HFD condition

Fenofibrate is a fibric acid derivative, which is already used in humans to lower cholesterol and triglyceride levels in blood through activation of peroxisome proliferator-activated receptor alpha (PPARα) and increased lipoprotein lipase acitivity.

Previous work suggested an increase in PPAR`s at mRNA level in *p48-Kras*^{G12D} mice on HFD thus the aim of fenofibrate treatment was to even further increase PPARα activation and check whether this could enhance pancreatic tumorigenesis.

Following 20 weeks of weekly fenofibrate treatment under HFD condition, similar to untreated animals *CO* and *p48-Kras*^{G12D} mice showed no significant weight difference **(Figure 4.11 A,B and C).**
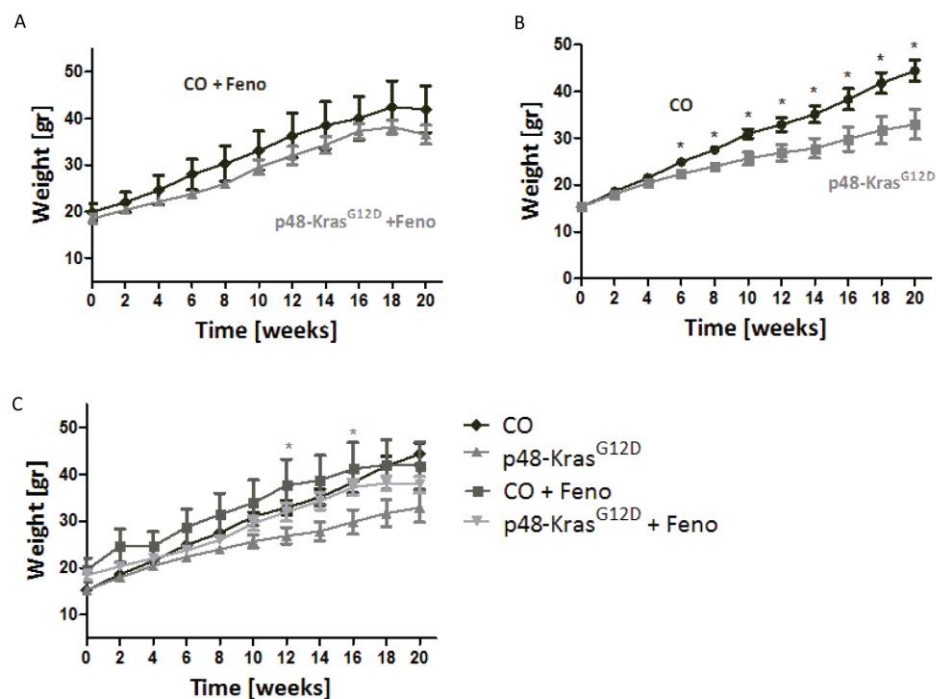
Figure 4.11: Weight curves for fenofibrate treated *CO* (n=3) and *p48-Kras*^{G12D} mice (n=6) (A) and untreated *CO* (n=6) and *p48-Kras*^{G12D} (n=10) animals (B). Fenofibrate treated and untreated animals were compared to each other and fenofibrate treated *p48-Kras*^{G12D} mice in comparison to untreated *p48-Kras*^{G12D} mice after 12 and 16 weeks showed significant weight gain (C). t-test: *p<0,05.

Considering the weight gain in fenofibrate-treated *p48-Kras*^{G12D} animals, we further checked the insulin sensitivity in mice, which underwent fenofibrate treatment. The glucose tolerance test showed that fenofibrate-treated mice had an improved insulin response independent of *Kras*^{G12D} activation **(Figure 4.12 A)**, which was confirmed by decreased fasting blood glucose levels **(Figure 4.12 B)**, suggesting expected enhancement in insulin sensitivity such as that described for humans following fenofibrate treatment.
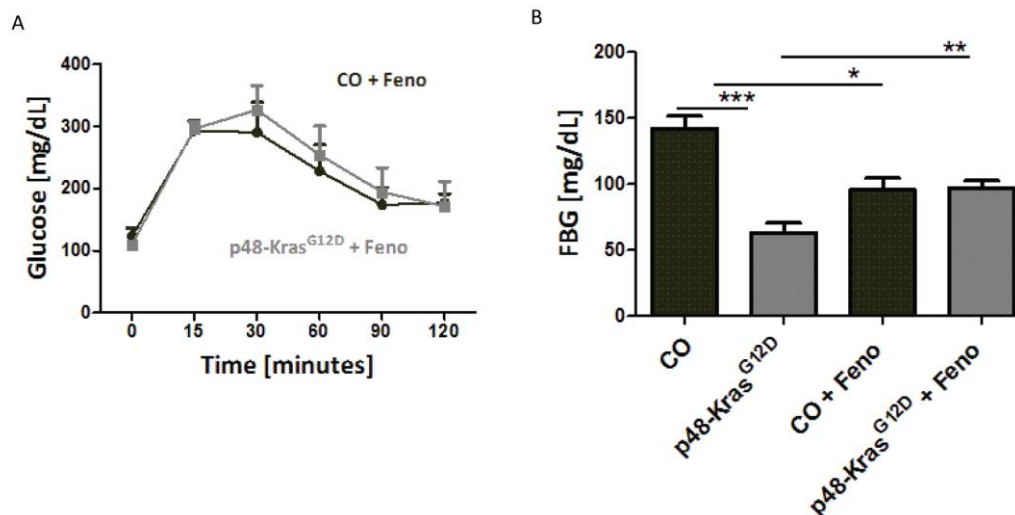
Figure 4.12: GTT results for fenofibrate-treated *CO* (n=3) and *p48-Kras*^{G12D} (n=5) animals (A). Fasting blood glucose levels compared to untreated *CO* (n=5) and *p48-Kras*^{G12D} (n=7) mice (B) after 20 weeks of HFD. t-test: *p<0,05; **p<0,01.

In order to clarify the effect of fenofibrate administration on pancreatic tumor development pathology in pancreata was evaluated. The tumor incidence in fenofibrate-treated mice was decreased to 29% as well as the architectural distortion was reduced to 74% **(Figure 4.13 A)**, suggesting decreased tumor incidence and tissue disruption compared to untreated *p48-Kras*^{G12D} animals. PanIN 1 lesions were found in all fenofibrate-treated *p48-Kras*^{G12D} animals. 86% of mice showed PanIN 2 however no PanIN 3 was observed. Considering the decreased architectural distortion in fenofibrate-treated animals compared to untreated mice **(Figure 4.13 A and B)**, an anti-tumorigenic effect of fenofibrate in pancreatic tumor development was clarified. Further Sirius red and Alcian blue stainings were performed **(Figure 4.13 C-J)** suggesting a reduction in fibrosis and mucus production in fenofibrate-treated mice in accordance with decreased tumorgenesis seen in these animals.
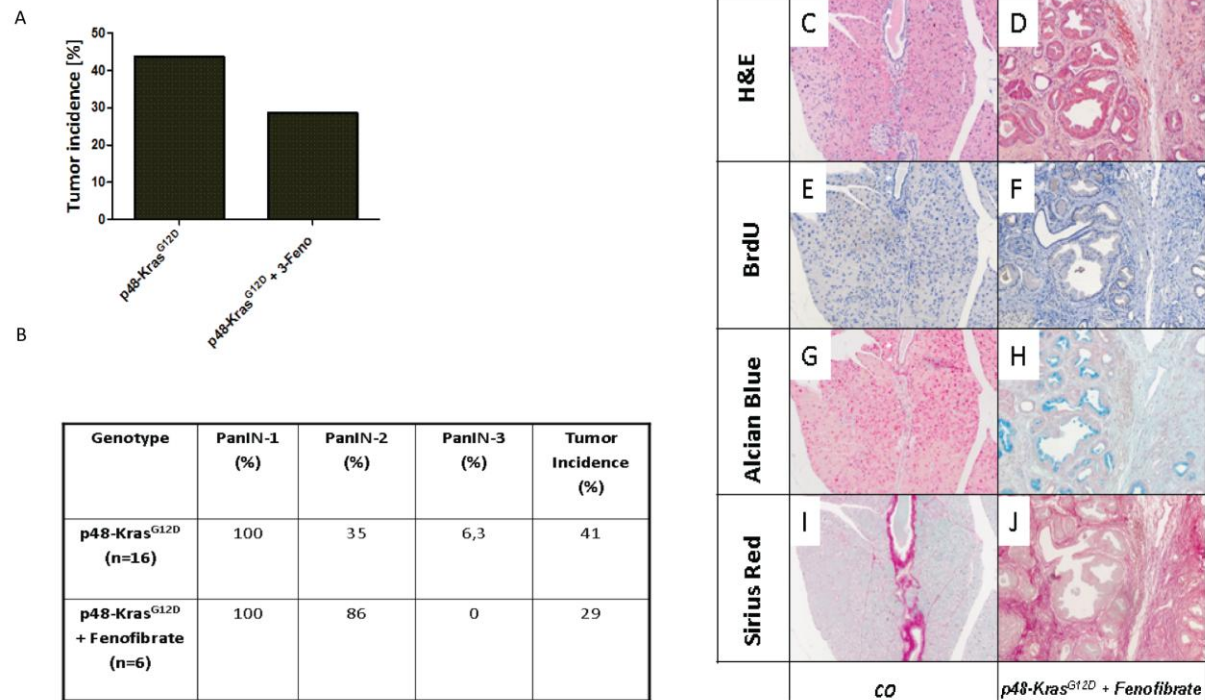
Figure 14.13: Tumor incidence and the frequency of PanIN lesions in *p48-Kras*[G12D] (n=17) mice and in fenofibrate-treated *p48-Kras*[G12D] (n=7) animals after 20 weeks on HFD (A + B). H&E (C +D), BrdU (E + F), Alcian Blue (G + H) and Sirius Red (I + J) staining of pancreas sections from fenofibrate-treated *CO* and *p48-Kras*[G12D] animals.

To further investigate the expression of genes involved in glycolysis and fat metabolism, RT-PCR was performed **(Figure 4.14)**. Expression of lipoprotein lipase (LPL) was significantly downregulated in fenofibrate-treated *p48-Kras*[G12D] mice compared to its *CO*s but no significant difference was exhibited compared to untreated *CO* and *p48-Kras*[G12D] animals **(Figure 4.14 A)**. SteCoA was significantly decreased in fenofibrate-treated mice although no significant difference in genes involved glucose metabolism was observed. Furthermore mRNA levels for inflammatory genes were checked and a significant decrease for TNFα was detected **(Figure 4.14 B)** suggesting a reduced lipogenesis and downregulated inflammatory response due to the decreased free fatty acids in the circulation following fenofibrate administration.
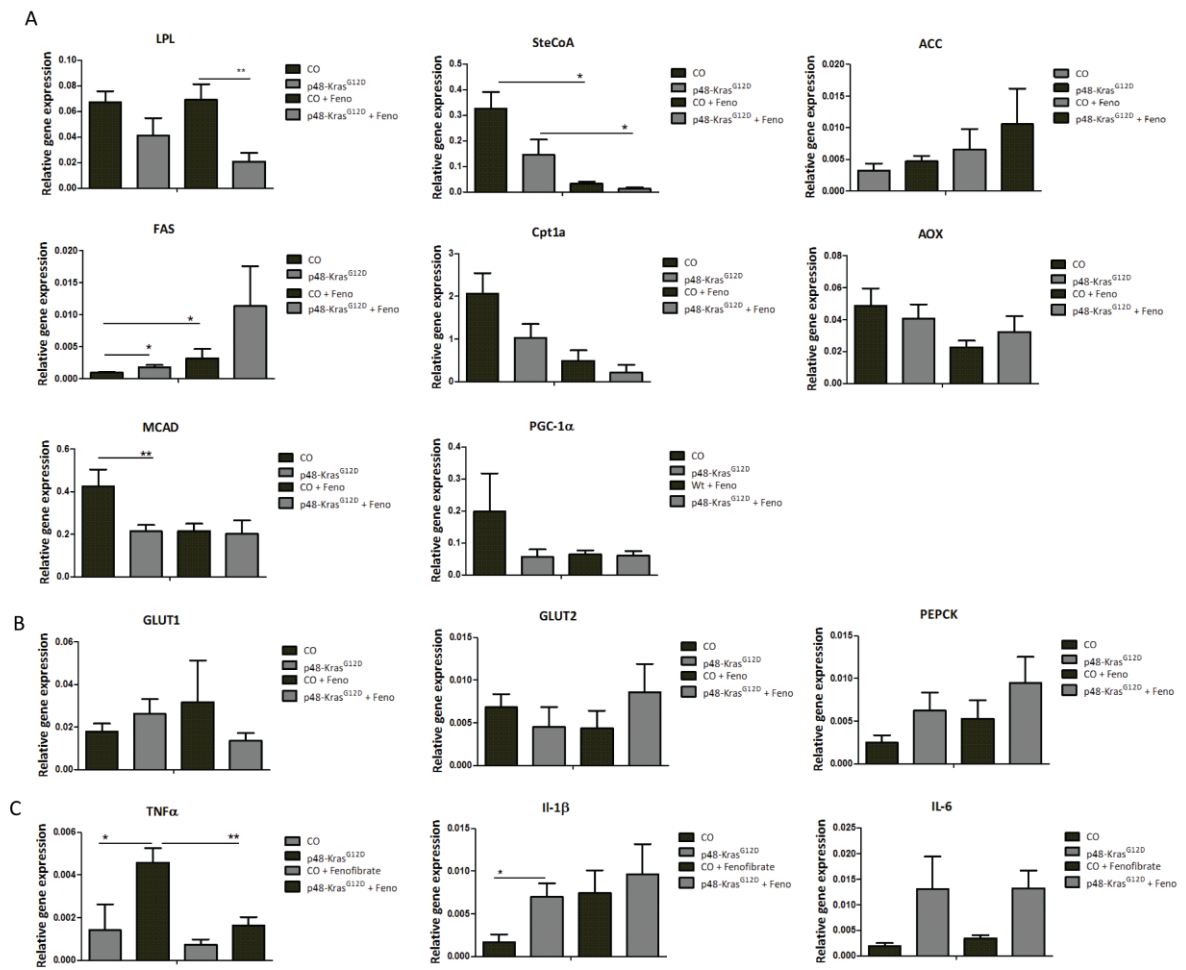
Figure 4.14: RT-PCR analysis of genes involved in fat (A) and glucose (B) metabolism and inflammatory response (C) in fenofibrate-treated *CO* (n=3) and *p48-Kras^{G12D}* (n=8) mice were compared to untreated *CO* (n=4) and *p48-Kras^{G12D}* (n=8) animals. t-test: *p<0,05; **p<0,01.

4.4 Inhibition of mitochondrial fatty acid ß-oxidation by Etomoxir treatment in *p48-KrasG12D* mice

Etomoxir is an inhibitor of the FA ß-oxidation and blocks the carnitine palmitoyltransferase 1A (Cpt1a), which is essential in transporting fatty acids into the mitochondrial matrix. The aim of the treatment was to see whether inhibition of FA ß-oxidation could shift metabolism towards glycolysis and if this could enhance tumorigenesis in *p48-Kras*^{G12D} mice on HFD.

When mice were treated with etomoxir no difference in weight gain was observed between *CO* and *p48-Kras*^{G12D} animals such as that seen in untreated mice under HFD conditions **(Figure 4.15 A, B and C)**.
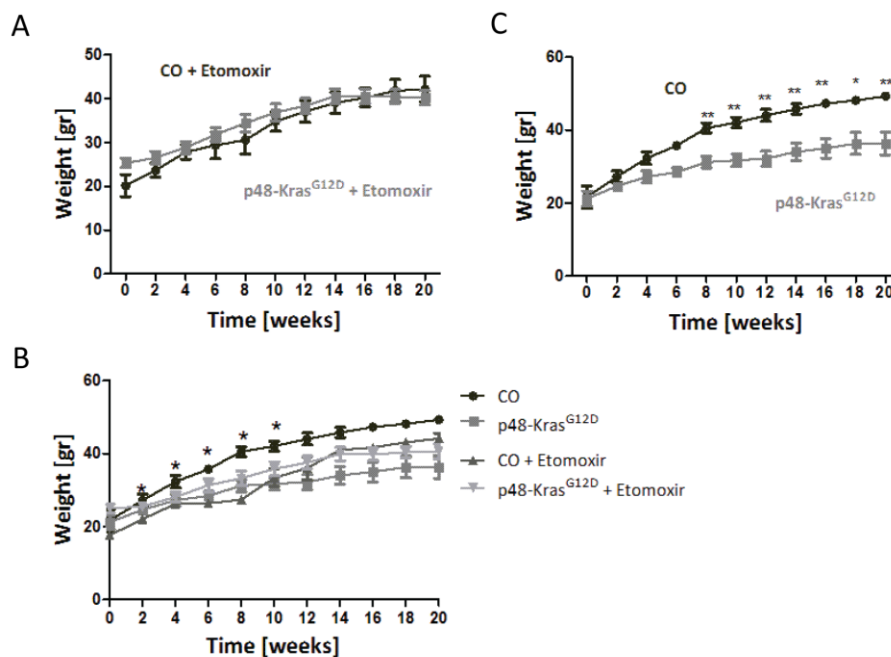
Figure 4.15: Weight curves from etomoxir-treated *CO* (n=3) and *p48-Kras*^{G12D} mice (n=7) (A) and untreated *CO* (n=6) and *p48-Kras*^{G12D} (n=10) animals (B). Etomoxir-treated and untreated animals were compared to each other and etomoxir-treated *CO* mice showed in comparison to untreated *CO* mice a significant weight loss after 2,4,6,8 and 10 weeks (C). t-test: *p<0,05; **p<0,01.

In order to check the influence of etomoxir on insulin sensitivity, glucose tolerance test was performed. Inhibitor treated *CO* and *p48-Kras*[G12D] mice exhibited hyperglycemia during the GTT, whereas the *p48-Kras*[G12D] mice still responded relatively better then *CO* animals in glucose clearance **(Figure 14.6 A)**. Etomoxir-treated *p48-Kras*[G12D] mice had a significant increased fasting blood glucose levels compared to untreated *p48-Kras*[G12D] mice **(Figure 14.6 B)** suggesting fatty acid ß-oxidation-associated weight loss and consequently improved insulin sensitivity was inhibited in *p48-Kras*[G12D] mice through etomoxir treatment.
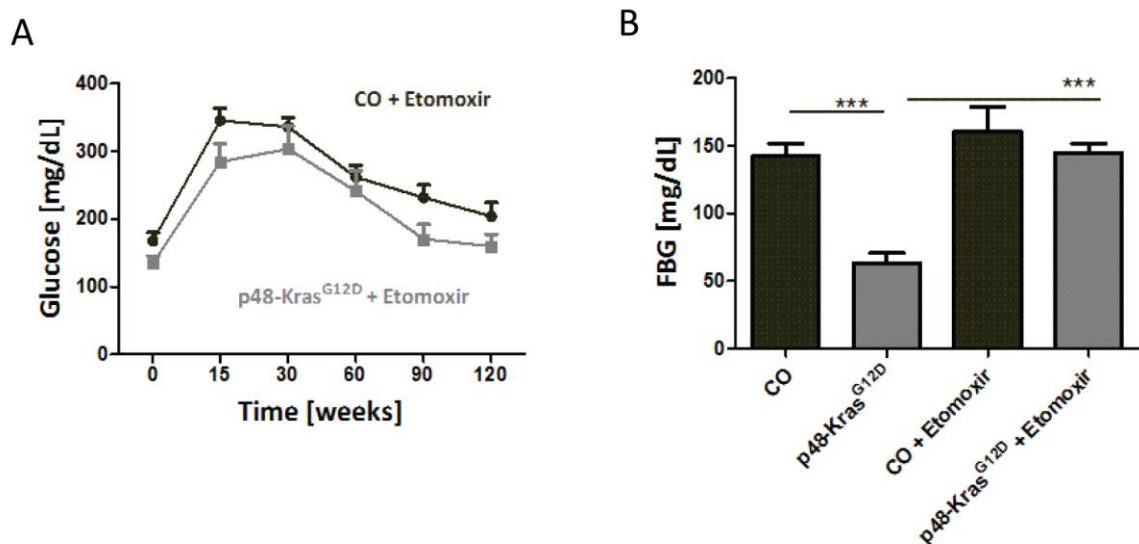
Figure 14.16: GTT results from etomoxir-treated *CO* (n=4) and *p48-Kras*[G12D] (n=8) animals (A) and their fasting blood glucose levels after 20 weeks of HFD compared to untreated *CO* (n=5) and *p48-Kras*[G12D] (n=7) mice (B). t-test: ***p<0,001.

In order to investigate the influence of etomoxir administration on the pancreatic tumorigenesis pathological evaluation was implemented. The tumor incidence in etomoxir-treated mice was 40% and the architectural distortion of the intact tissue was 91% **(Figure 4.17 A).** Similar to untreated *p48-Kras*[G12D] animals etomoxir-treated *p48-Kras*[G12D] mice showed nearly the same tumor incidence and tissue disruption. In 40% of the treated *p48-Kras*[G12D] animals PanIN 2 lesions were found but just one PanIN 3 was seen **(Figure 4.17 B)**. Further Sirius red and Alcian blue stainings were performed and compared to *CO* mice *p48-Kras*[G12D] animals that suggested similar levels of fibrosis and mucin secretion such as that seen in untreated *p48-Kras*[G12D] animals **(Figure 4.17 G-J)**.

These results imply that etomoxir treatment did not decrease the tumorigenesis in *p48-Kras^{G12D}* mice suggesting that pancreatic tumor cells preferred glycolysis more than mitochondrial FA ß-oxidation as the main bioenergetic pathway.

Genotype	PanIN-1 (%)	PanIN-2 (%)	PanIN-3 (%)	Tumor Incidence (%)
p48-Kras^{G12D} (n=16)	100	35	6,3	41
p48-Kras^{G12D} + Etomoxir (n=8)	100	40	12,5	40
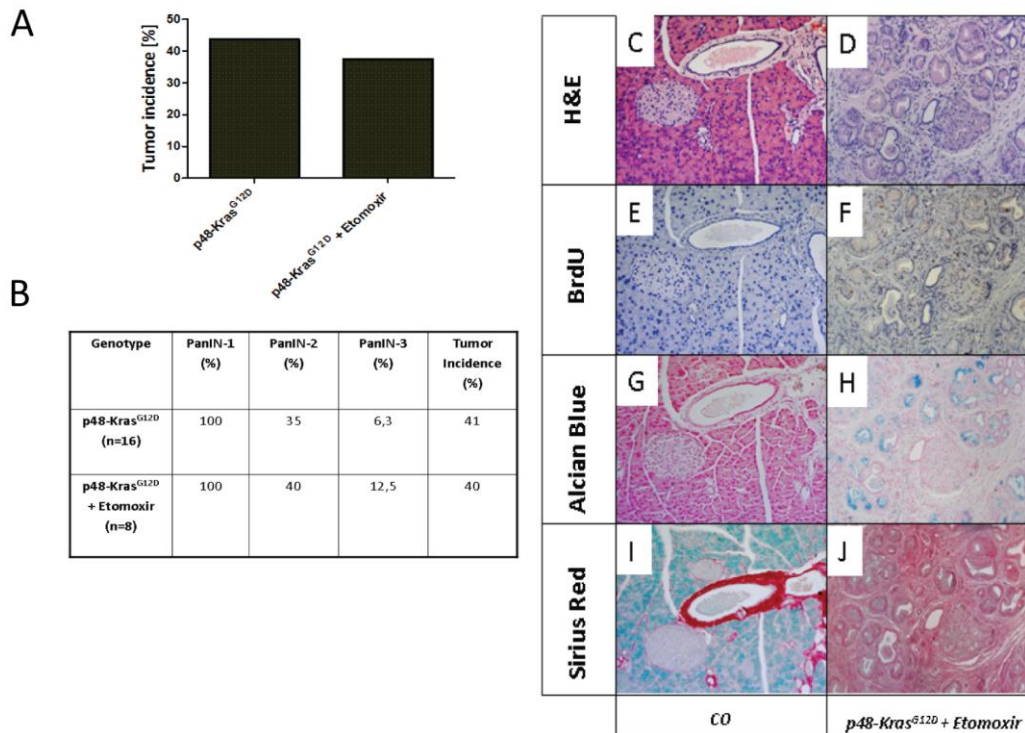
Figure 14.18: PanIN lesions and tumor incidence in *p48-Kras^{G12D}* (n=17) mice and in etomoxir-treated *p48-Kras^{G12D}* (n=8) animals after 20 weeks on HFD (A). H&E staining of *CO* (A) and *p48-Kras^{G12D}* (B) pancreas sections from etomoxir-treated animals. Stainings for BrdU (E + F), Alcian Blue (G + H) and Sirius Red (I + J).

To check whether any changes could be detected at the gene expression level, RT-PCR was performed. The inhibitor treatment showed an effect of the gene expression level of Cpt1a and MCAD, which were significantly downregulated compared to untreated animals **(Figure 14.18)**. The enzymes acetyl-CoA-carboxylase (ACC) and fatty acid synthase (FAS), which are essential in the fatty acid synthesis, were significantly reduced in etomoxir-treated *p48-Kras^{G12D}* animals compared to untreated *p48-Kras^{G12D}* animals **(Figure 14.18)**. Acetyl-CoA oxidase (AOX) was significantly downregulated compared to

etomoxir-treated *CO* and untreated *p48-Kras^{G12D}* animals. However the expression of lipoprotein lipase (LPL), which is involved in lipogenesis, was significantly upregulated in etomoxir-treated *p48-Kras^{G12D}* mice compared to untreated group **(Figure 14.19)**.

These results indicate decreased transport and catabolism of free fatty acids as well as reduced fatty acid synthesis in etomoxir-treated *p48-Kras*^{G12D} animals that lead to decreased levels of free fatty acids in the circulation thus increased insulin sensitivity seen in these mice.
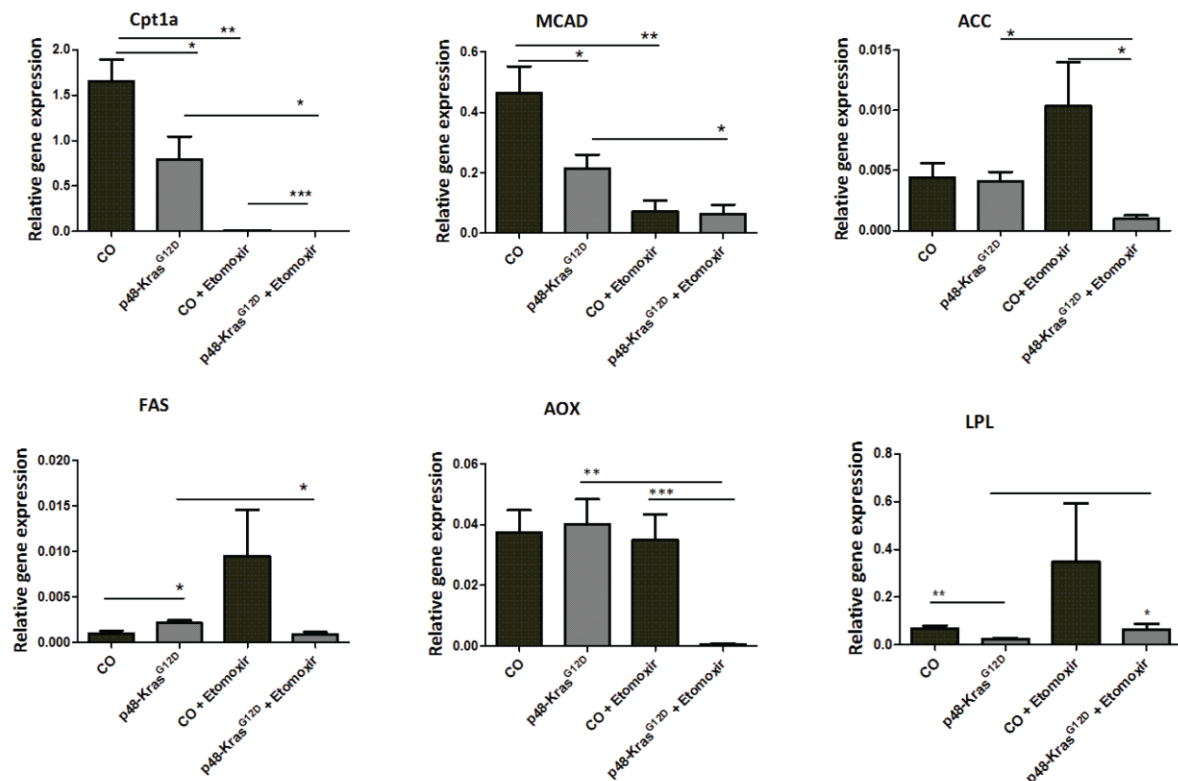
Figure 14.19: RT-PCR analysis of genes involved in fat metabolism in etomoxir-treated *CO* (n=3) and *p48-Kras*^{G12D} (n=4) mice as well as untreated *CO* (n=4) and *p48-Kras*^{G12D} (n=8) animals. t-test: *p<0,05; **p<0,01; ***p<0,001.

To asses the effect of Cpt1α inhibition via etomoxir on the respiratory capacity in treated animals, we measured oxygen consumption via Clark electrode. Considering the RCR of these animals, it was shown that the etomoxir-treated *p48-Kras*^{G12D} mice had a significantly lower respiratory capacity then untreated *p48-Kras*^{G12D} mice, which was in support of the mitochondrial content although no significant changes in citrate synthase activity were detected **(Figure 14.20 A, B and C)**. For the respiration capacity it was demonstrated that in etomoxir-treated *p48-Kras*^{G12D} mice the respiratory control ratio was significantly diminished compared to *p48-Kras*^{G12D} mice **(Figure 4.20 A)**. The

mitochondria content was increased however the citrate synthase activity was not significantly downregulated in etomoxir-treated *p48-Kras^{G12D}* mice **(Figure 4.20 B and C)**. Taken together these results imply a significant downregulation of oxidative phosphorylation through inhibition of Cpt1a via etomoxir and probably shift towards the glycolytic pathway, which is in accordance with increased tumor incidence in these animals.
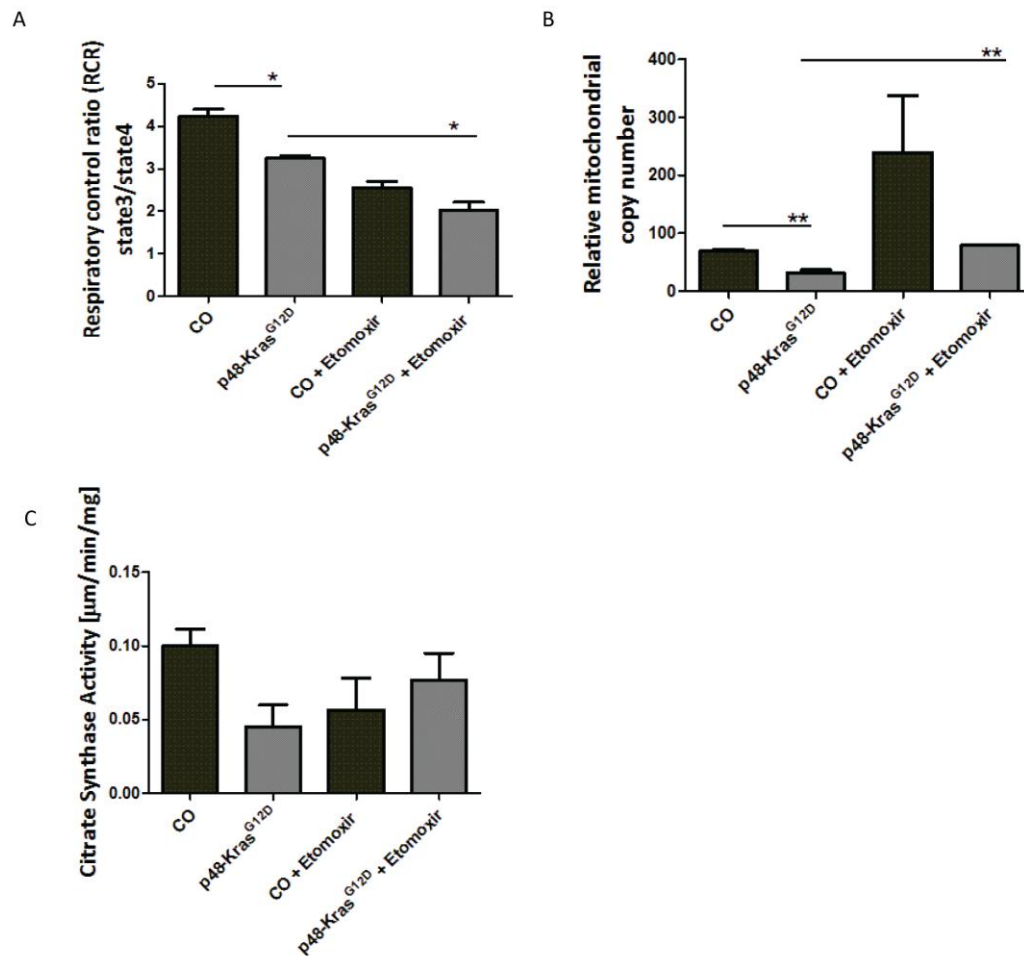
Figure 14.20: Follwing 20 weeks on HFD the pancreatic mitochondria from etomoxir-treated *CO* (n=2) and *p48-Kras^{G12D}* (n=3) mice as well as untreated *CO* (n=3) and *p48-Kras^{G12D}* (n=2) animals were isolated and the respiratory control rates were measured (A). The mitochondrial content from etomoxir-treated *CO* (n=3) and *p48-Kras^{G12D}* (n=3) mice as well as untreated *CO* (n=3) and *p48-Kras^{G12D}* (n=3) groups were investigated after 20 weeks on HFD (B). The citrate synthase activity was measured for etomoxir-treated and untreated animals (n=3) (C). t-test: *p<0,05; **p<0,01.

4.5   3-Bromopyruvate treatment does not change tumor incidence in *p48-Kras*^{G12D} mice

3-Bromopyruvate (3-BP), which is a pyruvate/lactate analogue, blocks glycolysis due to inhibition of hexokinase II. Further it seems to affect mitochondrial respiration however the underlying mechanisms are still poorly understood. It is proposed that the enzyme succinate dehydrogenase (SDH) is one of its target genes and so far it was demonstrated that it is a promising anti-cancer drug in mouse models of liver cancer.

Following 20 weeks of 3-BP treatment under HFD condition, *CO* and *p48-Kras*^{G12D} female mice showed no significant weight difference compared to each other and in comparison to untreated *CO* and *p48-Kras*^{G12D} animals **(Figure 4.21 A and B)**. Although the weight curves for the male *p48-Kras*^{G12D} mice showed no difference in between however a significant change was observed when compared to untreated *p48-Kras*^{G12D} males **(Figure 4.21 C and D)**. These results suggested a gender difference in 3-BP-treated male animals, which was clearly observed in male *p48-Kras*^{G12D} mice.
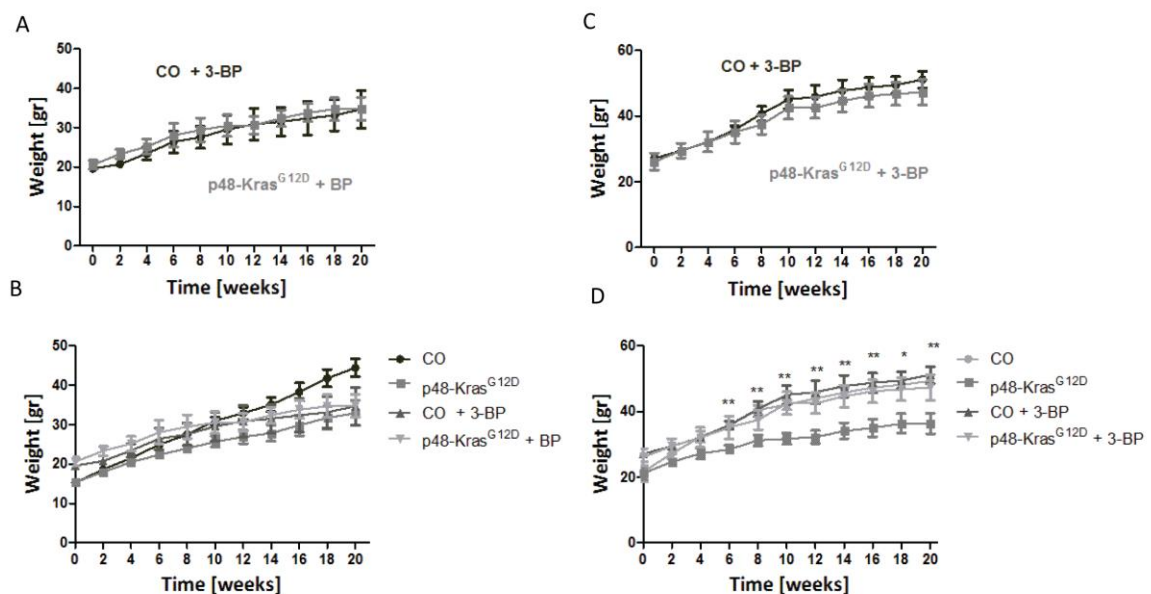
Figure 4.21: The weight curves for female mice treated with 3-BP [*CO* (n=4) and *p48-Kras*^{G12D} mice (n=5)] (A) and compared to untreated female *CO* (n=6) and *p48-Kras*^{G12D} animals (n=10) (B). The weight curves for male *CO* (n=5) and *p48-Kras*^{G12D} mice (n=5) showed no difference compared to each other (C). However 3-BP-treated male *p48-Kras*^{G12D} animals compared to untreated male *p48-Kras*^{G12D} mice had a significant weight gain at 6, 8, 10, 12, 14, 16, 18 and 20 weeks (D). t-test: *p<0,05; **p<0,01.

To analyze the outcome of 3-BP treatment on the insulin sensitivity GTT was performed. 3-BP-treated mice exhibited an impaired glucose tolerance during the GTT, whereas the *p48-Kras*[G12D] mice continued to show increased clearance of blood glucose **(Figure 4.21 A)**. Indeed, the fasting glucose levels were significantly increased in 3-BP-treated *p48-Kras*[G12D] mice compared to untreated *p48-Kras*[G12D] animals **(Figure 4.21 B)** suggesting inhibition of hexokinase II and enhanced accumulation of glucose although this was not associated to increased insulin sensitivity seen in these animals.
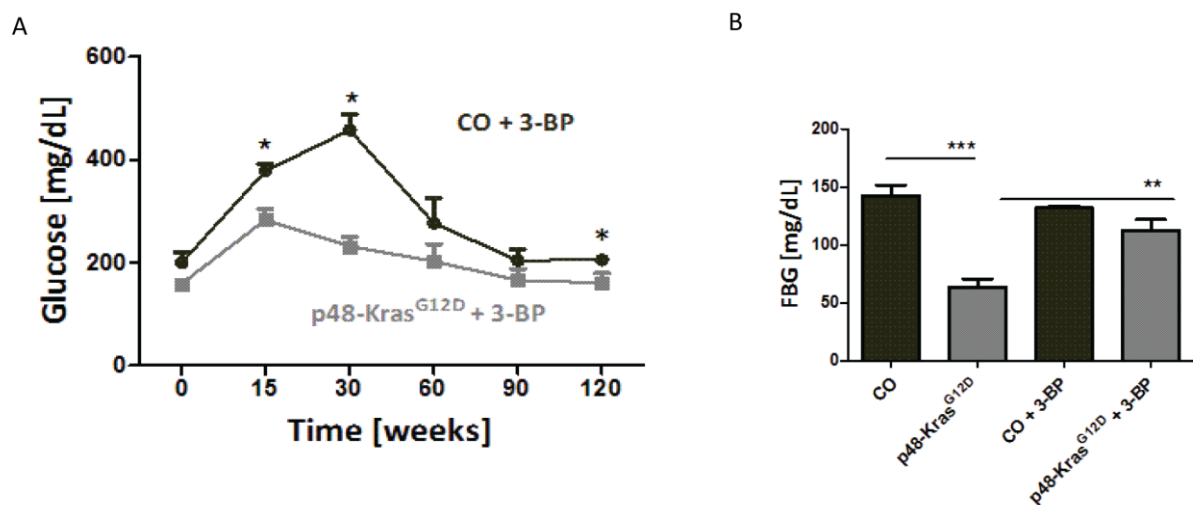
Figure 4.21: GTT results from 3-BP-treated male *CO* (n=3) and *p48-Kras*[G12D] (n=6) animals (A) and their fasting blood glucose levels after 20 weeks of HFD compared to untreated *CO* (n=5) and *p48-Kras*[G12D] (n=7) animals(B). t-test: *p<0,05; **p<0,01; ***p<0,001.

As 3-BP is proposed as a promising anti-tumor drug, we were highly interested in its effects in *p48-Kras*[G12D] mice that show enhanced pancreatic tumorigenesis under HFD conditions. The tumor incidence in 3-BP-treated mice was 40% and the architectural distortion of the intact tissue was 100% **(Figure 4.22 A).** Compared to untreated *p48-Kras*[G12D] animals, 3-BP-treated *p48-Kras*[G12D] mice showed nearly the same tumor incidence and tissue disruption. Similar to untreated group in 40% of the treated *p48-Kras*[G12D] animals PanIN 2 lesions were found. Further Sirius red and Alcian blue stainings were performed and compared to *p48-Kras*[G12D] animals **(Figure 4.22 B)**. However nearly the same levels of fibrosis and mucus production were seen in 3-BP-treated *p48-Kras*[G12D] mice compared to untreated *p48-Kras*[G12D] animals. These results suggested no anti-tumorigenic effect for 3-BP during pancreatic tumor development.
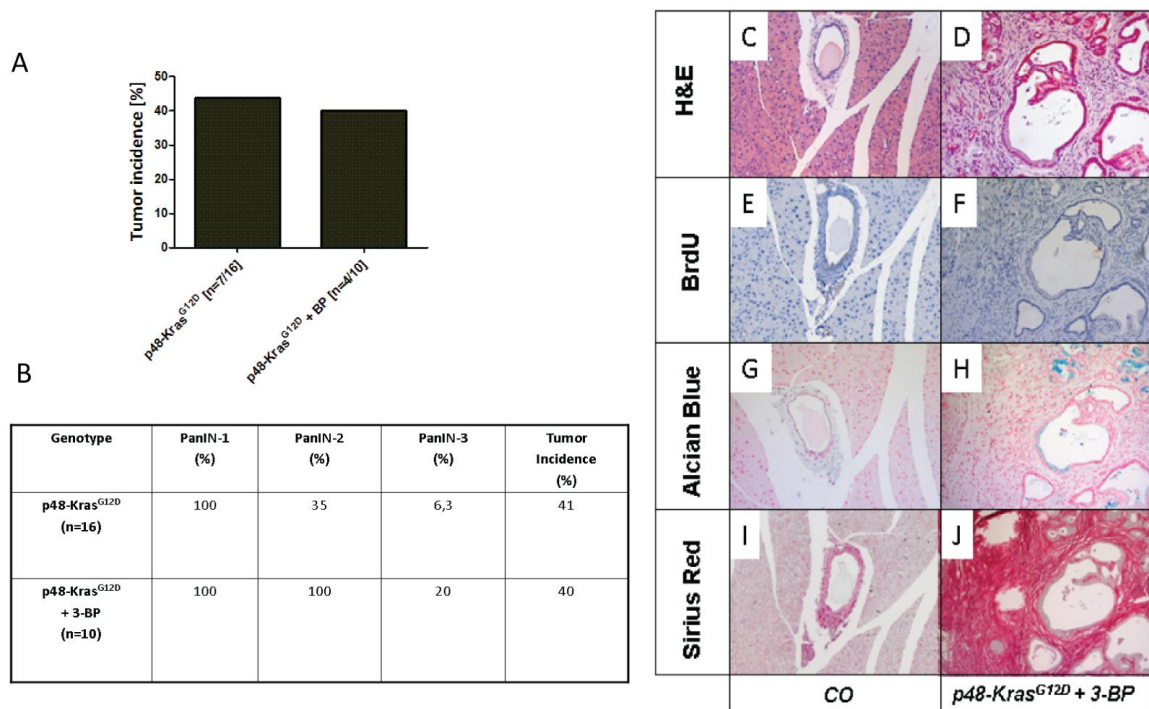
Figure 4.22: PanIN lesions and tumor incidence in untreated *p48-Kras*^{G12D} (n=17) mice and in 3-BP-treated *p48-Kras*^{G12D} (n=8) animals after 20 weeks on HFD (A and B). H&E staining for pancreas sections from 3-BP-treated *CO* (C) and *p48-Kras*^{G12D} (D) animals. Further stainings for BrdU (E + F), Alcian Blue (G + H) and Sirius Red (I + J).

To address the influence of the 3-BP treatment on mitochondrial oxidative phosphorylation, measurements using Clark electrode was performed. 3-BP treatment led to a significant decrease in oxidative phosphorylation in *p48-Kras*^{G12D} animals compared to *CO* and untreated *p48-Kras*^{G12D} mice **(Figure 4.23 A)**. Further the relative mitochondrial copy number was significantly downregulated in *p48-Kras*^{G12D} animals compared to untreated *p48-Kras*^{G12D} mice, whereas the citrate synthase activity was not significantly changed **(Figure 4.23 B and C)** thereby suggesting diminished oxidative phosphorylation and decreased mitochondrial content in *p48-Kras*^{G12D} animals due to 3-BP treatment probably through inhibition of the SDH.
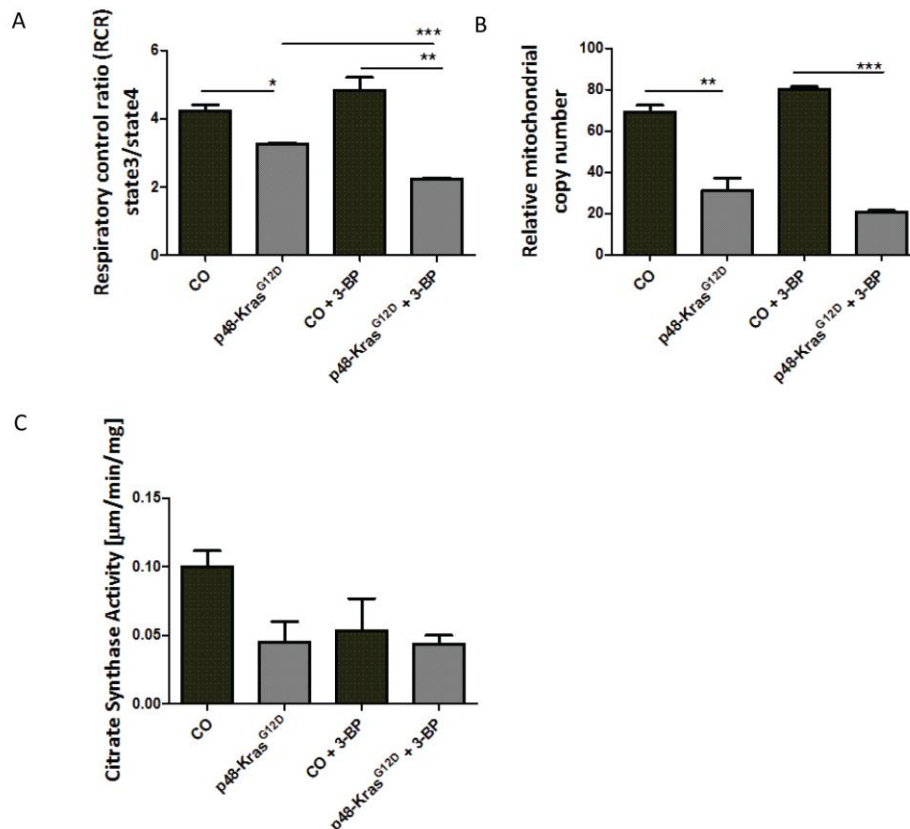
Figure 4.23: Following 20 weeks on HFD the pancreatic mitochondria from 3-BP-treated *CO* (n=3) and *p48-Kras*^{G12D} (n=3) mice as well as that of untreated *CO* (n=3) and *p48-Kras*^{G12D} (n=2) mice animals were isolated and their respiratory control rates were measured (A). The mitochondrial content from 3BP-treated *CO* (n=3) and *p48-Kras*^{G12D} (n=3) mice as well as that of untreated *CO* (n=3) and *p48-Kras*^{G12D} (n=3) animals was investigated after 20 weeks on HFD (B). The citrate synthase activity was shown for 3-BP-treated and untreated animals (n=3) (C). t-test: *p<0,05; **p<0,01; ***p<0,001.

4.6 Effect of pancreas-specific SIRT1-deletion during HFD-enhanced tumorigenesis in *p48-Kras*^{G12D} mice

Sirtuin 1 (SIRT1), a multifaceted NAD$^+$-dependent deacetylase, is activated by caloric restriction and modulates gene expression according to the energy status of the cell. This enzyme is an important regulator of metabolic processes including fatty acid ß-oxidation, gluconeogenesis, mitochondrial activity and senescence. It is overexpressed in several tumour types thus it is important to investigate its function during pancreatic tumorigenesis.

SIRT1-deficent animals had no difference in weight gain when compared to each other. However in comparison to *p48-Kras*^{G12D} mice, *SIRT1*$^{fl/fl}$*-p48-Kras*^{G12D} mice showed a significant difference at 14, 16 and 18 weeks on HFD **(Figure 4.24 A)**. Indeed the weight

gain seemed also to be in accordance with an impaired glucose tolerance since $SIRT1^{fl/fl}$-$p48$-$Kras^{G12D}$ mice exhibited a significantly elevated fasting blood glucose levels when compared to $p48$-$Kras^{G12D}$ animals **(Figure 4.24 B)**. Taken together these results indicated insulin resistance in SIRT1-deficient mice through increased weight gain observed in these animals.
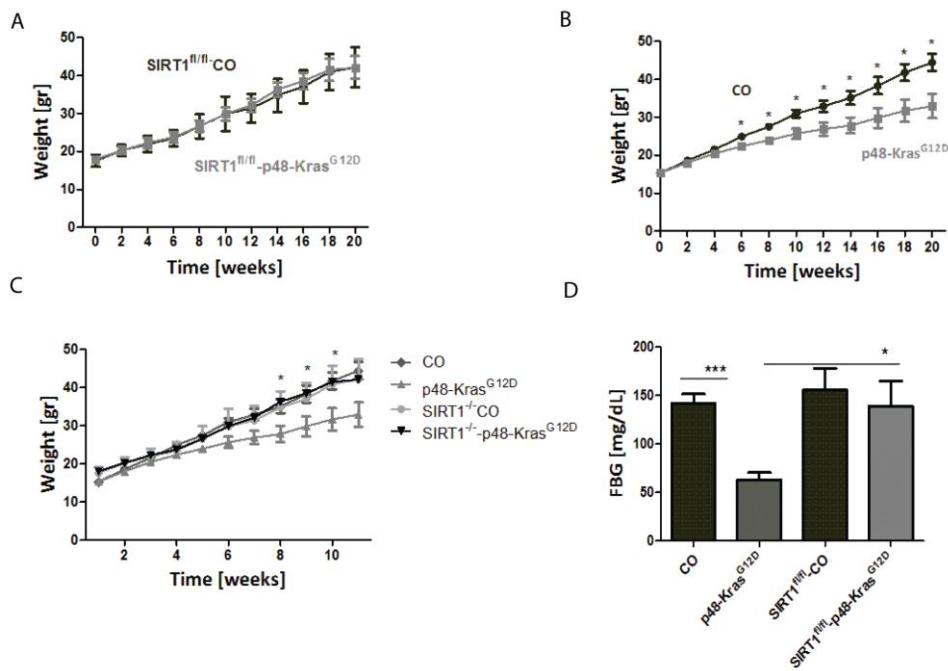
Figure 4.24: Weight curves from $SIRT1^{fl/fl}$-CO (n=4) and $SIRT1^{fl/fl}$-$p48$-$Kras^{G12D}$ mice (n=6) (A) and CO (n=6) and $p48$-$Kras^{G12D}$ mice (n=10) (B). $SIRT1^{fl/fl}$-$p48$-$Kras^{G12D}$ mice showed significant weight gain compared to $p48$-$Kras^{G12D}$ animals at 14, 16 and 18 weeks (C). Fasting blood glucose levels indicated that $SIRT1^{fl/fl}$ mice were hyperglycemic (D). t-test: *p<0,05; ***p<0,001.

To address the effect of pancreas-specific SIRT1-deficency during pancreatic tumorigenesis, we evaluated H&E stained pancreata. The pathological evaluation demonstrated that the pancreas from $SIRT1^{fl/fl}$-$p48$-$Kras^{G12D}$ mice had PanIN 1 and 2 lesions, whereas no PanIN 3 was detected. The tumor incidence was 43% and the architectural distortion was 95% that was similar to that seen in $p48$-$Kras^{G12D}$ animals **(Figure 4.25)** suggesting no rescue due to SIRT1-deficency was seen during PDAC development.
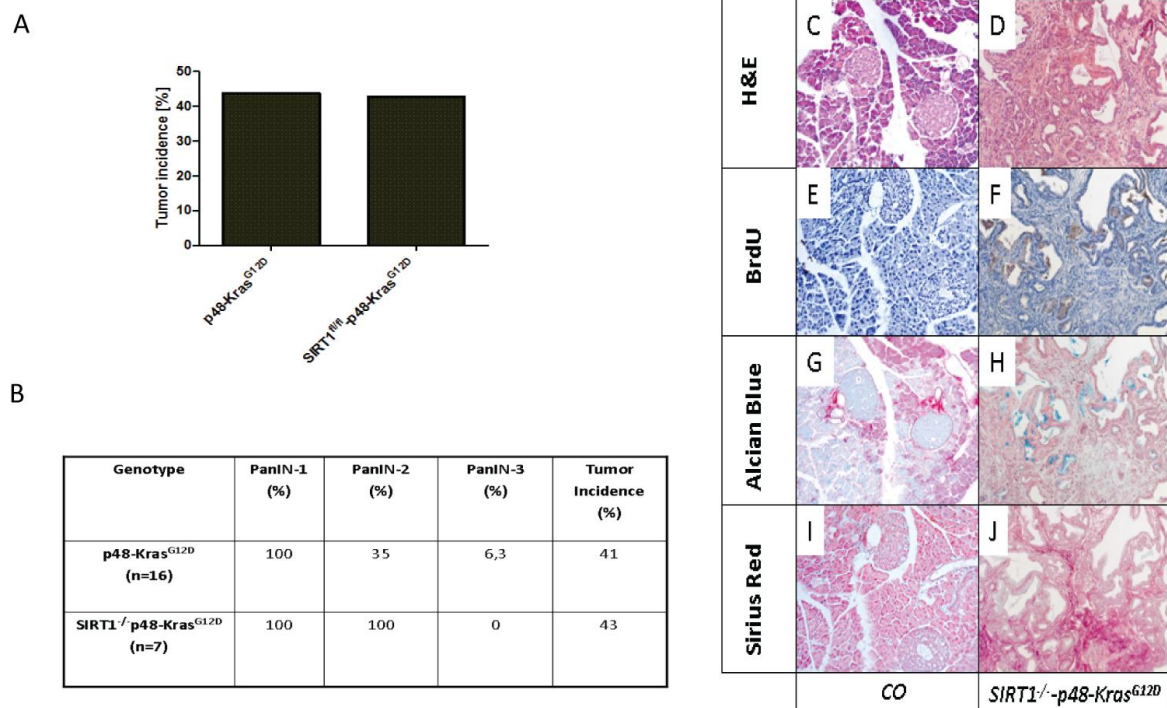
Figure 4.25: PanIN lesions and tumor incidence in *p48-Kras^{G12D}* (n=17) mice and in *SIRT1$^{fl/fl}$-p48-Kras^{G12D}* (n=7) animals after 20 weeks on HFD (A). H&E staining, BrdU (C + D), Alcian Blue (E + F) and Sirius Red (G + H) from *SIRT1$^{fl/fl}$-CO* (A) and *SIRT1$^{fl/fl}$-p48-Kras^{G12D}* pancreata.

Although no difference was observed in SIRT1-deficent animals during tumorigenesis as compared to *p48-Kras^{G12D}* mice, we wanted to investigate whether the SIRT1-deficent mice showed a difference in the respiratory capacity. The respiration ratio was checked in 12 months old *SIRT1$^{fl/fl}$* under normal diet (ND) conditions using Clark electrode. *SIRT1$^{fl/fl}$-p48-Kras^{G12D}* mice had a higher respiratory capacity then the *SIRT1$^{fl/fl}$-CO* mice **(Figure 4.26 A)** whereas *SIRT1$^{fl/fl}$-CO* animals showed a decreased RCR in comparison to *CO* mice. Indeed the SIRT1 deficiency had reversed the phenotype in *CO* and *p48-Kras^{G12D}* mice. Importantly the oxidative phosphorylation was diminished in SIRT1 deficient animals independent of whether mice were kept on ND or HFD that was further confirmed through the relative mitochondrial content **(Figure 4.24 26)**. However the citrate synthase activity was increased in *SIRT1$^{fl/fl}$-p48-Kras^{G12D}* mice **(Figure 4.26 C)**. These results suggested an influence of SIRT1-deficency on decreased mitochondrial content as well as a compensatory upregulation of the citrate synthase activity in *p48-Kras^{G12D}* animals.
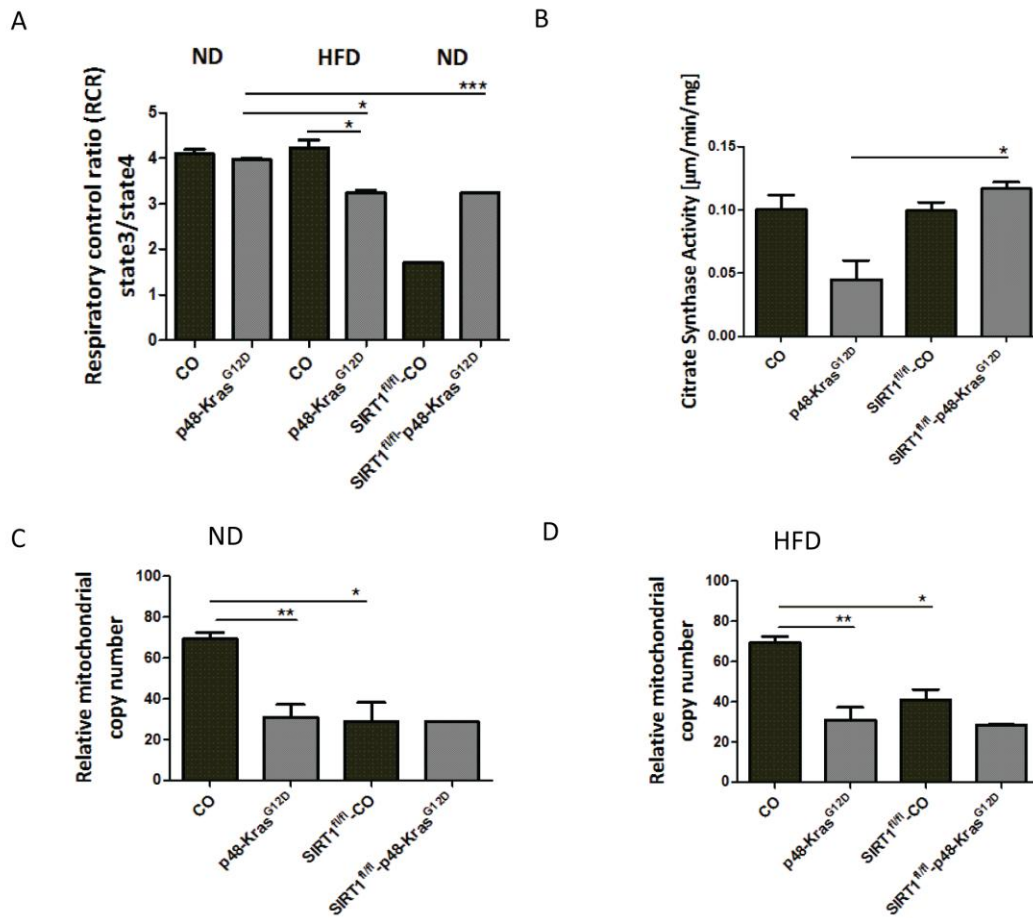
Figure 4.26: Following 12 months on ND the pancreatic mitochondria from $SIRT1^{fl/fl}$-CO (n=1) and $SIRT1^{fl/fl}$-$p48$-$Kras^{G12D}$ (n=2) animals as well as the pancreatic mitochondria from CO (n=3) and $p48$-$Kras^{G12D}$ (n=2) mice, which had been 20 weeks either on ND or HFD were isolated and the respiratory control rates were measured (A). The citrate synthase activity for $SIRT1^{fl/fl}$-CO (n=3), $SIRT1^{fl/fl}$-$p48$-$Kras^{G12D}$ (n=3), CO (n=3) and $p48$-$Kras^{G12D}$ (n=3) mice fed for 20 weeks with HFD (B). The mitochondrial content from $SIRT1^{fl/fl}$-CO (n=3) and $SIRT1^{fl/fl}$-$p48$-$Kras^{G12D}$ (n=3) mice, kept for 12 months on ND (C) as well as from $SIRT1^{fl/fl}$ -mice kept for 20 weeks on HFD (D) were compared to CO (n=3) and $p48$-$Kras^{G12D}$ (n=3) animals, which received HFD for 20 weeks. t-test: *p<0,05; **p<0,01.

In order to get more insight into the effects of SIRT1-deficency on the different complexes of the electron transfer chain, we performed WB and RT-PCR analysis. No difference in complex V was detectable between $p48$-$Kras^{G12D}$ mice and $SIRT1^{fl/fl}$-$p48$-$Kras^{G12D}$ mice at the protein level. However for the complexes IV, III, and I, a downregulation in $SIRT1^{fl/fl}$-$p48$-$Kras^{G12D}$ mice was demonstrated. Further the results at the protein level were confirmed through RT-PCR suggesting a significant decrease in $SIRT1^{fl/fl}$-$p48$-$Kras^{G12D}$ mice for the subunits of complex IV and I. However the upregulation in complex II in $SIRT1^{fl/fl}$-$p48$-$Kras^{G12D}$ mice compared to $p48$-$Kras^{G12D}$ animals could not be confirmed with the RT-

PCR results. These results implicated no effect on the subunits of the respiratory chain in SIRT1-deficient mice compared to *CO* and *p48-Kras^{G12D}* animals **(Figure 4.27 A + B)**.
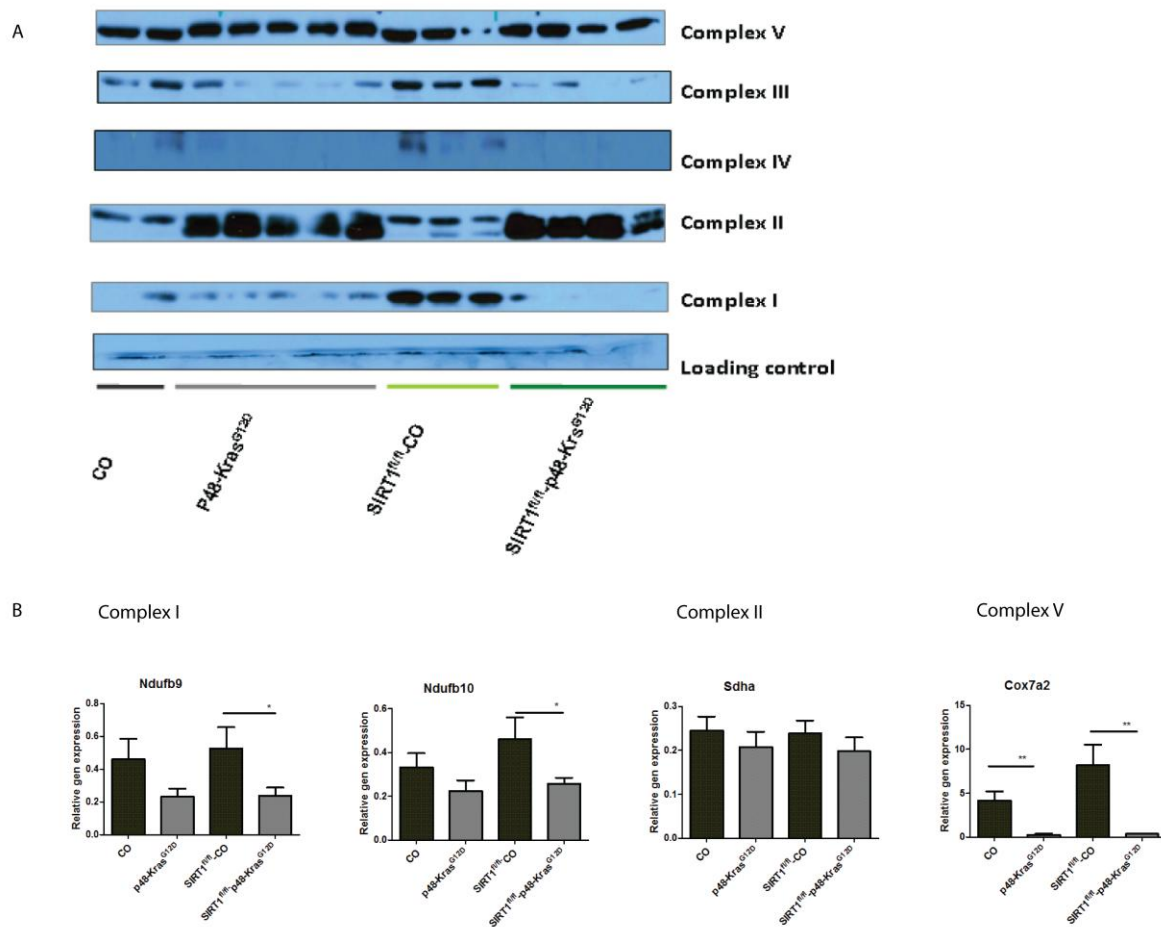
Figure 4.27: Western blot from *CO*, *p48-Kras^{G12D}*, *SIRT1$^{fl/fl}$-CO* and *SIRT1$^{fl/fl}$-p48-Kras^{G12D}* pancreata using the anti-OXPHOS antibody (A) and RT-PCR analysis of Ndufb9, Ndufb10, Sdha and Cox7a2, the subunits of complex I, II and IV, respectively (B). t-test: *p<0,05; **p<0,01.

Further we wanted to investigate the expression of genes involved in glycolysis and fat metabolism in SIRT1-deficient mice compared to *CO* and *p48-Kras^{G12D}* **(Figure 4.28 A and B)**. As for the genes involved in glycolysis, the major difference was seen for glucose-6-phosphatase (G6Pase) that is involved in catabolism of glucose, which was significantly increased in SIRT1-deficient mice. Additionally the mRNA levels for the glucose transporter 2 (GLUT2) was significantly decreased in *SIRT1$^{fl/fl}$-p48-Kras^{G12D}* mice compared to *p48-Kras^{G12D}* animals. Further genes involved in gluconeogenesis was affected by the SIRT1-deficiency, which was shown by the significantly upregulated mRNA levels for phosphoenolpyruvate kinase (PEPCK) in these animals **(Figure 4.28 A)**. Morever genes involved in lipogenesis such as fatty acid synthase (FAS), Steroly-CoA desaturase (SteCoA),

acetyl-CoA carboxylase (ACC) and lipoprotein lipase (LPL) were significantly decreased in $SIRT1^{fl/fl}$-$p48$-$Kras^{G12D}$ mice compared to $SIRT1^{fl/fl}$-CO mice, whereas ACC, LPL and FAS were highly increased in $SIRT1^{fl/fl}$-CO mice in comparison to CO animals. Another gene increased in $SIRT1^{fl/fl}$-CO mice in comparison to CO mice was the peroxisome proliferator-activated receptor γ (PPARγ). Further the expression of carnitine palmitoyltransferase1a (Cpt1α) was much higher in $SIRT1^{fl/fl}$-$p48$-$Kras^{G12D}$ mice then $SIRT1^{fl/fl}$-CO and $p48$-$Kras^{G12D}$ animals. Also the expression of the microsomal triglyceride transfer protein (MTTP) was significantly upregulated in SIRT1-deficent mice. Taken together these results suggested upregulated glycolytic flux due to the increased G6Pase in SIRT-deficent mice as well an enhanced transport of free fatty acids across the mitochondria membrane by upregulation of Cpt1α **(Figure 4.28 B)**.
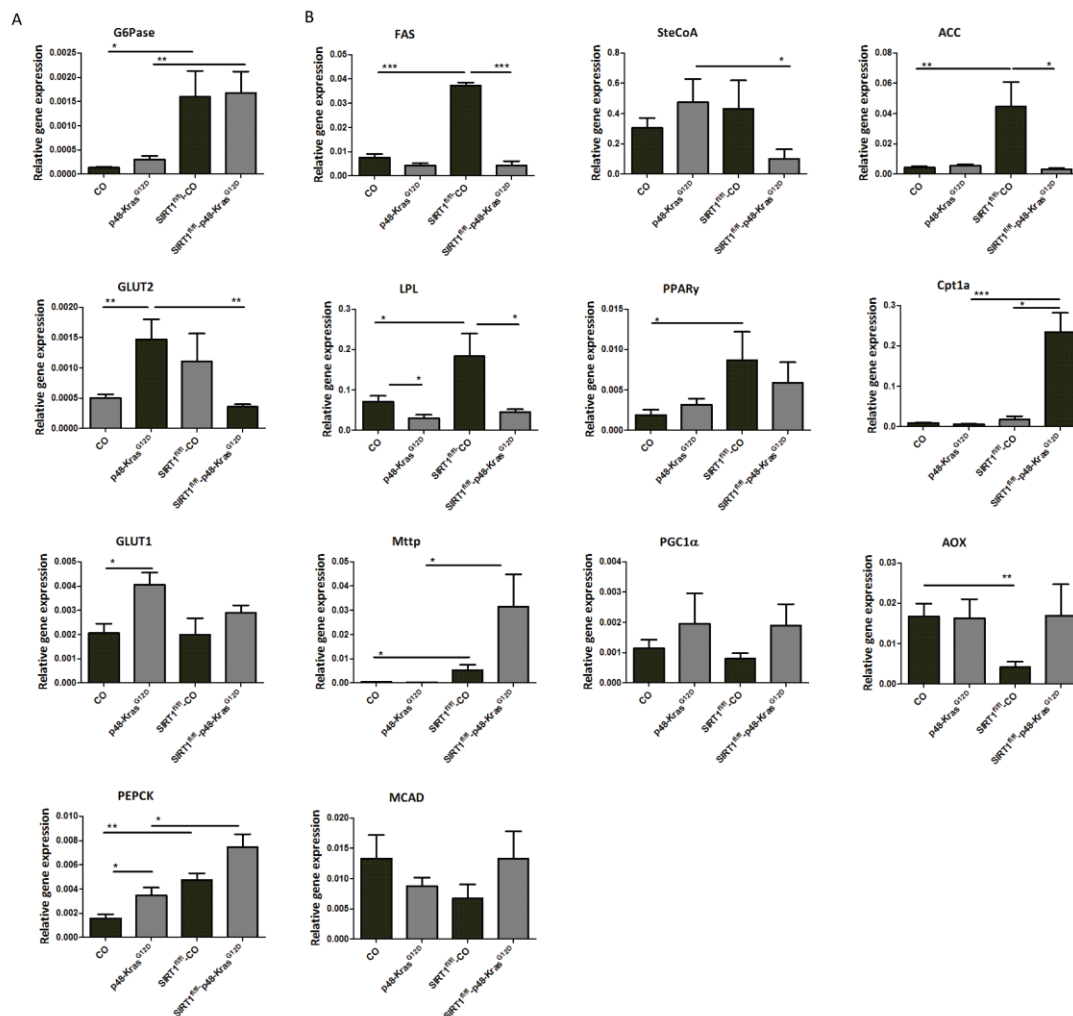
Figure 4.28: RT-PCR analysis of the pancreata from $SIRT1^{fl/fl}$-CO (n=5) and $SIRT1^{fl/fl}$-$p48$-$Kras^{G12D}$ (n=8) mice and untreated CO (n=4) and $p48$-$Kras^{G12D}$ (n=8) animals on genes involved in glucose (A) and fat metabolism (B). t-test: *p<0,05; **p<0,01.

4.7 Decreased tumor incidence in *PPARγ$^{fl/fl}$-p48-Kras^{G12D}* animals under HFD conditions

The PPAR family, which consists of three members: PPARα, PPARβ/δ and PPARγ, can in response to endogenous and exogenous ligands modulate the expression of their target genes and act as transcription factors. PPARγ (PG) is expressed majorly in adipose tissue where it regulates the generation and differentiation of adipocytes and it also is included in inflammatory responses. To investigate its role in insulin sensitivity and pancreatic tumorgenesis mice with pancreas-specific knockout of PPARγ were kept under HFD for 20 weeks.

Regarding the weight curves for *PG$^{fl/fl}$* mice, no significant difference in weight gain was seen until the 18. and 20. weeks on HFD. When compared to *CO* and *p48-Kras^{G12D}* mice, no difference in weight gain was observed **(Figure 4.29 A, B and C)** suggesting no effect of PG-deficiency on the weight gain *p48-Kras^{G12D}* mice.
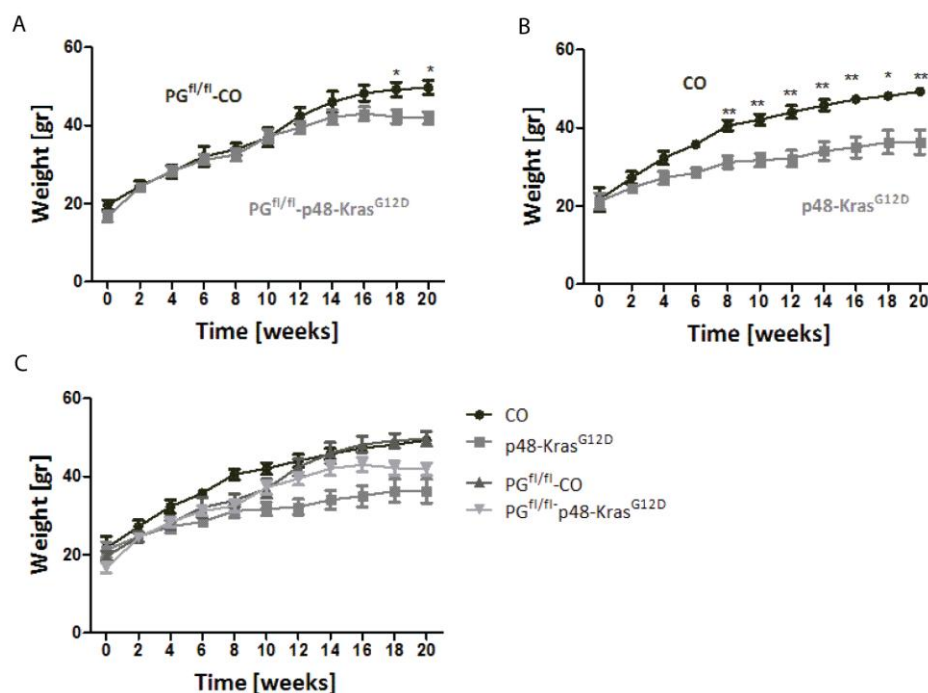
Figure 4.29: Weight curves from *PG$^{fl/fl}$-CO* (n=4), *PG$^{fl/fl}$-p48-Kras^{G12D}* mice (n=7) (A), *CO* (n=6) and *p48-Kras^{G12D}* animals (n=10) (B). *PG$^{fl/f}$* mice showed no significant difference in weight gain compared to *CO* and *p48-Kras^{G12D}* animals at 14, 16 and 18 weeks (C). t-test: *p<0,05; **p<0,01.

Further to verify the role of PG-deficiency during pancreatic tumorigenesis, pancreata sections were evaluated. Importantly $PG^{fl/fl}$-$p48$-$Kras^{G12D}$ mice showed no cancer development **(Figure 4.30 A)**. In accordance with total rescue in tumorigenesis 33% of the intact tissue architecture was disrupted and only PanIN 1 lesions were detected whereas in $p48$-$Kras^{G12D}$ mice the architectural distortion was seen in 95-100% of the tissue and all PanIN 1, 2 and 3 lesions were seen.

A

B

Genotype	PanIN-1 (%)	PanIN-2 (%)	PanIN-3 (%)	Tumor Incidence (%)
p48-Kras^{G12D} (n=16)	100	35	6,3	41
PG$^{-/-}$-p48-Kras^{G12D} (n=2)	100	0	0	0
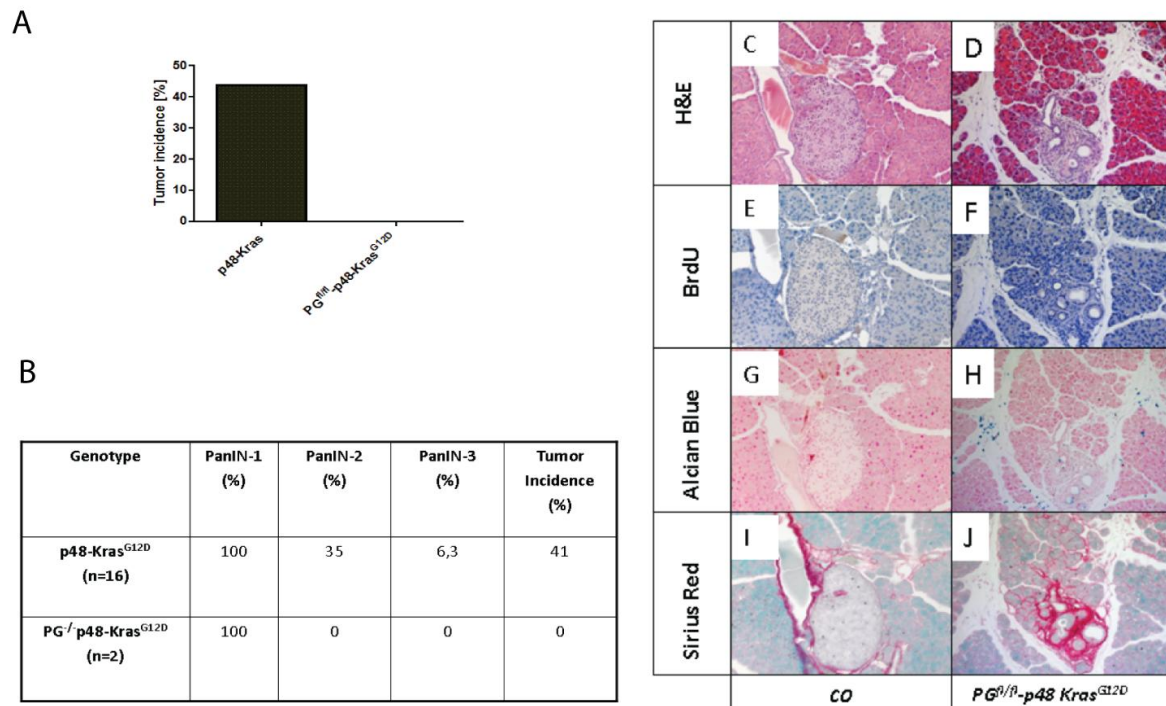
Figure 4.30: Tumor incidence and PanIN lesions in $p48$-$Kras^{G12D}$ (n=17) mice and $PG^{-/-}$-$p48$-$Kras^{G12D}$ (n=8) animals after 20 weeks on HFD (A and B). H&E (C + D), BrdU (E + F), Alcian Blue (G + H) and Sirius Red (I + J) staining of pancreas sections from $PG^{-/-}$-CO (A) and $PG^{-/-}$-$p48$-$Kras^{G12D}$ mice.

Further these findings were supported through Sirius red and Alcian blue staining, which indicated less fibrosis and mucin production in $PG^{fl/fl}$-$p48$-$Kras^{G12D}$ mice compared to $p48$-$Kras^{G12D}$ animals **(Figure 4.30 G-J)** suggesting decreased transformation of the tissue.

Furthermore we wanted to check the insulin sensitivity in PG-deficent animals thus performed GTT. However the insulin sensitivity was not positively influenced through the PG-deficency **(Figure 4.31 A)**. $PG^{fl/fl}$-CO and $PG^{fl/fl}$-p48-Kras^{G12D} mice were hyperglycemic although the $PG^{fl/fl}$-p48-Kras^{G12D} animals responded significantly better then the $PG^{fl/fl}$-CO mice during GTT.
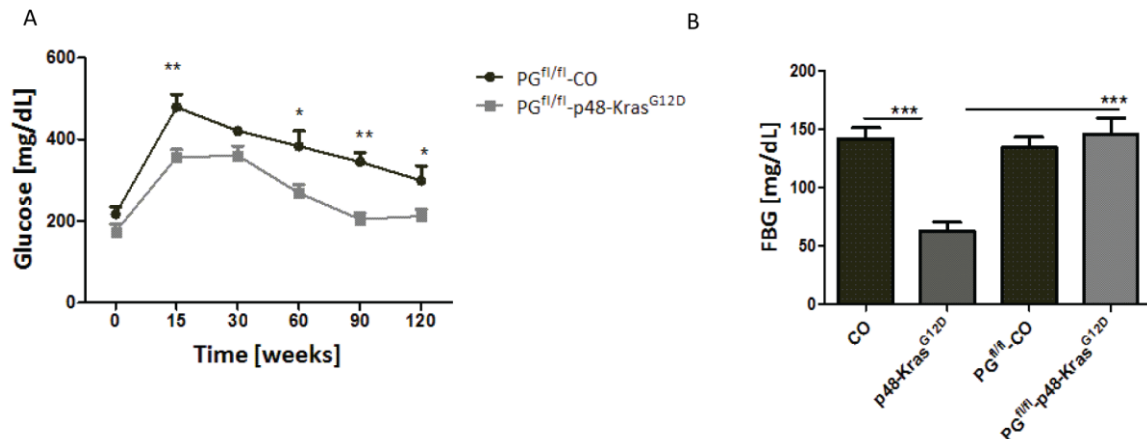
Figure 4.31: GTT results from $PG^{fl/fl}$-CO (n=3) and $PG^{fl/fl}$-p48-Kras^{G12D} (n=7) animals (A) and their fasting blood glucose levels after 20 weeks on HFD compared to untreated CO (n=5) and p48-Kras^{G12D} (n=7) mice (B). t-test: *p<0,05; **p<0,01; ***p<0,001

Based on the fact that PPARγ is involved in the lipid metabolism, we were interested to check the PG-deficiency on the respiratory capacity compared to CO and p48-Kras^{G12D} animals. The RCR`s demonstrated that $PG^{fl/fl}$-p48-Kras^{G12D} mice had significantly increased OXPHOS activity compared to p48-Kras^{G12D} animals whereas in between the $PG^{fl/fl}$-mice no difference was observed **(Figure 2.32 A)**. The citrate synthase activity suggested the same although the mitochondrial content was not significantly upregulated in $PG^{fl/fl}$-p48-Kras^{G12D} mice **(Figure 4.32 B and C)** suggesting increased oxidative phosphorylation and citrate synthase activity in p48-Kras^{G12D} animals due the PG-deficiency.
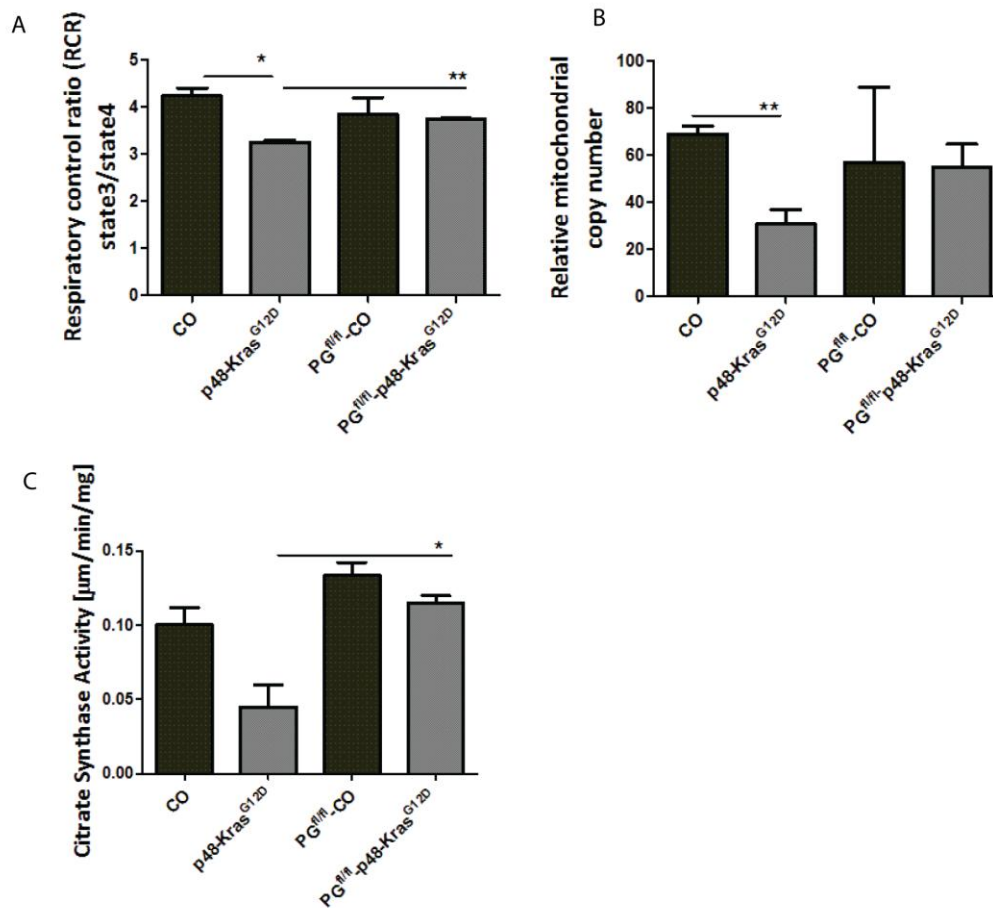
Figure 4.32: Following 20 weeks on HFD the pancreatic mitochondria from $PG^{fl/fl}$-*CO* (n=2) and $PG^{fl/fl}$-*p48-Kras*^{G12D} (n=3), *CO* (n=3) and *p48-Kras*^{G12D} (n=2) mice were isolated and the respiratory control rates were measured (A). The mitochondrial content from $PG^{fl/fl}$-*CO* (n=3), $PG1^{fl/fl}$-*p48-Kras*^{G12D} (n=3), *CO* (n=3) and *p48-Kras*^{G12D} (n=3) mice were defined after 20 weeks on HFD (B) as well the citrate synthase activity (n=3) (C). t-test: *p<0,05; **p<0,01.

4.8 PPARα-deficiency protects against HFD-accelerated tumorigenesis

PPARα, another family member of the PPAR`s is mainly expressed in tissues that show high beta-oxidation activity such as liver, intestinal absorptive, skeletal and cardiac muscle cells. This transcription factor is a central modulator of lipid homeostasis and its target genes are involved in β-oxidation especially in the mobilization and catabolism of fatty acids.

To investigate the effect of PPARα during PDAC whole body knockout of PPARα (PA) was used. The weight curves suggested that PA-deficiency had an impact on the phenotype of $p48$-$Kras^{G12D}$ mice. Although the $PA^{-/-}$-CO and $PA^{-/-}$-$p48$-$Kras^{G12D}$ animals showed no difference in between however $PA^{-/-}$-CO mice were significantly leaner than their CO littermates **(Figure 4.33 A, B and C)** suggesting an effect of PA-deficiency in improving weight gain in these animals.
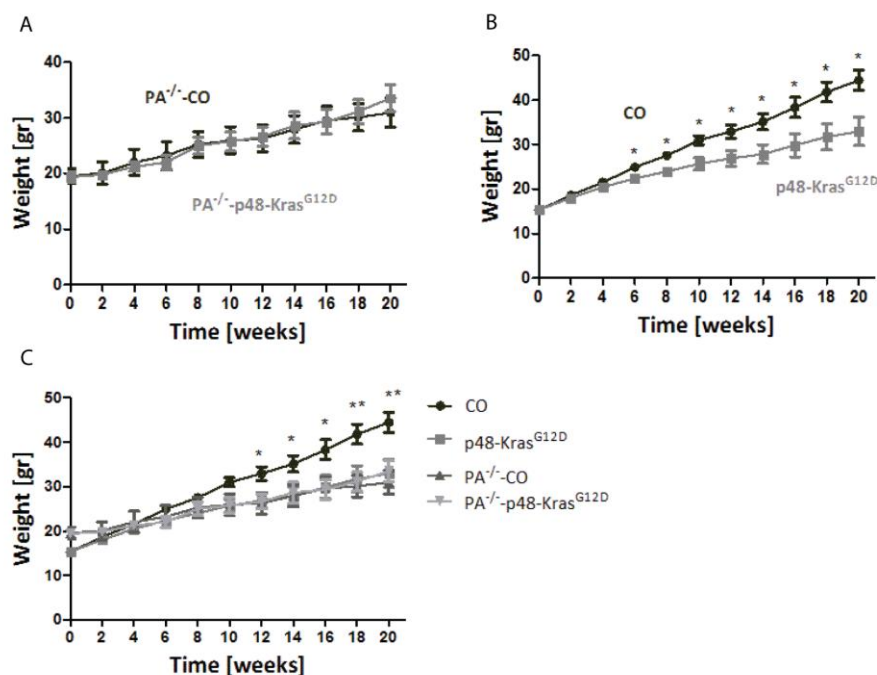
Figure 4.33: Weight curves from $PA^{-/-}$-CO (n=6) and $PA^{-/-}$-$p48$-$Kras^{G12D}$ mice (n=5) (A) and CO (n=6) and $p48$-$Kras^{G12D}$ mice (n=10) (B). $PA^{-/-}$-CO mice showed significant weight loss compared to CO animals at 12, 14, 16, 18 and 20 weeks (C). t-test: *p<0,05; **p<0,01.

Considering the weight curves we were highly interested to check the insulin sensitivity in the PA-deficent mice by GTT. The fasting blood glucose levels suggested that the $PA^{-/-}$ mice were insulin sensitive, which indeed was confirmed by GTT **(4.34 B and C)**. The $PA^{-/-}$ mice did not exhibit a difference in glucose tolerance such as that described for *CO* and *p48-Kras*^{G12D} mice on HFD. These results demonstrated an increased insulin response in the PA-deficent mice probably through decreased body weight .
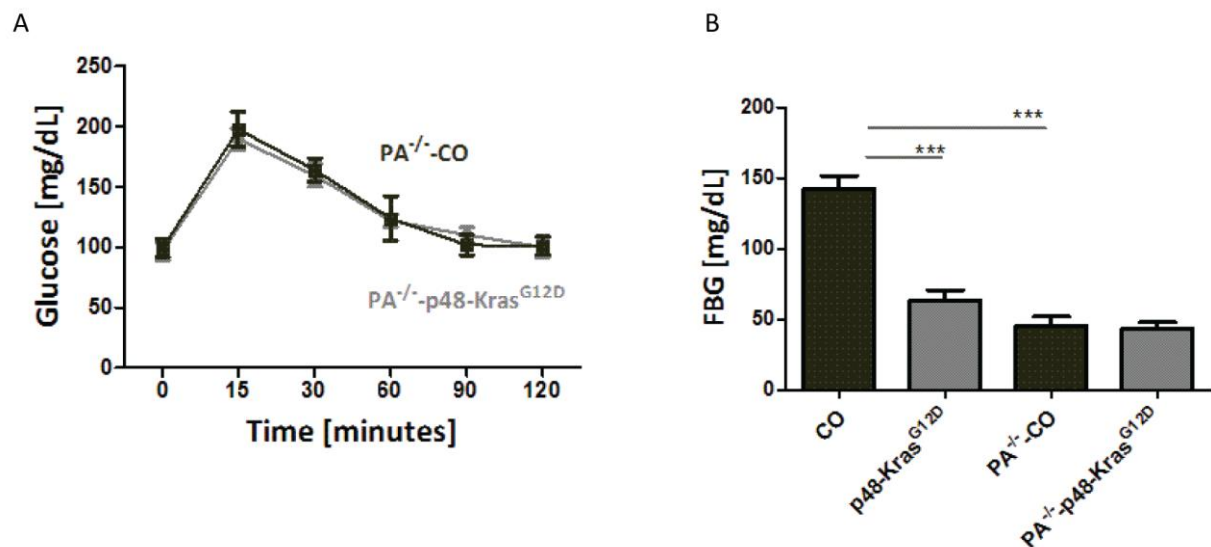
Figure 4.34: GTT results from $PA^{-/-}$-*CO* (n=4) and *p48-Kras*^{G12D} (n=4) animals (A). Fasting blood glucose levels after 20 weeks of HFD compared to *CO* (n=5) and *p48-Kras*^{G12D} (n=7) mice (B). t-test: ***p<0,001.

Furthermore we checked the histology of the pancreata from $PA^{-/-}$-*p48-Kras*^{G12D} animals and the most striking result was seen for the tumor incidence, which PA-deficiency caused a complete rescue of the phenotype in *p48-Kras*^{G12D} mice. The disruption of intact tissue architecture was limited to 34% and 50 % PanIN 2 lesions were detected **(Figure 4.35 A and B)**. Further less fibrotic areas were seen in $PA^{-/-}$-*p48-Kras*^{G12D} animals compared to *p48-Kras*^{G12D} as well as less mucins production and decreased proliferation rates were observed **(Figure 4.35 C-J)**. These results suggested an important role for PA in PDAC development.

A

B

Genotype	PanIN-1 (%)	PanIN-2 (%)	PanIN-3 (%)	Tumor Incidence (%)
p48-Kras^{G12D} (n=16)	100	35	6,3	41
PA$^{-/-}$-p48-Kras^{G12D} (n=8)	100	50	0	0
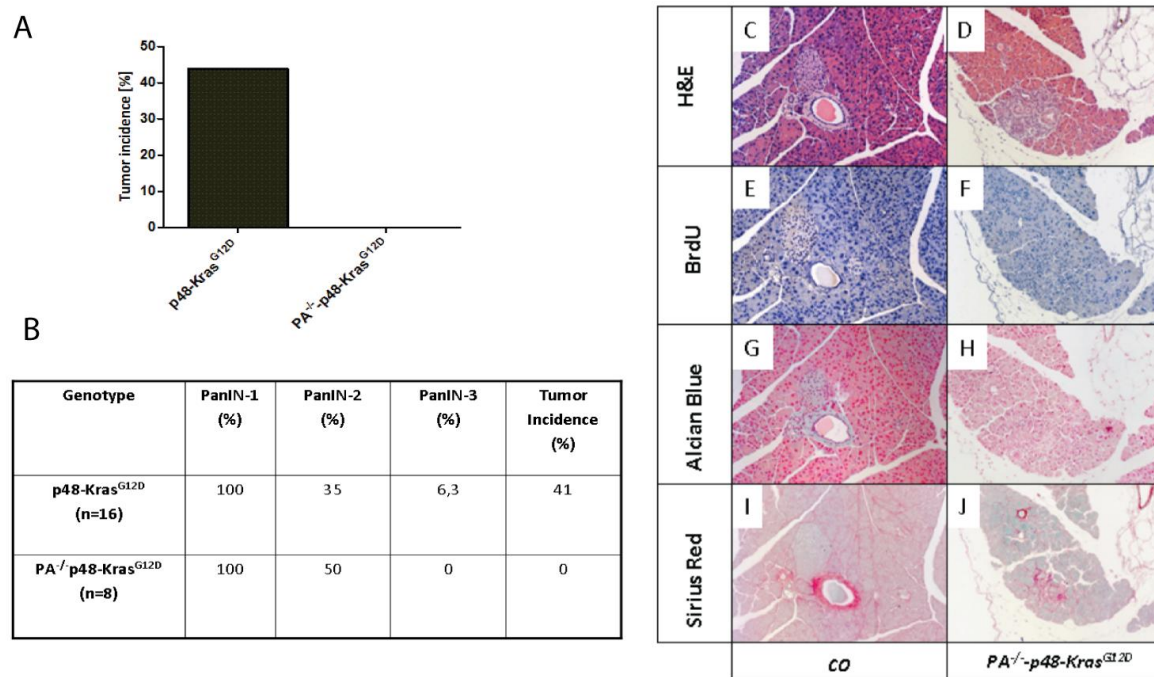
Figure 4.35: PanIN lesions and tumor incidence in *p48-Kras^{G12D}* (n=17) mice and *PA$^{-/-}$-p48-Kras^{G12D}* (n=8) animals after 20 weeks on HFD (A and B). H&E (C + D), BrdU (E + F), Alcian Blue (G + H) and Sirius Red (I + J) staining of pancreas sections from *PA$^{-/-}$-CO* (A) and *PA$^{-/-}$-p48-Kras^{G12D}* mice.

In order to analyze the role of PA on the mitochondrial oxygen consumption, we performed respiratory measurement using the Clark electrode. It was demonstrated that *PA$^{-/-}$* mice showed overall lower oxidative phosphorylation levels then *CO* and *p48-Kras^{G12D}* animals on HFD **(Figure 4.36 A)**. Further even a reversed phenotype was seen in *CO* and *p48-Kras^{G12D}* mice compared to *PA$^{-/-}$* animals. Whereas these result were not completely consistent with the mitochondrial content, which demonstrated a significant decrease in *PA$^{-/-}$-CO* mice compared to *CO* animals but no downregulation in the mitochondrial content in *PA$^{-/-}$-p48-Kras^{G12D}* mice compared to *p48-Kras^{G12D}* mice was detected **(Figure 4.36 B)**. Further the reversed phenotype seen in RCR results was not confirmed since there was a significant decrease in mitochondrial content in *PA$^{-/-}$-p48-Kras^{G12D}* mice compared *PA$^{-/-}$-CO* mice. In contrast the citrate synthase activity also supported the reversed phenotype but in comparison to *CO* and *p48-Kras^{G12D}* mice the *PA$^{-/-}$-p48-Kras^{G12D}* animals kept showing increased viable mitochondria **(Figure 4.36 C)** suggesting that PA-deficiency is responsible for the decreased mitochondrial content and diminished RCR levels probably through its involvement in the mitochondrial biogenesis.

Indeed the increased citrate synthase activity observed in $PA^{-/-}$-p48-Kras^{G12D} mice could be to compensate the lower mitochondrial content in these animals.
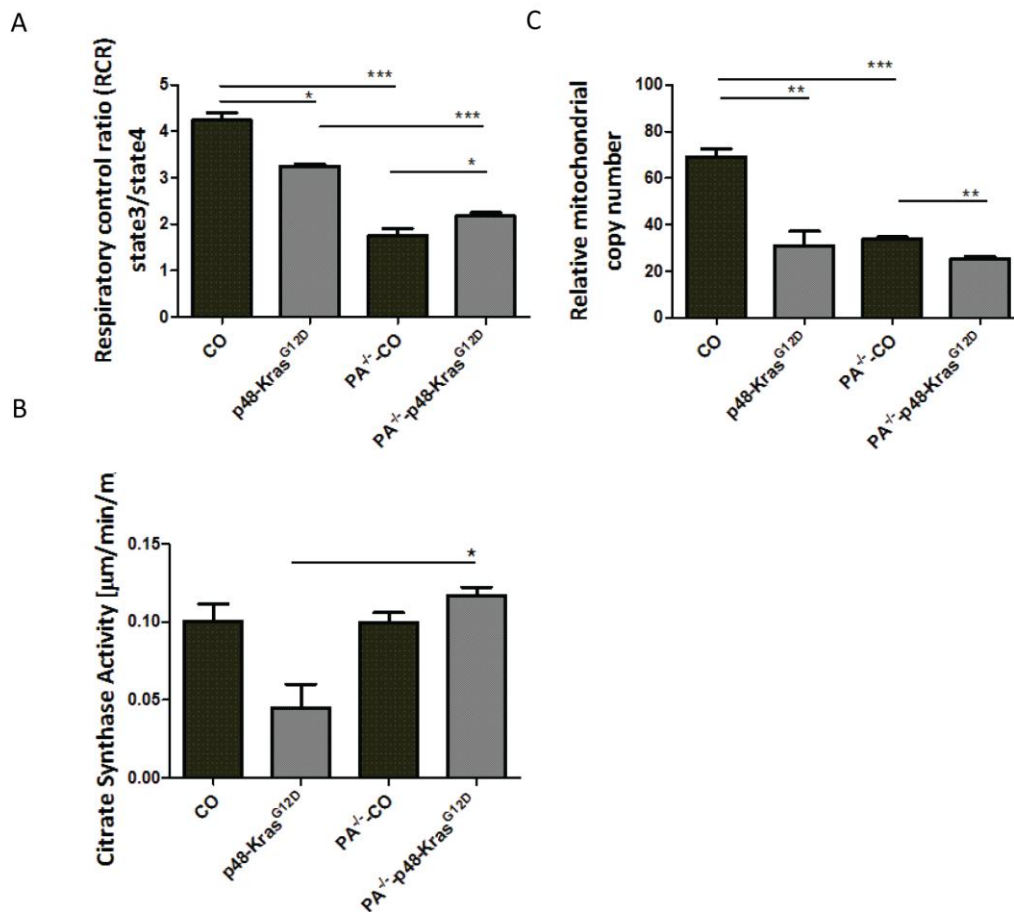
Figure 4.36: Following 20 weeks on HFD the pancreatic mitochondria from $PA^{-/-}$-CO (n=1), $PA^{-/-}$-p48-Kras^{G12D} (n=2), CO (n=3) and p48-Kras^{G12D} (n=2) mice were isolated and the respiratory control rates were measured (A). The mitochondrial content from $PA^{-/-}$-CO (n=3), $PA^{-/-}$-p48-Kras^{G12D} (n=3), CO (n=3) and p48-Kras^{G12D} (n=3) animals was defined after 20 weeks on HFD (B) as well as the citrate synthase activity (n=3) (C). t-test: *p<0,05; **p<0,01; ***p<0,001.

Further we checked the subunits of the respiratory chain at the protein and the mRNA level. Complex V was upregulated in $PA^{-/-}$-p48-Kras^{G12D} mice compared to p48-Kras^{G12D} mice, whereas no differences were observed for complex III and I **(Figure 4.37)**. Complex II was decreased in $PA^{-/-}$-p48-Kras^{G12D} mice compared to p48-Kras^{G12D} mice but this was not confirmed through the RT-PCR results while checking another subunit of complex II.
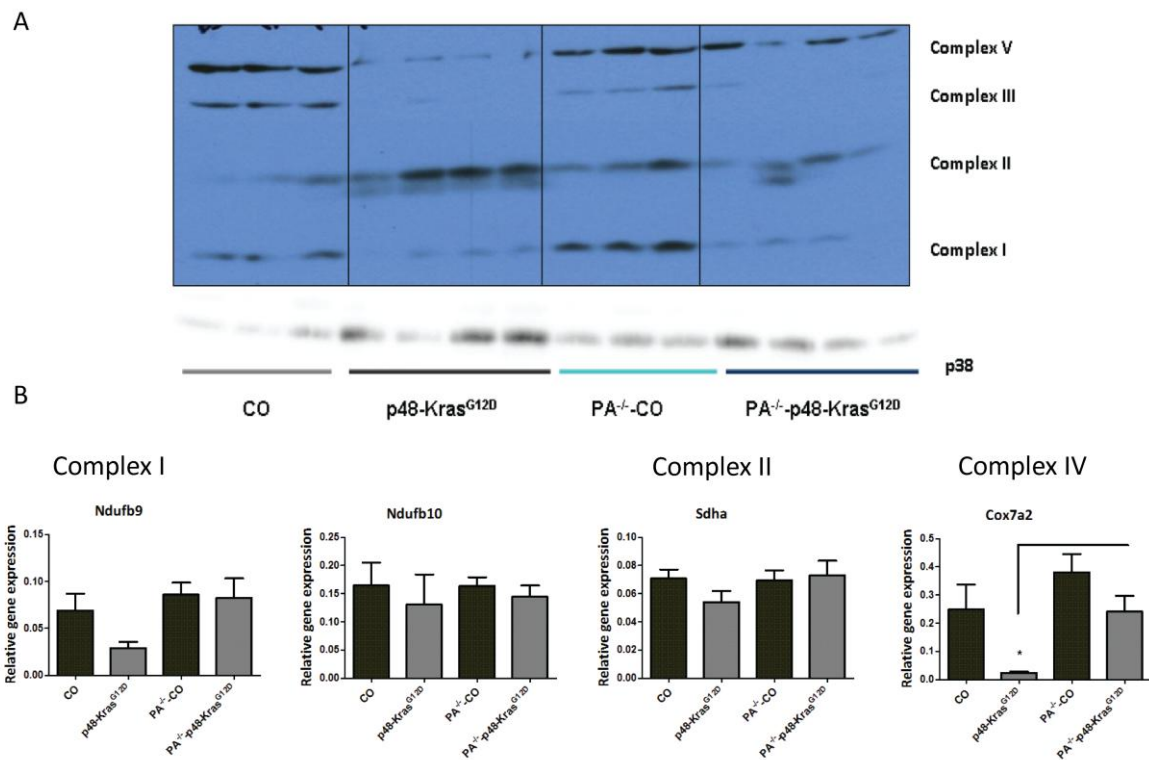
Figure 4.37: Western blot of pancreata from *CO, p48-Kras^G12D, PA^-/- -CO and PA^-/- -p48-Kras^G12D* mice using an anti-OXPHOS antibody. RT-PCR analyses were carried out to detect the subunits of complex I, II and IV. t-test: *p<0,05.

The mRNA levels of genes involved in fat and glucose metabolism were checked via RT-PCR. Genes involved in fat metabolism showed that the PA-deficiency in mice had an effect on the regulation of couple of target genes, which are under direct control of *PA^-/-* **(Figure 4.38 A)** such as MCAD, LPL, PGC-1α as well as Cpt1α. Indeed the phenotype was even reversed and the Cpt1a mRNA level was significantly upregulated in *PA^-/- -p48-Kras^G12D* mice compared to *PA^-/- -CO`s*. However PPARγ gene expression was significantly diminished in *PA^-/- -p48-Kras^G12D* mice compared to *p48-Kras^G12D* animals.
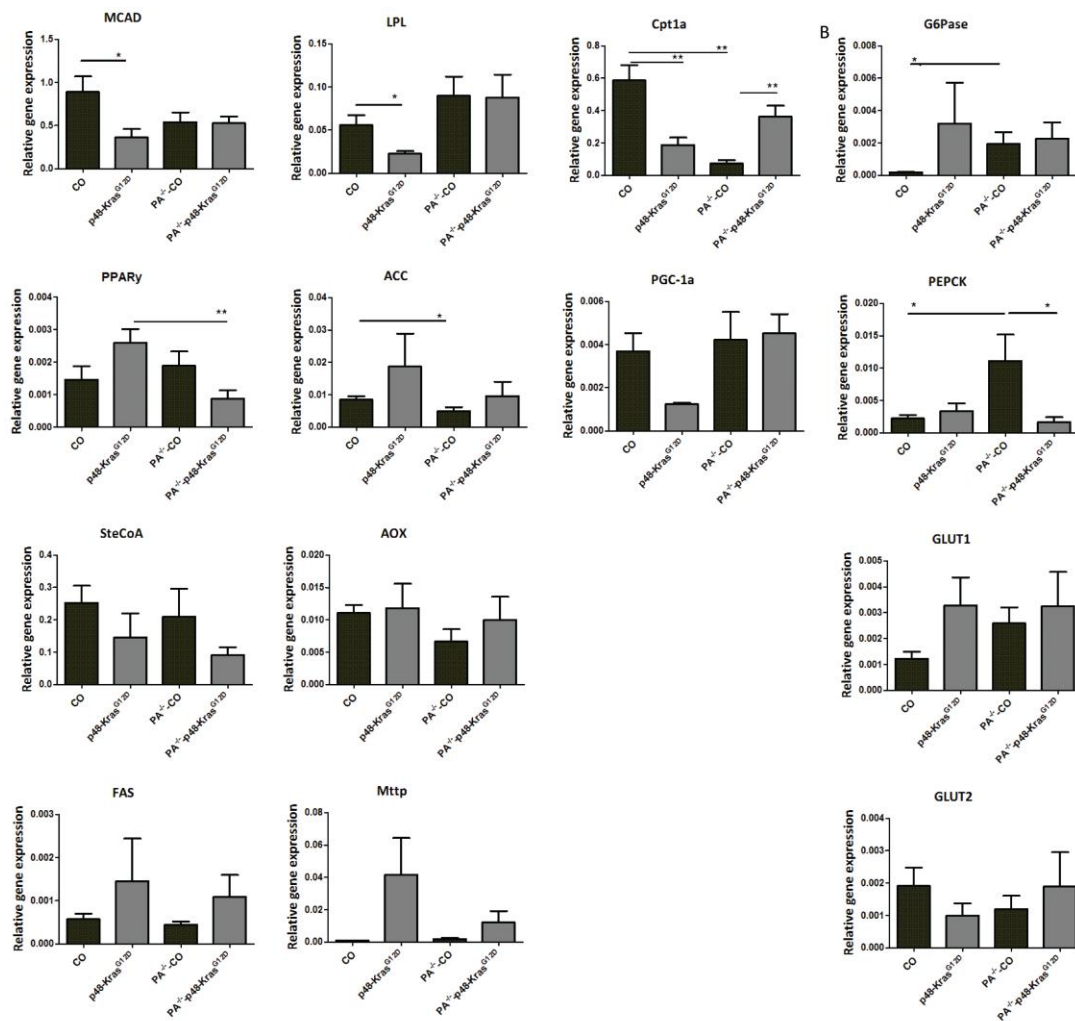
Figure 4.38: RT-PCR analysis of pancreata from *PA⁻/⁻-CO* (n=6), *PA⁻/⁻-p48-Kras^G12D* (n=8), *CO* (n=4) and *p48-Kras^G12D* (n=8) animals on genes involved in fat (A) and glucose metabolism (B). t-test: *p<0,05; **p<0,01.

Regarding genes involved in the glucose metabolism, G6Pase seemed to be under direct control of PA. Further PEPCK expression was reversed in PA-deficient mice and was significantly downregulated in *PA⁻/⁻-p48-Kras^G12D* mice compared to *p48-Kras^G12D* animals whereas it was significantly increased in *PA⁻/⁻-CO* mice compared to *CO* littermates **(Figure 4.38 B)**. These results suggested an increased free fatty acid transport across the mitochondrial membrane and a diminished gluconeogenesis in *PA⁻/⁻-p48-Kras^G12D* animals.

4.9 Decreased inflammatory response in 2-DG treated *p48-Kras*^G12D and *PA*^-/- *p48-Kras*^G12D mice during pancreatic tumorigenesis

We successfully demonstrated that the energy metabolism plays a very important role in *p48-Kras*^G12D mice during pancreatic tumorigenesis. Hanahan et al. proposed beside deregulation of cellular energetics as well as increased inflammation as one of the hallmarks of cancer (Hanahan and Weinberg 2011). Since we were able to significantly decrease tumor incidence in 2-DG treated *p48-Kras*^G12D animals and even rescue the phenotype in *PA*^-/- *p48-Kras*^G12D mice by manipulating the energy metabolism, we were further interested in their inflammatory response. Over the last years tumor-associated macrophages (TAMs) became more and more important in tumor development. It is suggested that they are M2 polarized and significantly increased in several cancer types (An, Sood et al. 1987; Leek, Lewis et al. 1996; Solinas, Germano et al. 2009). Our previous work showed that HFD-induced obesity enhances inflammation thus promotes pancreatic tumorigenesis in *p48-Kras*^G12D animals (Khasawneh, Schulz et al. 2009). Therefore we wanted to investigate the inflammatory response in the pancreas cells via through Fluorescence Activated Cell Sorting (FACS) and check whether altered energy homeostasis has any effect on inflammation and macrophage polarization.

In our experiments we used the monocytes-macrophage marker CD11b+ in combination with Gr1$^+$, F4/80$^+$, IL-4, IL-13, TNFα and IFNγ to check the levels of inflammatory cell as well as cytokines that are selected differentially by M1 or M2 macrophages. We could demonstrate that HFD increased the amount of inflammatory cells in *p48-Kras*^G12D mice on HFD compared to those kept on ND (**Figure 39 A-D, 40 A-D, 41 A-D**). Regarding the 2-DG *p48-Kras*^G12D mice and *PA*^-/--*p48-Kras*^G12D, which exhibit decreased tumor incidence, we successfully showed reduction in neutrophils and macrophages suggesting anti-inflammatory effect of 2-DG treatment as well as the *PA*^-/--deficiency (**Figure 39 C-D**). Although the cell percentage of CD11b+ -F4/80+ was not significantly diminished in these two groups, a tendency towards a decrease was evident in the animals (**Figure 39 A-B**).
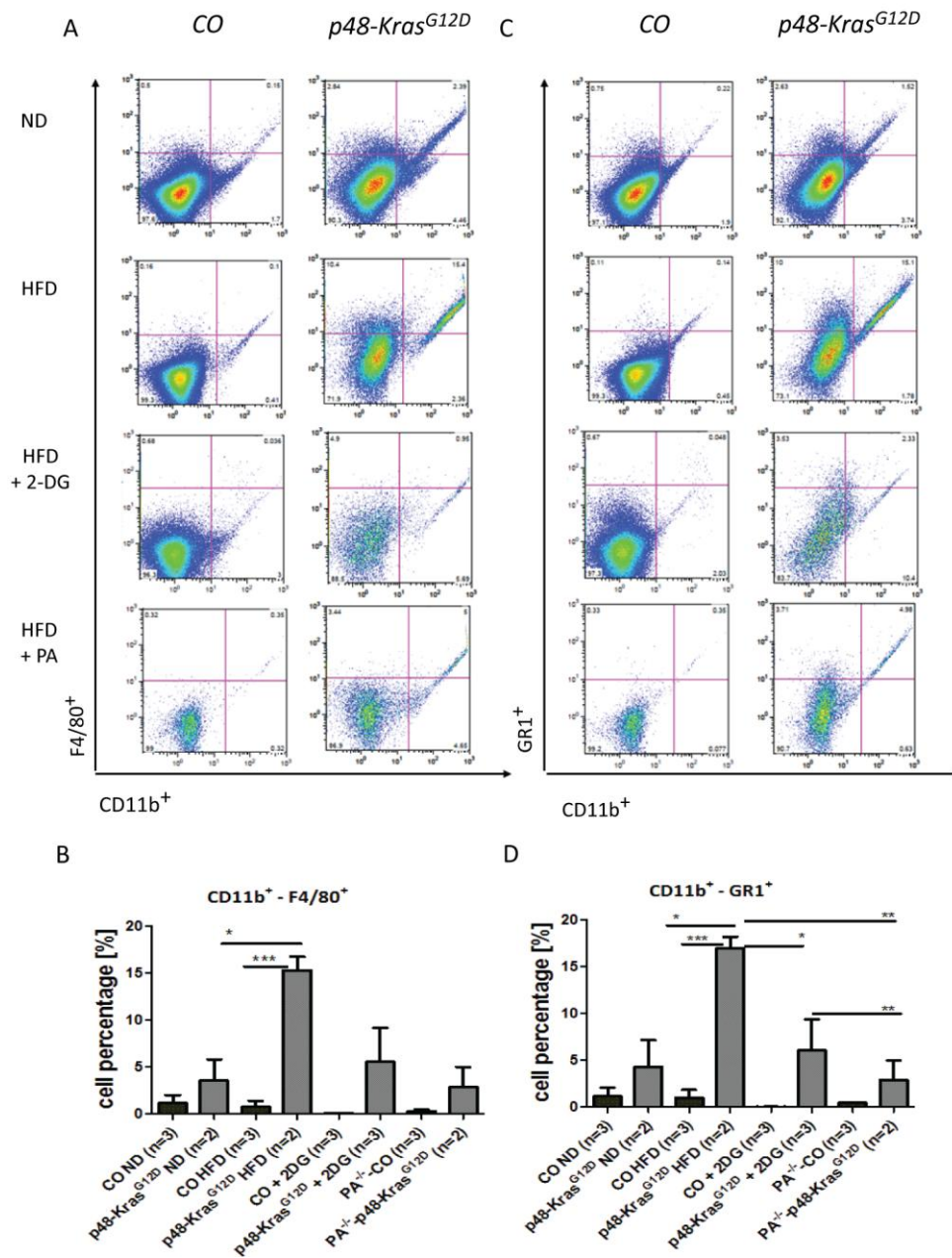
Figure 39: FACS analysis of inflammatory cells in *CO* and *p48-Kras^G12D^* animals as well as 2-DG treated *CO*, *p48-Kras^G12D^* animals and *PA^-/-^*-deficent mice kept on ND or HFD for 20 weeks (A-D). t-test: *p<0,05; **p<0,01; ***p<0,001.

It is widely accepted that in several cancer types the level of TAMs is increased and that they are mainly M2 polarized. Therefore we checked IL-4 and IL-13 in the isolated pancreas cells. In accordance with the pervious results we demonstrated that HFD upregulated the number of M2 macrophages in *p48-Kras^G12D^*. However the 2-DG treatment as well as the *PA^-/-^*-deficiency lead to reduced M2 macrophage polarization in

p48-Kras[G12D] mice suggesting less inflammation in these animals due to the changes in bioenergetic pathways (**Figure 40 A-D**).
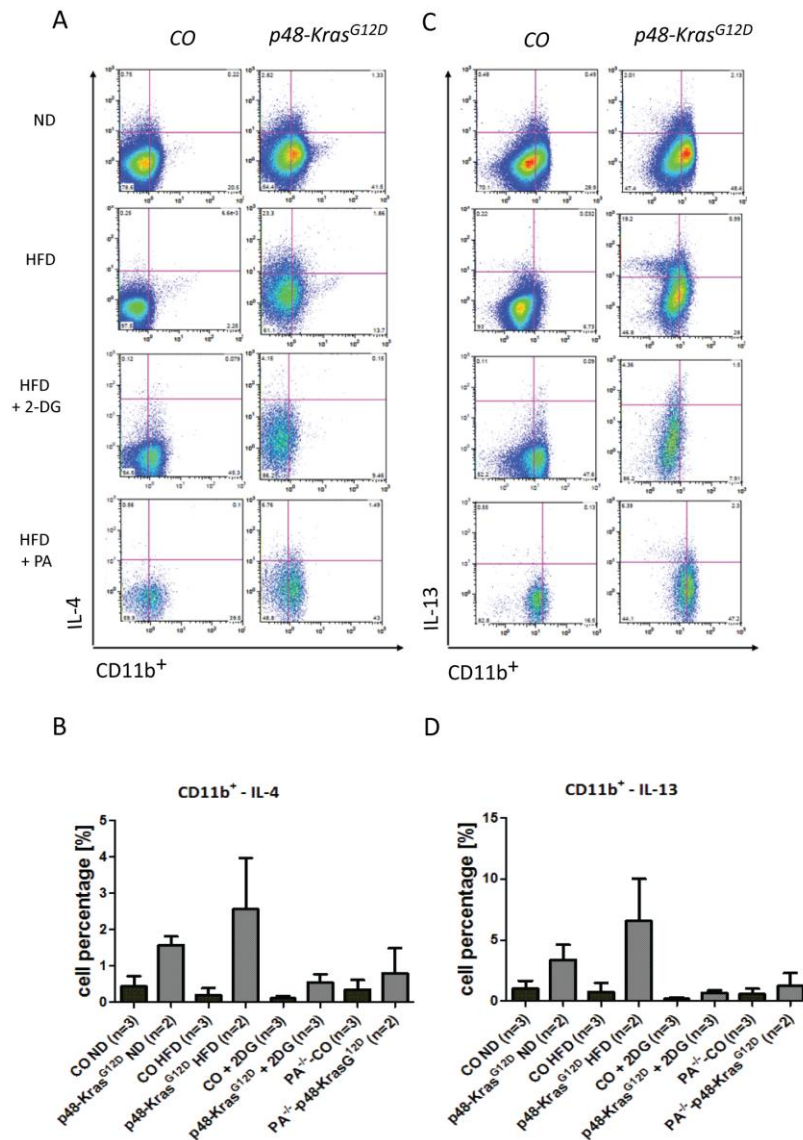
Figure 40: FACS analysis for M2 polarization in *CO* and *p48-Kras*[G12D] animals, 2-DG treated *CO, p48-Kras*[G12D] mice as well as *PA*^{-/-}-deficent mice kept on ND or HFD for 20.weeks (A-D). t-test: not significant (ns).

Other markers such as TNFα and IFNγ were used to investigate the M1 polarization (**Figure 41 A-D**). Again *p48-Kras*[G12D] animals on HFD showed an increased inflammation compared to those on ND, whereas 2-DG treated *p48-Kras*[G12D] and *PA*^{-/-}-*p48-Kras*[G12D] mice exhibited a reduced M1 phenotype suggesting less inflammatory response in these

animals. Taken together these results demonstrated less inflammation in 2-DG treated *p48-Kras*^{G12D} and *PA*$^{-/-}$-*p48-Kras*^{G12D} mice due to the reduced tumor incidence probably owning to the switch from glycolysis to oxidative phosphorylation.

Indeed macrophage polarization towards M1 or M2 phenotype in *p48-Kras*^{G12D} mice on HFD may be closely linked to the metabolic shift observed in these animals since 2-DG *p48-Kras*^{G12D} and *PA*$^{-/-}$- *p48-Kras*^{G12D} mice showed decreased glycolytic rates and M2 polarization.
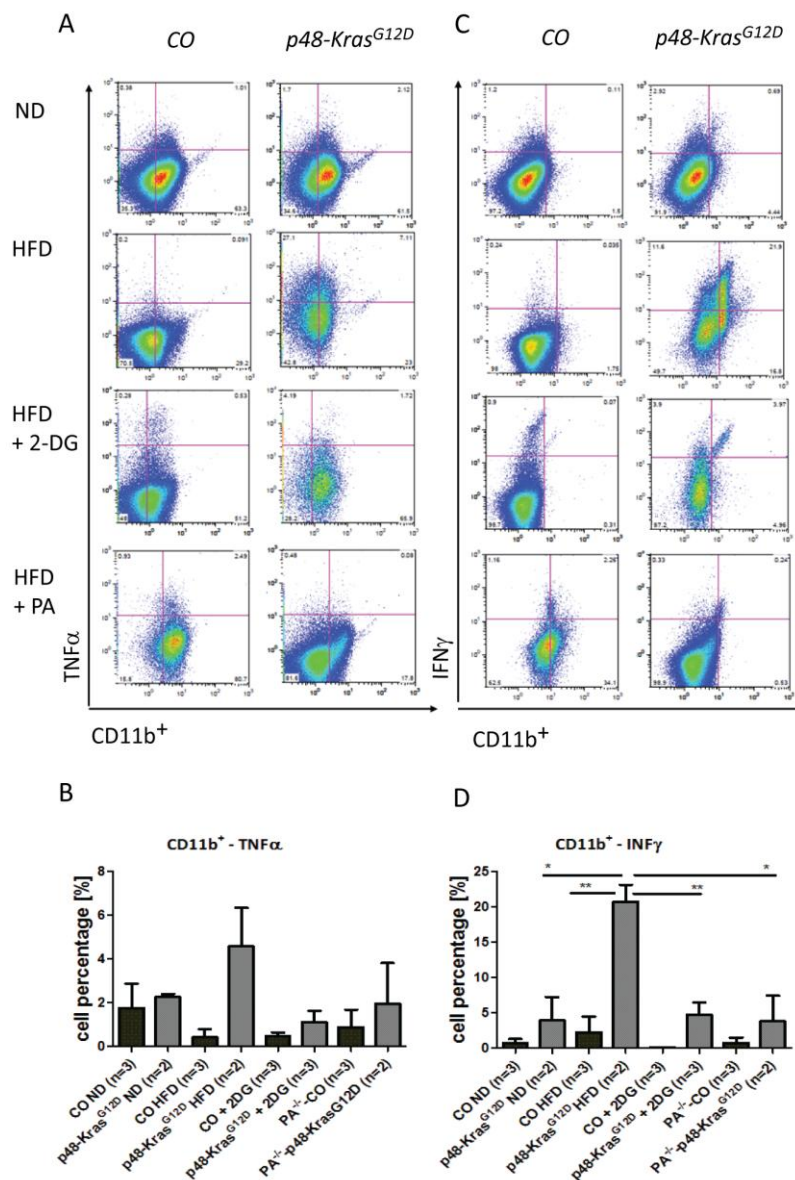
Figure 41: FACS analysis for M1 macrophages in *CO* and *p48-Kras*^{G12D} animals, 2-DG treated *CO, p48-Kras*^{G12D} mice as well as *PA*$^{-/-}$-deficent mice kept on ND or HFD for 20.weeks (A-D). t-test: *p<0,05; **p<0,01.

5. Discussion

5.1 Warburg Effect

Otto Warburg's findings in 1920´s considering the metabolic shift in tumor cells from oxidative phosphorylation to glycolysis is now considered as an essential basis for cancer research (Warburg 1930). Warburg suggested that the shift from oxidative phosphorylation to glycolysis is based on mitochondrial dysfunction however that has not been confirmed in most of the cancer cells. But apart from this, the increased glucose uptake serves for detection of most human primary cancers and metastasis and is used as an important tool in the clinical field. The FDG-PET analysis uses a radioactive-labelled glucose analogue, 2-DG, which is taken into the cells via glucose transporters but can not be further metabolized and accumulates in the cytoplasm. Cells with highly increased need of glucose, such as most cancer cells, use the glucose analogue. They become detected by metabolic trapping, which is visible on the PET image. It is shown that cancer types with an extreme high demand of glucose have more aggressive behaviour and that they are more invasive, which is in accordance with a very poor prognosis (Postovit, Adams et al. 2002; Gatenby and Gillies 2004; Mochiki, Kuwano et al. 2004). Unfortunately, the FGD-PET has also drawbacks considering the sensitivity and the specificity in detection. Regarding the specificity, especially immune cells are known to uptake also FDG, which then may lead to false positive results. Further the sensitivity is limited when lesions are smaller than 0.8 cm^3 (Gatenby and Gillies 2004). The main disadvantage of FDG-PET is that not all cancer cells rely on glycolysis and/or switch to glycolysis as the preferred energy source. (Liu 2006; Moreno-Sanchez, Rodriguez-Enriquez et al. 2007; Bensinger and Christofk 2012).

Since Warburg discovered the dependency of most cancer cells on glycolysis, still the questions remain: Why do most cancer cells choose the less efficient energetic pathway? The exact reason and molecular mechanisms for the glycolytic phenotype seen in cancer cells are poorly understood. Until now many researches tried to find answers and provide different hypothesis regarding the advantages for cancer cells. First, decreased oxygen levels (hypoxia) in tumor tissue contributes to a "glycolytic switch" through the activation of genes involved in glycolysis via the HIF-1α activation (Brahimi-Horn and Pouyssegur 2006; Pelicano, Martin et al. 2006). However it is shown that even in the presence of

oxygen cancer cells maintain a high glycolytic rate (Pedersen 2007). Second, highly dividing cells have an increased need for carbon precursors to generate building blocks, which are provided in increased numbers through high glycolytic rates. Glycolytic building blocks serve to feed the pentose phosphate pathway and thus promote the biosynthesis of nucleic acids, phospholipids, fatty acids and cholesterol (Pedersen 2007; DeBerardinis, Lum et al. 2008; Weinberg, Hamanaka et al. 2010). Third, energy supply in the form of ATP is much faster during glycolysis. Based on the less time and effort, the ATP outcome is similar or even higher when compared to oxidative phosphorylation (Guppy, Greiner et al. 1993; Pfeiffer, Schuster et al. 2001; Lopez-Lazaro 2008) and further many more building blocks can be provided. Fourth, reactive oxygen species (ROS), which are produced during oxidative phosphorylation, can be even harmful to cancer cells (Milane, Duan et al. 2011). However Kaelin et al. proposed a proliferation promoting effect by increased ROS production via the inhibition of growth inhibitory phosphatases (Kaelin and Thompson 2010). Fifth, the high lactate production lead to low pH in cancer cells and this is suggested as a massive growing advantage for tumor cells (Gatenby and Gillies 2004). It is pointed out that the acidosis does not harm cancer cells but protects them from the immune system and further promote normal cells to become invasive (Pedersen 2007; Lopez-Lazaro 2008; Milane, Duan et al. 2011). Indeed our studies suggest that *p48-Kras^{G12D}* mice that show enhanced tumorigenesis during HFD significantly depend on glycolysis although the OXPHOS is also used.

5.2 Can metabolic changes during tumorigenesis be used as a potential marker in PDAC?

PDAC is one of the worst cancer types with an extreme high mortality rate and a median survival of 6 to 9 months (Rasheed, Matsui et al. 2012). The asymptotic course of the disease, high metastatic potential, resistance to radiation and chemotherapy and lack of a highly efficient detection method contribute to very poor prognosis and lead to 5-year survival rate of 4 % (Hidalgo 2010; Hill, Li et al. 2012; Rasheed, Matsui et al. 2012). Considering the detection of pancreatic cancer by FDG-PET, controversial results for the sensitivity and the specificity as well as for false positive results are discussed (Bensinger and Christofk 2012; Herrmann, Erkan et al. 2012). However the FDG-PET analysis is still not optimized for the detection of early precursor lesions and furthermore the location of

the pancreas exacerbates the explicit diagnosis in human patients. However it might be possible to find other metabolic features during pancreatic tumorigenesis that can be used as a marker for the detection of PDAC. Here it would be important to know at which time point these metabolic changes occur and whether these could be used to detect already-existing precursor lesions.

5.3 Obesity accelerates pancreatic tumor progression and metabolic changes in *p48-Kras*[G12D] mice

During our studies the PDAC mouse model with oncogenic *Kras*[G12D] activation in the exocrine pancreas served as a great tool because it recapitulates human disease. Besides around 90% of all pancreatic cancer patients have a mutation in the *Kras* gene (Hruban, Iacobuzio-Donahue et al. 2001; Pour, Pandey et al. 2003; Tuveson, Shaw et al. 2004; Hezel, Kimmelman et al. 2006). Based on our previous work we were able to clearly demonstrate that HFD accelerated PanIN development with significant changes in inflammatory responses and bioenergetic pathways (Khasawneh, Schulz et al. 2009). Now we show that not only early tumor promotion but also tumor progression was clearly increased in *p48-Kras*[G12D] animals during HFD. We could successfully demonstrate that obesity plays an important role in pancreatic cancer development and could confirm previous results suggesting an increased inflammatory response in *p48-Kras*[G12D] mice due to the significantly upregulated pro-inflammatory cytokines, IL-1β and TNFα. Enhanced cytokines were probably due to the increased free fatty acid levels in the circulation, which lead to a low-grade inflammation. Furthermore metabolic changes in *p48-Kras*[G12D] mice during pancreatic tumorigenesis were demonstrated, which showed a decreased transport of long-chain fatty acids to the inner mitochondrial membrane and a diminished mitochondrial fatty acid ß-oxidation. Also a significantly reduction in the respiratory capacity was observed in *p48-Kras*[G12D] mice kept on HFD. Even the mitochondrial content was significantly decreased in *p48-Kras*[G12D] animals suggesting lower mitochondrial respiratory rates in these mice and increased dependency on another bioenergetic pathway such as glycolysis. However the RT-PCR results for couple of genes involved in glycolysis showed no significant differences between *CO* and *p48-Kras*[G12D] mice. This could be due to the fact that other glycolytic genes are upregulated, which were not checked in our experimental system or it is the enzymatic rates that are changed, which

we could not measure directly or pancreatic cancer cells can also use alternative metabolic pathways other than glycolysis such as the glutamine pathway. Also glutamine is the most abundant nutrient used by mammalian cells as bioenergetic substrate, which is necessary for the generation of energy, macromolecules and cell survival. Non-transformed cells seem to use only a small amount of glutamine for macromolecular biosynthesis and energy production. In contrast, glutamine is consumed in large amounts in tumor cells and provides biosynthetic precursors instead of breaking it down completely for energy use (DeBerardinis, Mancuso et al. 2007). In pancreatic cancer patients around 85% are suffering from cachexia and some groups suggested that this skeletal muscle wasting is linked to glutamine metabolism because muscles store around 90% of all glutamine in the body (Tisdale 2009; Vasseur, Afzal et al. 2009; DeBerardinis and Cheng 2010). Further metabolic studies are required to confirm the preference of pancreatic tumor cells on glycolysis such as measuring the lactate amount as well as to check their dependency on glutamine metabolism in our mouse model..

5.4 Can modulation of glycolysis and/or oxidative phosphorylation via pharmacological drugs be potentially used as a potential therapeutic approach for pancreatic tumorigenesis?

5.4.1 2-DG treatment decreases tumor incidence in *p48-Kras*[G12D] mice

Glycolysis plays an important role during pancreatic tumorigenesis (Ying, Kimmelman et al. 2012). Strikingly we could successfully demonstrate that the inhibition of glycolysis by 2-DG significantly decreased the tumor incidence in *p48-Kras*[G12D] animals. Furthermore the treatment increased the mitochondrial respiration in *p48-Kras*[G12D] mice suggesting an enforced switch to oxidative phosphorylation and a certain capability of pancreatic cancer cells to adapt to a different energy source. Considering the mitochondrial content the same downregulation was observed in 2-DG treated *p48-Kras*[G12D] mice compared to *CO* littermates and untreated animals. However the citrate synthase activity was significantly increased in 2-DG treated *p48-Kras*[G12D] mice compared to untreated *p48-Kras*[G12D] mice, implicating enhanced citrate synthase activity as a compensatory effect in 2-DG treated *p48-Kras*[G12D] mice to maintain their energy status. Coleman et al. demonstrated that human pancreatic cancer cell line treated with 2-DG show increased cytotoxicity however

in accordance with our results *in vivo* studies showed as well an anti-tumorigenic effect of 2-DG with an additionally increased sensitivity to irradiation without obvious cell toxicity (Coleman, Asbury et al. 2008). Further Goldberg et al. reported recently that in phase 1 clinical trails the single administration of 2-DG shows some anti-tumorigenic effects in patients with solid tumors and further no toxicity was observed by the treatment (Goldberg, Israeli et al. 2012). It becomes more and more evident that 2-DG treatment might be a potential therapeutic approach in pancreatic cancer and in combination with irradiation as well as the use of Ras-inhibitors the anti-tumorigenic effect could even be increased (Coleman, Asbury et al. 2008; Goldberg, Israeli et al. 2012).

5.4.2 3-Bromopyruvate treatment does not serve as potential therapeutic drug in *p48*-*Kras*^{G12D} animals

3-Bromopyruvate, another glycolytic inhibitor, which is a promising anti-cancer drug in pancreatic, hepatocellular carcinoma and human cancer cell lines including leukemia, lymphoma, and neuroblastoma (Xu, Pelicano et al. 2005; Xu, Pelicano et al. 2005; Pereira da Silva, El-Bacha et al. 2009; Bhardwaj, Rizvi et al. 2010; Akers, Fang et al. 2011; Levy, Zage et al. 2012; Tang, Yuan et al. 2012). Besides *in vitro* studies also *in vivo* experiments supported these findings. Ko et al. demonstrated that 3-BP is able to destroy advanced cancers in tumor-bearing rats (Ko, Smith et al. 2004) without harming normal cells. Further Ko et al. reported about the first human case study in 16 year old patient with hepatocellular carcinoma (Ko, Verhoeven et al. 2012). The authors implicated that the young patient lived longer then expected and had an improved life quality (Ko, Verhoeven et al. 2012). This alkyling agent is proposed to block glycolysis via the inhibition of hexokinase II and glyceraldehyde 3-phosphate dehydrogenase (GAPDH) as well as mitochondrial oxidative phosphorylation through the repression of succinate dehydrogenase (Dell'Antone 2006; Ganapathy-Kanniappan, Vali et al. 2010). In many malignant tumors hexokinase II is predominantly overexpressed and it is know that this isoform bounds on the outer mitochondrial membrane protein such as voltage dependent anion channel where it has access to mitochondrial produced ATP (Mathupala, Ko et al. 2009; Nakano, Miki et al. 2012). 3-BP seems to disassociate hexokinase II and induces cell death through increased ATP depletion in cancer cells however the underlying molecular mechanism for induced cell death is poorly understood

(Pastorino, Shulga et al. 2002; Robey and Hay 2005; Kim, Ahn et al. 2008; Nakano, Miki et al. 2012).

Although 3-BP is described for potential cancer treatment, however we could not confirm the anti-tumorigenic effect in PDAC mouse model. One possibility might be that the studies suggesting an anti-tumorigenic effect in pancreatic cancer were performed *in vitro* and are not comparable to our *in vivo* model (Bhardwaj, Rizvi et al. 2010). However *in vivo* pancreatic and hepatocellular xenograft tumors showed also a tumor reducing effect in solid tumor but Cao et al. proposed that the 3-BP efficiency is 3 fold higher under hypoxic conditions compared to normoxia. Since we did not checked the hypoxic conditions in our system, the efficiency of 3-BP might be decreased due to normoxia. Regarding its inhibitory effect on oxidative phosphorylation, we indeed observed a significantly decreased mitochondrial respiration in 3-BP-treated *p48-Kras^{G12D}* animals and untreated *p48-Kras^{G12D}* mice. In accordance the mitochondrial content was significantly reduced in 3-BP treated *p48-Kras^{G12D}* mice however the treatment had no effect on the citrate synthase activity. Another explanation for the missing anti-tumorigenic effect might be an increased inhibitory effect on OXPHOS rather then on glycolysis of 3-BP, which leads to the same tumor incidence observed in untreated animals. Bhardweay et al suggested that an increased crosstalk between different bioenergetic pathways takes place and that the inhibition of both glycolysis and OXPHOS is a promising anticancer treatment. However we observed that pancreatic cancer mainly rely on glycolysis and the switch to mitochondrial respiration comes along with decreased tumor incidence in our mouse model during HFD-induced obesity. An inhibition of OXPHOS might even support cancer development and if 3-BP is administered in combination with a glycolysis inhibitor, it should be clarified that both inhibit with the same efficiency the two pathways to avoid an imbalance, which even can promote tumorigenesis. Taken together 3-BP treatment in the concentration we administrated was not effective in the therapy of pancreatic tumorigenesis in *p48-Kras^{G12D}* mice.

5.4.3 Etomoxir treatment leads to potential inhibition of FA ß-oxidation but does not show anti-tumorigenic effect during PDAC development

Etomoxir is known to inhibit FA ß-oxidation via blocking the Cpt1α. Interestingly etomoxir-treated *p48-Kras*^{G12D} mice showed the same weight gain as their *CO* littermates suggesting a decreased FA ß-oxidation thus increased fatty acid storage in the body. In accordance, etomoxir-treated *p48-Kras*^{G12D} animals showed significantly impaired insulin sensitivity probably due to the increased body weight observed in these mice. Further the mitochondrial oxidative phosphorylation was significantly downregulated in etomoxir-treated animals compared to untreated group, suggesting a reduced ATP-production through respiratory chain. Indeed Pike et al. suggested an additionally inhibitory effect of etomoxir on the respiratory chain *in vitro* (Pike, Smift et al. 2010). We could show the tumor incidence in etomoxir-treated *p48-Kras*^{G12D} mice was similar to untreated animals thus proving a higher dependency of *p48-Kras*^{G12D} animals on glycolysis compared to oxidative phosphorylation. However Pike et al. proposed that intact FA ß-oxidation promotes tumorigenesis through providing NAPDH to main the antioxidant system, which stands contradictory to our findings where we demonstrate reduced tumor incidence by enhanced mitochondrial respiration (Pike, Smift et al. 2011). Furthermore increased OXPHOS not only provides NAPDH but also reactive oxygen species (ROS), which are mainly produced via the electron chain. Based on our findings we hypothesize that the balance between ROS and the antioxidant system is still intact in our system, however it is necessary to check the ROS amount in etomoxir-treated and untreated animals.

5.4.4 PPARα agonist fenofibrate enhances FA ß-oxidation and decreases tumor incidence in *p48-Kras*^{G12D} mice

In humans fenofibrate is used to lower cholesterol and triglycerides in the circulation through enhanced activation of the peroxisome proliferator-activated receptor α (PPARα). Indeed, we were able to demonstrate an improved insulin response in fenofibrate-treated animals compared to untreated group. It is suggested that increased activation of PPARa leads to decreased cell proliferation *in vivo* and *in vitro* as well as decreased angiogenesis (Panigrahy, Kaipainen et al. 2008). Furthermore the apoptosis induced-cell death is activated through increased activation of PPARα by fenofibrate

(Thuillier, Anchiraico et al. 2000; Panigrahy, Kaipainen et al. 2008). Regarding the tumor incidence in fenofibrate treated *p48-Kras*[G12D] mice, we observed a clear reduction compared to untreated *p48-Kras*[G12D] mice, suggesting an anti-tumorigenic effect of the PPARα agonist fenofibrate in our system. Additionally the pro-inflammatory cytokine TNFα was significantly downregulated in fenofibrate-treated *p48-Kras*[G12D] animals suggesting reduced inflammatory response through the enhanced lipolysis in fenofibrate-treated mice thus reduced tumor incidence, which is supported by several groups that showed an anti-inflammatory effect of PPARα as well as PPARγ (Jiang, Ting et al. 1998; Poynter and Daynes 1998).The complete underlying molecular mechanism that promote the anti-inflammatory effect by the agonist fenofibrate has not been fully understood however it is suggested that particularly the inhibition of the nuclear factor-κB (NF-κB) pathway is involved (Delerive, De Bosscher et al. 1999; Delerive, Gervois et al. 2000; Toyoda, Kamei et al. 2008).

5.5 Involvement of nuclear receptors in cancer development: Peroxisome proliferator-activated receptor (PPAR`s) as potential targets in pancreatic cancer?

Nuclear receptors are multifunctional ligand induced transcription factors, which bind to DNA and regulate genes involved in many cellular processes including differentiation, homoeostasis, inflammation and energy metabolism (Shaw, Evans et al. 2010; Tang, Chen et al. 2011). The transcription factors are activated through the binding of small compounds such as steroids, retinoids, and thyroid hormones or through synthetic ligands (Zhang, Burch et al. 2004). Similar to the mouse genome which encodes for 49 of the receptors the human genome encodes for 48 nuclear receptors (Zhang, Burch et al. 2004; Tang, Chen et al. 2011). More and more evidence raised over the last years that nuclear receptors are as well involved in the development of different cancer types including prostate cancer, acute myeloid leukemia, breast, liver and primary colon cancer (Peters, Aoyama et al. 1998; Gupta, Tan et al. 2000; Bradbury, Khanim et al. 2005; Huffman, Grizzle et al. 2007; Stunkel, Peh et al. 2007).

5.5.1 Peroxisome proliferator-activated receptor γ as a promising therapeutic target in PDAC

Controversial results are published considering the role of PPARγ in tumor cells (Motomura, Okumura et al. 2000). Brockman and others demonstrated an anti-proliferating effect in human colon carcinoma cells by ligand induced upregulation of PPARγ (Brockman, Gupta et al. 1998; Sarraf, Mueller et al. 1998). In contrast it was shown that an upregulation of PPARγ supports the colonic tumorigenesis in mice (Lefebvre, Chen et al. 1998; Saez, Tontonoz et al. 1998). Over the last years more evidence appeared that the overexpression of PPARγ might play an important role in tumorigenic processes and is linked to several cancer types including pancreatic cancer (Motomura, Okumura et al. 2000; Kristiansen, Jacob et al. 2006; Eibl 2008). Additionally our group showed a significantly upregulation of PPARγ in *p48-Kras^{G12D}* animals during HFD-induced obesity (Khasawneh, Schulz et al. 2009).

Most strikingly we found total rescue during tumorigenesis in *p48-Kras^{G12D}* mice by a pancreas-specific deletion of *PG.* Although the underlying mechanism is not clearly understood, however we hypothesize that through downregulation of glycolytic genes, e.g. GLUT`s, hexokinase II and pyruvate kinase (Panasyuk, Espeillac et al. 2012), and increased fatty acid levels in the circulation *PG*-deficiency supported the shift from glycolysis to oxidative phosphorylation. In accordance with our hypothesis we observed a significant upregulation in the mitochondrial respiration in *PG$^{fl/fl}$-p48-Kras^{G12D}* mice compared to *p48-Kras^{G12D}* animals as well as an increased citrate synthase activity. However the mitochondrial content was not significantly upregulated compared to *p48-Kras^{G12D}* animals and *CO* littermates. Further it would be beneficial to measure metabolic products such as lactate to confirm our hypothesis as well as expression levels of genes involved in fat and glucose metabolism. So far, we can conclude that the pancreas-specific *PG* deletion is efficient to rescue the phenotype during HFD-induced obesity in *p48-Kras^{G12D}* mice however the molecular mechanism is not fully known.

5.5.2 Peroxisome proliferator-activated receptor α (PPARα)-deficiency protects against tumorigenesis in *p48-Kras*^{G12D} during HFD-induced obesity

PPARα is an important regulator of lipid oxidation. As being a ligand inducible transcription factor it directly regulates genes involved in FA ß-oxidation such as Cpt1α, AOX, LPL and MCAD (Fruchart, Staels et al. 2001). Further PPARα can also be activated through exogenous agonists such as different fibrates including fenofibrate, ciprofibrate, bezafibrate, and others. Guerre-Millo et al. demonstrated that the treatment of rodents with PPARα agonist leads to decreased triglyceride in the circulation and thus a significant improvement in insulin sensitivity (Guerre-Millo, Gervois et al. 2000). In this study the authors suggested enhanced FA oxidation and reduced ectopic lipid storage in non-adipose tissues could be the underlying mechanism to improved insulin sensitivity (Haluzik and Haluzik 2006). However Guerre-Millo et al. demonstrated one year later that PPARα-null mice even under HFD-induced obesity remain insulin sensitive (Guerre-Millo, Rouault et al. 2001). Indeed we also observed increased insulin response in *PA*-deficent animals under HFD condition and further decreased weight gain in *PA*$^{-/-}$-*p48-Kras*^{G12D} animals compared to *p48-Kras*^{G12D} mice suggesting increased insulin sensitivity due to the decreased body weight in *PA*$^{-/-}$-*p48-Kras*^{G12D} mice. Since *PA* is known to be involved in fatty acid metabolism we showed a significantly diminished respiration control rate in *PA*-deficent mice compared to *p48-Kras*^{G12D} animals and *CO* littermates probably due to reduced mitochondrial biogenesis induced by *PA*-deletion. However the reversed phenotype in *PA*-deficent mice still suggested an increased dependency of *PA*$^{-/-}$-*p48-Kras*^{G12D} animals on OXPHOS compared to *PA*$^{-/-}$-*CO* animals. Therefore we hypothesize that the increased citrate synthase activity observed in *PA*$^{-/-}$-*p48-Kras*^{G12D} mice reflects a compensatory effect for decreased mitochondrial content seen in these animals. We demonstrated a total rescue in *PA*$^{-/-}$-*p48-Kras*^{G12D} mice, which is in accordance with our hypothesis that *p48-Kras*^{G12D} animals rely more on glycolysis then OXPHOS and therefore we suggested a reduced glycolysis due to *PA*-deficiency. Controversial results were published regarding the role of *PA* in tumorigenesis. Several studies pointed out that increased activation via agonists such as fenofibrate suppresses tumor growth *in vitro* and *in vivo* through inhibition of uncontrolled cell proliferation, angiogenesis, apoptosis and its anti-inflammatory effects (Saidi, Holland et al. 2006; Panigrahy, Kaipainen et al. 2008; Riccardi, Mazzon et al. 2009; Pyper, Viswakarma et al. 2010). In contrast it was

demonstrated that *PA* agonists lead to liver cancer in rodents, however it is not completely understood if increased *PA*-activation causes liver malignancy or the agonist itself. Especially increased proliferation was observed in breast cancer cell lines (Suchanek, May et al. 2002; Kurokawa, Shimomura et al. 2011).

We propose that *PA*-deficiency in *p48-Kras^{G12D}* animals lead to upregulated OXPHOS and reduced glycolysis thus reduced tumor incidence. However the increased glycolytic rate has still to be proven. Nevertheless we suggest that PPARα may serve as a potential therapeutic target during pancreatic adenocarcinoma.

5.5.3   Pancreas-specific SIRT1 deletion does not affect pancreatic tumorigenesis

Sirtuin 1 (SIRT1), a multifaceted NAD$^+$-dependent deacetylase, is an important regulator of cell survival as well as metabolic processes including lipid metabolism and gluconeogenesis (Kong, Wang et al. 2009). It has been demonstrated that SIRT1 is significantly increased in human prostate cancer and primary colon cancer as well as in skin cancers including squamous cell carcinoma, basal cell carcinoma, Bowen's disease, and actinic keratosis (Bradbury, Khanim et al. 2005; Hida, Kubo et al. 2007; Huffman, Grizzle et al. 2007; Stunkel, Peh et al. 2007). The exact mechanisms by which SIRT1 is involved in cancer development is under debate but at least one of the possible explanations arise from its effect on mitochondrial activity.

A significantly decreased respiratory control rate in SIRT1-deficent mice was observed compared to *CO* mice and *p48-Kras^{G12D}* animals kept on ND. However compared to *p48-Kras^{G12D}* animals and *CO* littermates kept on HFD only *SIRT1^{fl/fl}-CO* mice seem to have a decreased RCR. Furthermore independent on HFD or ND diet, SIRT1-deficency led to significantly reduced mitochondrial content suggesting involvement of SIRT1 in the mitochondrial biogenesis. This is supported by the finding that SIRT1 regulates the peroxisome proliferator-activated receptor γ (PPARγ) coactivator 1α (PGC-1α), which is known to be involved in mitochondrial biogenesis and induces further mitochondrial FA ß-oxidation in different tissue types (Chen, Yao et al. 2008). However Gurd et al. showed controversial results in mammalian muscle cells and proposed that SIRT1 protein expression does not play an obligatory role in mitochondrial biogenesis and oxidative capacity in rat skeletal and heart muscle (Gurd, Yoshida et al. 2009). Furthermore we could not detect differences for several subunits of mitochondrial OXPHOS suggesting

these subunits were not affected by the SIRT1-deficiency. These results implicate a strong tissue-specific effect of SIRT1 and that SIRT1-deficency had a clear influence on mitochondrial biogenesis in pancreatic tumorigenesis under both ND and HFD conditions. Although the mRNA levels of PGC-1α were not significantly changed in SIRT1-deficent mice the G6Pase was significantly increased in SIRT1-deficent animals suggesting an enhanced glycolysis in these mice. However PEPCK was significantly increased in SIRT-deficent animals suggesting an enhanced gluconeogenesis. The diminished mitochondrial content observed in SIRT1-deficent mice as well as an increased glycolysis could explain the similar tumor incidence seen in *p48-Kras*^G12D^ animals, suggesting the *p48-Kras*^G12D^ mouse model relies more on glycolysis then oxidative phosphorylation. Taken together these results implicated SIRT1-deficency had no inhibitory effect in pancreatic tumorigenesis.

5.6 Is Macrophage polarization linked to energy metabolism and pancreatic cancer development?

Inflammation is one of the cancer hallmarks and it is known that the tumor environment consists mainly of inflammatory cells that have tumor promoting properties (Balkwill and Mantovani 2001; Hanahan and Weinberg 2011). Tumor cells release several cytokines, which recruit leukocytes such as macrophages, neutrophils, dendritic cells and lymphocytes. These inflammatory cells promote tumor development through the release of growth factors and further support angiogenesis as well as DNA instability (Coussens and Werb 2002; Balkwill 2004). It is widely accepted that chronic inflammation is associated with promoting tumorigenesis. Further HFD-induced obesity supports low-grade inflammation during pancreatic cancer. Khawasneh et al. demonstrated that in the *p48-Kras*^G12D^ mouse model the PanIN development was significantly increased during HFD and now we could show that also tumor progression was upregulated under HFD-diet condition (Khasawneh, Schulz et al. 2009).

In accordance we showed that HFD diet causes increased inflammation in *p48-Kras*^G12D^ animals, which was due to enhanced inflammatory cells. However significantly reduced inflammatory response was observed in 2-DG treated and *PA*-deficent mice compared to untreated animals on HFD. Since we were able to significantly decrease the tumor incidence via 2-DG treatment and *PA*-deficiency, one possible explanation for decreased

inflammatory response is the reduced tumor incidence in 2-DG treated mice and in *PA*$^{-/-}$-*p48-Kras*^{G12D} animals. But apart from this more and more evidence arise that there is also a crosstalk between immune cells such as macrophages and metabolic pathways (Bhargava and Lee 2012). Macrophages can adapt to environmental stimuli and accordingly show a distinct phenotype, which goes along with changed metabolic phenotype. It is suggested that M1 phenotype relies more on glycolysis, whereas M2 phenotype uses FA oxidation as a main energy source. Most of the tumor-associated macrophages (TAMs) exhibit M2 phenotype, which comes along with poor prognosis in different cancer types including invasive pancreatic cancer (Kamper, Bendix et al. 2011; Kurahara, Shinchi et al. 2011). Pavlides et al. suggested that cancer-associated fibroblasts can also shift their metabolic phenotype to glycolysis and promote thus tumor development by releasing glycolytic products such as pyruvate and lactate. These energy-rich products are transferred to other cancer cells and thereby support their growth (Pavlides, Whitaker-Menezes et al. 2009). Therefore it seems that metabolic features and tumor microenvironment are closely linked. Recently Bhargava et al. proposed that inflammatory mediators such as cytokines and several lipids use the same common signaling pathways (Bhargava and Lee 2012). Further they suggested an activation of M2 macrophages by some omega-3-fatty acids whereas M1 phenotype is mediated by saturated fatty acids, ceramides and cholesterol crystals (Bhargava and Lee 2012). Although we were not able to make a conclusion about the preferred macrophage phenotype in pancreatic cancer since M2 and M1 are both upregulated under HFD, we hypothesize that eventually due to the 2-DG administration and the *PA*-deficiency, macrophage polarization was influenced in the direction of FA acid oxidation, which additionally promotes an increased oxidative phosphorylation in these groups through mediators, which are not known yet.

So far very little is known about the crosstalk between metabolic features of inflammatory cells and immune response, however a better understanding might provide further therapeutic targets in cancer development.

6. Summary

PDAC mouse model with oncogenic $Kras^{G12D}$ activation serves as a tool for the investigation of pancreatic carcinogenesis. The constitutive expression of the $Kras^{G12D}$ in the exocrine pancreas in combination with HFD-induced obesity led to acceleration of tumorigenesis in mice. It is widely accepted that metabolic derangements during tumor development are one of the very important hallmarks of cancer and provide tumor cells with different advantages such as promoting excessive cell proliferation, adaption to hypoxic conditions and many more. Glycolysis is the preferred bioenergy source in most of the tumor types, however still less is known about host-tumor connection regarding energetic shifts during different stages of tumorigenesis.

We aimed in our study to address which pathway is mainly preferred in pancreatic cancer and how tumor development is influenced by the interference of metabolic pathways due to pharmacological drugs or additionally knockout of genes involved in metabolism. Therefore we performed metabolic studies such as oxygen consumption measurements via Clark electrode as well as defining mitochondrial content/ viability in the well-established $p48\text{-}Kras^{G12D}$ mouse model.

As our main finding, we could successfully demonstrate that the PPARα whole body knockout caused a significant reduction in pancreatic tumor incidence in $p48\text{-}Kras^{G12D}$ mice. We hypothesized that the downregulated tumorigenesis is probably due to preference of mitochondrial respiration as main energy source instead of glycolysis. Although the mitochondrial respiration is diminished in PA-deficent animals however a high citrate synthase activity was observed especially in $PA^{-/-}\text{-}p48\text{-}Kras^{G12D}$ mice supporting increased mitochondrial activity. In accordance we observed an increased mRNA level of Cpt1a suggesting enhanced transport of long fatty acid into mitochondria.

Additionally we could show significantly impaired insulin sensitivity in PPARα-deficient animals which was in accordance with reduced weight gain as well as significantly reduced inflammatory response observed in these mice.

Furthermore we demonstrate that the pancreas-specific deletion of PPARγ is also sufficient enough to significantly reduce tumor incidence in $p48\text{-}Kras^{G12D}$ animals and cause upregulation of mitochondrial respiration capacity. Due to significantly increased respiration control rates and citrate synthase activity in these animals, we propose a strong dependency of $PG^{-/-}\text{-}p48\text{-}Kras^{G12D}$ mice on oxidative phosphorylation.

Summary

In accordance the glycolysis inhibitor 2-Deoxyglucose shifts energy metabolism in *p48-Kras*[G12D] mice towards mitochondria that goes along well with significantly reduced tumor incidence in *p48-Kras*[G12D] animals under HFD condition.

In addition we showed reduced tumor incidence in fenofibrate treated *p48-Kras*[G12D] mice probably through enhanced oxidative phosphorylation and diminished inflammatory response. However further metabolic studies have to be performed in order to show the dependency on mitochondrial respiration in fenofibrate-treated *p48-Kras*[G12D] animals.

Our results demonstrate that pancreatic tumorigenesis in *p48-Kras*[G12D] animals clearly rely on glycolysis and the inhibition of the glycolytic pathway lead to reduced tumor development and increased mitochondrial respiration. Further our findings strongly suggested an important role of the nuclear receptors PPARγ and PPARα in the development of PDAC and that PPAR`s inhibitors could be useful in therapeutic treatment however further studies are required to identify the underlying molecular mechanisms. We could successfully show that metabolic changes play a quite important role in pancreatic cancer development and further we suggest that the imaging of changes in biogenetic pathways could be potential used in early prognosis for PDAC patients.

7. Abbreviations

A

Ab - Antibody

ACC - Acetyl-CoA Carboxylase

ADP - Adenosine Bisphosphate

AOX - Acetyl-CoA Oxidase

ATP - Adenosine Triphosphate

B

BrdU - Bromodesoxyuridine

BSA - Bovine Serum Albumine

C

CAT - Catalase

COX - Cytochrome C Oxidase

CP - Chronic Pancreatitis

Cpt - Carnitine Palmitoyltransferase

D

DNA - Deoxyribonucleic Acid

dNTP - Deoxynucleotide Trisphosphate

E

ECM - Extra-cellular Matrix

EDTA - Ethylenediaminetetraacetic Acid

EMA - Ethidium Monoazide Bromide

F

FA - Fatty Acid

FACS - Fluorescence Assisted Cell Sorting

FAD - Flavin Adenine Dinucleotide

FAS - Fatty Acid Synthase

FCCP - Carbonylcyanide-p-trifluoromethoxyphenylhydrazone

FCS - Fetal Calf Serum

FDG - Fluoro Deoxyglucose

G

GAPDH - Glyceraldehyde-3-phosphate Dehydrogenase

GI - Gastrointestinal

GLUT - Glucose Transporter

GPx - Glutathione Peroxidase

GTT - Glucose Tolerance Test

G6Pase - Glucose 6-phosphatase

H

HFD – High Fat Diet

HIF - Hypoxia-inducible Factor

H&E - Haematoxylin & Eosin

I

i.p. - intraperitoneal

IFN - Interferon

IHC - Immunohistochemistry

IL - Interleukin

K

KO - Knock-out

K-ras - Kirsten-Ras

L

LDH - Lactate Dehydrogenase

LKB - Liver Kinase B1

LPL - Lipoprotein Lipase

LPS - Lipopolysaccharide

M

MAPK - Mitogen-Activated Protein Kinase

MCAD - Medium-chain Acyl-coenzyme A Dehydrogenase

Mttp - Microsomal Triglyceride Transfer Protein

N

NAD **-** Nicotinamide Adenine Dinucleotide

ND - Normal Diet

P

PanIN - Pancreatic Intraepithelial Neoplasms

PBS - Phosphate Buffered Saline

PCR - Polymerase Chain Reaction

PDCA - Pancreatic Ductal Adenocarcinoma

PET - Positron Emission Tomography

PEPCK - Phosphoenolpyruvate Carboxykinase

PFA - Paraformaldehyde

PFK - Phosphofructokinase

PGC - Peroxisome proliferator-activated Receptor-gamma Coactivator

PK - Pyruvate Kinase

PPAR - Peroxisome Proliferator-activated Receptor

PPP - Pentose Phosphate Pathway

R

RAS - Rat Sarcoma

RAF- Rat Fibrosarcoma

RCR - Respiratory Control Rate

RNA - Ribonucleic Acid

ROS - Reactive Oxygen Species

RT - Real-Time

S

SCO2 - Cytochrome C Oxidase 2

SDH - Succinate Dehydrogenase

SDS - Sodium Dodecyl Sulfate

SIRT - Sirtuin

SOD - Superoxide Dismutase

SteCoA - Stearoly-CoA Desaturase

T

TAM - Tumor-associated Macrophages

TCA - Tricarboxylic Acid

TIGAR - TP53-induced Glycolysis And Apoptosis Regulator

TNF - Tumor Necrosis Factor

TS Thymidylate Synthase

T2DM - Type 2 Diabetes Mellitus

W

WB - Western Blotting

8. References

(1999). "Cancer risks in BRCA2 mutation carriers. The Breast Cancer Linkage Consortium." J Natl Cancer Inst **91**(15): 1310-1316.

Acharya, A., I. Das, et al. (2010). "Redox regulation in cancer: a double-edged sword with therapeutic potential." Oxid Med Cell Longev **3**(1): 23-34.

Adhikary, S. and M. Eilers (2005). "Transcriptional regulation and transformation by Myc proteins." Nat Rev Mol Cell Biol **6**(8): 635-645.

Aguirre, A. J., N. Bardeesy, et al. (2003). "Activated Kras and Ink4a/Arf deficiency cooperate to produce metastatic pancreatic ductal adenocarcinoma." Genes Dev **17**(24): 3112-3126.

Ahlgren, J. D. (1996). "Epidemiology and risk factors in pancreatic cancer." Semin Oncol **23**(2): 241-250.

Akers, L. J., W. Fang, et al. (2011). "Targeting glycolysis in leukemia: a novel inhibitor 3-BrOP in combination with rapamycin." Leuk Res **35**(6): 814-820.

Aller, E. E., I. Abete, et al. (2011). "Starches, sugars and obesity." Nutrients **3**(3): 341-369.

Altenberg, B. and K. O. Greulich (2004). "Genes of glycolysis are ubiquitously overexpressed in 24 cancer classes." Genomics **84**(6): 1014-1020.

An, T., U. Sood, et al. (1987). "In situ quantitation of inflammatory mononuclear cells in ductal infiltrating breast carcinoma. Relation to prognostic parameters." Am J Pathol **128**(1): 52-60.

Argiles, J. M. and F. J. Lopezsoriano (1990). "Why Do Cancer-Cells Have Such a High Glycolytic Rate." Medical Hypotheses **32**(2): 151-155.

Balkwill, F. (2004). "Cancer and the chemokine network." Nat Rev Cancer **4**(7): 540-550.

Balkwill, F. and A. Mantovani (2001). "Inflammation and cancer: back to Virchow?" Lancet **357**(9255): 539-545.

Bensaad, K., A. Tsuruta, et al. (2006). "TIGAR, a p53-inducible regulator of glycolysis and apoptosis." Cell **126**(1): 107-120.

Bensinger, S. J. and H. R. Christofk (2012). "New aspects of the Warburg effect in cancer cell biology." Semin Cell Dev Biol.

Bhardwaj, V., N. Rizvi, et al. (2010). "Glycolytic enzyme inhibitors affect pancreatic cancer survival by modulating its signaling and energetics." Anticancer Res **30**(3): 743-749.

Bhargava, P. and C. H. Lee (2012). "Role and function of macrophages in the metabolic syndrome." Biochem J **442**(2): 253-262.

Bingle, L., C. E. Lewis, et al. (2006). "Macrophages promote angiogenesis in human breast tumour spheroids in vivo." Br J Cancer **94**(1): 101-107.

Bishop-Bailey, D. (2011). "PPARs and angiogenesis." Biochem Soc Trans **39**(6): 1601-1605.

Biswas, S. K. and A. Mantovani (2012). "Orchestration of metabolism by macrophages." Cell Metab **15**(4): 432-437.

Blagih, J. and R. G. Jones (2012). "Polarizing macrophages through reprogramming of glucose metabolism." Cell Metab **15**(6): 793-795.

Bos, J. L. (1989). "ras oncogenes in human cancer: a review." Cancer Res **49**(17): 4682-4689.

Bos, J. L., E. R. Fearon, et al. (1987). "Prevalence of ras gene mutations in human colorectal cancers." Nature **327**(6120): 293-297.

References

Bradbury, C. A., F. L. Khanim, et al. (2005). "Histone deacetylases in acute myeloid leukaemia show a distinctive pattern of expression that changes selectively in response to deacetylase inhibitors." Leukemia **19**(10): 1751-1759.

Brahimi-Horn, C. and J. Pouyssegur (2006). "The role of the hypoxia-inducible factor in tumor metabolism growth and invasion." Bull Cancer **93**(8): E73-80.

Brockman, J. A., R. A. Gupta, et al. (1998). "Activation of PPARgamma leads to inhibition of anchorage-independent growth of human colorectal cancer cells." Gastroenterology **115**(5): 1049-1055.

Buchholz, M., A. Schatz, et al. (2006). "Overexpression of c-myc in pancreatic cancer caused by ectopic activation of NFATc1 and the Ca2+/calcineurin signaling pathway." EMBO J **25**(15): 3714-3724.

Burns, K. A. and J. P. Vanden Heuvel (2007). "Modulation of PPAR activity via phosphorylation." Biochim Biophys Acta **1771**(8): 952-960.

Calle, E. E., C. Rodriguez, et al. (2003). "Overweight, obesity, and mortality from cancer in a prospectively studied cohort of U.S. adults." N Engl J Med **348**(17): 1625-1638.

Chang, C. C., J. Y. Shih, et al. (2004). "Connective tissue growth factor and its role in lung adenocarcinoma invasion and metastasis." J Natl Cancer Inst **96**(5): 364-375.

Chaput, J. P. and A. Tremblay (2009). "Obesity and physical inactivity: the relevance of reconsidering the notion of sedentariness." Obes Facts **2**(4): 249-254.

Chen, G. P., L. Yao, et al. (2008). "Tissue-specific effects of atorvastatin on 3-hydroxy-3-methylglutarylcoenzyme A reductase expression and activity in spontaneously hypertensive rats." Acta Pharmacol Sin **29**(10): 1181-1186.

Chu, D., W. Kohlmann, et al. (2010). "Identification and screening of individuals at increased risk for pancreatic cancer with emphasis on known environmental and genetic factors and hereditary syndromes." JOP **11**(3): 203-212.

Clark, C. E., S. R. Hingorani, et al. (2007). "Dynamics of the immune reaction to pancreatic cancer from inception to invasion." Cancer Res **67**(19): 9518-9527.

Coleman, M. C., C. R. Asbury, et al. (2008). "2-deoxy-D-glucose causes cytotoxicity, oxidative stress, and radiosensitization in pancreatic cancer." Free Radic Biol Med **44**(3): 322-331.

Coussens, L. M. and Z. Werb (2002). "Inflammation and cancer." Nature **420**(6917): 860-867.

Dang, C. V. (2010). "Rethinking the Warburg effect with Myc micromanaging glutamine metabolism." Cancer Res **70**(3): 859-862.

Dang, C. V., A. Le, et al. (2009). "MYC-induced cancer cell energy metabolism and therapeutic opportunities." Clin Cancer Res **15**(21): 6479-6483.

Dang, C. V. and G. L. Semenza (1999). "Oncogenic alterations of metabolism." Trends Biochem Sci **24**(2): 68-72.

Daynes, R. A. and D. C. Jones (2002). "Emerging roles of PPARs in inflammation and immunity." Nat Rev Immunol **2**(10): 748-759.

de Martel, C., A. E. Llosa, et al. (2008). "Helicobacter pylori infection and development of pancreatic cancer." Cancer Epidemiol Biomarkers Prev **17**(5): 1188-1194.

DeBerardinis, R. J. and T. Cheng (2010). "Q's next: the diverse functions of glutamine in metabolism, cell biology and cancer." Oncogene **29**(3): 313-324.

DeBerardinis, R. J., J. J. Lum, et al. (2008). "The biology of cancer: metabolic reprogramming fuels cell growth and proliferation." Cell Metab **7**(1): 11-20.

DeBerardinis, R. J., A. Mancuso, et al. (2007). "Beyond aerobic glycolysis: transformed cells can engage in glutamine metabolism that exceeds the requirement for protein and nucleotide synthesis." Proc Natl Acad Sci U S A **104**(49): 19345-19350.

Delerive, P., K. De Bosscher, et al. (1999). "Peroxisome proliferator-activated receptor alpha negatively regulates the vascular inflammatory gene response by negative cross-talk with transcription factors NF-kappaB and AP-1." J Biol Chem **274**(45): 32048-32054.

Delerive, P., P. Gervois, et al. (2000). "Induction of IkappaBalpha expression as a mechanism contributing to the anti-inflammatory activities of peroxisome proliferator-activated receptor-alpha activators." J Biol Chem **275**(47): 36703-36707.

Dell'Antone, P. (2006). "Inactivation of H+-vacuolar ATPase by the energy blocker 3-bromopyruvate, a new antitumour agent." Life Sci **79**(21): 2049-2055.

Dressel, U., T. L. Allen, et al. (2003). "The peroxisome proliferator-activated receptor beta/delta agonist, GW501516, regulates the expression of genes involved in lipid catabolism and energy uncoupling in skeletal muscle cells." Mol Endocrinol **17**(12): 2477-2493.

Eibl, G. (2008). "The Role of PPAR-gamma and Its Interaction with COX-2 in Pancreatic Cancer." PPAR Res **2008**: 326915.

Eilers, M. and R. N. Eisenman (2008). "Myc's broad reach." Genes Dev **22**(20): 2755-2766.

Escribese, M. M., M. Casas, et al. (2012). "Influence of low oxygen tensions on macrophage polarization." Immunobiology.

Everhart, J. and D. Wright (1995). "Diabetes mellitus as a risk factor for pancreatic cancer. A meta-analysis." JAMA **273**(20): 1605-1609.

Fantin, V. R., J. St-Pierre, et al. (2006). "Attenuation of LDH-A expression uncovers a link between glycolysis, mitochondrial physiology, and tumor maintenance." Cancer Cell **9**(6): 425-434.

Fearon, E. R. and B. Vogelstein (1990). "A genetic model for colorectal tumorigenesis." Cell **61**(5): 759-767.

Feige, J. N., M. Lagouge, et al. (2008). "Specific SIRT1 activation mimics low energy levels and protects against diet-induced metabolic disorders by enhancing fat oxidation." Cell Metab **8**(5): 347-358.

Fernandez, E., C. La Vecchia, et al. (1994). "Family history and the risk of liver, gallbladder, and pancreatic cancer." Cancer Epidemiol Biomarkers Prev **3**(3): 209-212.

Fogg, V. C., N. J. Lanning, et al. (2011). "Mitochondria in cancer: at the crossroads of life and death." Chin J Cancer **30**(8): 526-539.

Fruchart, J. C., B. Staels, et al. (2001). "PPARS, metabolic disease and atherosclerosis." Pharmacol Res **44**(5): 345-352.

Galaris, D., V. Skiada, et al. (2008). "Redox signaling and cancer: the role of "labile" iron." Cancer Lett **266**(1): 21-29.

Ganapathy-Kanniappan, S., M. Vali, et al. (2010). "3-bromopyruvate: a new targeted antiglycolytic agent and a promise for cancer therapy." Curr Pharm Biotechnol **11**(5): 510-517.

Gao, P., I. Tchernyshyov, et al. (2009). "c-Myc suppression of miR-23a/b enhances mitochondrial glutaminase expression and glutamine metabolism." Nature **458**(7239): 762-765.

Gatenby, R. A. and R. J. Gillies (2004). "Why do cancers have high aerobic glycolysis?" Nat Rev Cancer **4**(11): 891-899.

References

Genkinger, J. M., D. Spiegelman, et al. (2009). "Alcohol intake and pancreatic cancer risk: a pooled analysis of fourteen cohort studies." Cancer Epidemiol Biomarkers Prev **18**(3): 765-776.

Giardiello, F. M., J. D. Brensinger, et al. (2000). "Very high risk of cancer in familial Peutz-Jeghers syndrome." Gastroenterology **119**(6): 1447-1453.

Giles, G. I. (2006). "The redox regulation of thiol dependent signaling pathways in cancer." Curr Pharm Des **12**(34): 4427-4443.

Gold, E. B. and S. B. Goldin (1998). "Epidemiology of and risk factors for pancreatic cancer." Surg Oncol Clin N Am **7**(1): 67-91.

Goldberg, L., R. Israeli, et al. (2012). "FTS and 2-DG induce pancreatic cancer cell death and tumor shrinkage in mice." Cell Death Dis **3**: e284.

Green, D. R. and J. E. Chipuk (2006). "p53 and metabolism: Inside the TIGAR." Cell **126**(1): 30-32.

Greenlee, R. T., M. B. Hill-Harmon, et al. (2001). "Cancer statistics, 2001." CA Cancer J Clin **51**(1): 15-36.

Greer, J. B. and D. C. Whitcomb (2009). "Inflammation and pancreatic cancer: an evidence-based review." Curr Opin Pharmacol **9**(4): 411-418.

Guan, Y., Y. Zhang, et al. (2002). "The Role of PPARs in the Transcriptional Control of Cellular Processes." Drug News Perspect **15**(3): 147-154.

Guerra, C., A. J. Schuhmacher, et al. (2007). "Chronic pancreatitis is essential for induction of pancreatic ductal adenocarcinoma by K-Ras oncogenes in adult mice." Cancer Cell **11**(3): 291-302.

Guerre-Millo, M., P. Gervois, et al. (2000). "Peroxisome proliferator-activated receptor alpha activators improve insulin sensitivity and reduce adiposity." J Biol Chem **275**(22): 16638-16642.

Guerre-Millo, M., C. Rouault, et al. (2001). "PPAR-alpha-null mice are protected from high-fat diet-induced insulin resistance." Diabetes **50**(12): 2809-2814.

Guppy, M., E. Greiner, et al. (1993). "The role of the Crabtree effect and an endogenous fuel in the energy metabolism of resting and proliferating thymocytes." Eur J Biochem **212**(1): 95-99.

Gupta, R. A., J. Tan, et al. (2000). "Prostacyclin-mediated activation of peroxisome proliferator-activated receptor delta in colorectal cancer." Proc Natl Acad Sci U S A **97**(24): 13275-13280.

Gurd, B. J., Y. Yoshida, et al. (2009). "The deacetylase enzyme SIRT1 is not associated with oxidative capacity in rat heart and skeletal muscle and its overexpression reduces mitochondrial biogenesis." J Physiol **587**(Pt 8): 1817-1828.

Haemmerle, G., T. Moustafa, et al. (2011). "ATGL-mediated fat catabolism regulates cardiac mitochondrial function via PPAR-alpha and PGC-1." Nat Med **17**(9): 1076-1085.

Hahn, S. A., B. Greenhalf, et al. (2003). "BRCA2 germline mutations in familial pancreatic carcinoma." J Natl Cancer Inst **95**(3): 214-221.

Haluzik, M. M. and M. Haluzik (2006). "PPAR-alpha and insulin sensitivity." Physiol Res **55**(2): 115-122.

Hanahan, D. and R. A. Weinberg (2011). "Hallmarks of cancer: the next generation." Cell **144**(5): 646-674.

He, W., Y. Barak, et al. (2003). "Adipose-specific peroxisome proliferator-activated receptor gamma knockout causes insulin resistance in fat and liver but not in muscle." Proc Natl Acad Sci U S A **100**(26): 15712-15717.

Herrmann, K., M. Erkan, et al. (2012). "Comparison of 3'-deoxy-3'-[(1)(8)F]fluorothymidine positron emission tomography (FLT PET) and FDG PET/CT for the detection and characterization of pancreatic tumours." Eur J Nucl Med Mol Imaging **39**(5): 846-851.

Hezel, A. F., A. C. Kimmelman, et al. (2006). "Genetics and biology of pancreatic ductal adenocarcinoma." Genes Dev **20**(10): 1218-1249.

Hida, Y., Y. Kubo, et al. (2007). "Strong expression of a longevity-related protein, SIRT1, in Bowen's disease." Arch Dermatol Res **299**(2): 103-106.

Hidalgo, M. (2010). "Pancreatic cancer." N Engl J Med **362**(17): 1605-1617.

Hill, R., Y. Li, et al. (2012). "Cell Intrinsic Role of Cox-2 in Pancreatic Cancer Development." Mol Cancer Ther.

Hodarnau, A., S. Dancea, et al. (1973). "Isolation of highly purified mitochondria from rat pancreas." J Cell Biol **59**(1): 222-227.

Hood, D. A., R. Zak, et al. (1989). "Chronic stimulation of rat skeletal muscle induces coordinate increases in mitochondrial and nuclear mRNAs of cytochrome-c-oxidase subunits." Eur J Biochem **179**(2): 275-280.

Hossain, P., B. Kawar, et al. (2007). "Obesity and diabetes in the developing world--a growing challenge." N Engl J Med **356**(3): 213-215.

Hruban, R. H., N. V. Adsay, et al. (2006). "Pathology of genetically engineered mouse models of pancreatic exocrine cancer: consensus report and recommendations." Cancer Res **66**(1): 95-106.

Hruban, R. H., M. Goggins, et al. (2000). "Progression model for pancreatic cancer." Clin Cancer Res **6**(8): 2969-2972.

Hruban, R. H., C. Iacobuzio-Donahue, et al. (2001). "Molecular pathology of pancreatic cancer." Cancer J **7**(4): 251-258.

Hruban, R. H., G. M. Petersen, et al. (1998). "Genetics of pancreatic cancer. From genes to families." Surg Oncol Clin N Am **7**(1): 1-23.

Huffman, D. M., W. E. Grizzle, et al. (2007). "SIRT1 is significantly elevated in mouse and human prostate cancer." Cancer Res **67**(14): 6612-6618.

Imai, T., R. Takakuwa, et al. (2004). "Peroxisome proliferator-activated receptor gamma is required in mature white and brown adipocytes for their survival in the mouse." Proc Natl Acad Sci U S A **101**(13): 4543-4547.

Isaksson, B., F. Jonsson, et al. (2002). "Lifestyle factors and pancreatic cancer risk: a cohort study from the Swedish Twin Registry." Int J Cancer **98**(3): 480-482.

Jaffee, E. M., R. H. Hruban, et al. (2002). "Focus on pancreas cancer." Cancer Cell **2**(1): 25-28.

James, W. P. (2008). "WHO recognition of the global obesity epidemic." Int J Obes (Lond) **32 Suppl 7**: S120-126.

Jiang, C., A. T. Ting, et al. (1998). "PPAR-gamma agonists inhibit production of monocyte inflammatory cytokines." Nature **391**(6662): 82-86.

Johnson, K. A., L. Rosenblum-Vos, et al. (2000). "Response to genetic counseling and testing for the APC I1307K mutation." Am J Med Genet **91**(3): 207-211.

Kaelin, W. G., Jr. and C. B. Thompson (2010). "Q&A: Cancer: clues from cell metabolism." Nature **465**(7298): 562-564.

Kahn, B. B. (1998). "Type 2 diabetes: when insulin secretion fails to compensate for insulin resistance." Cell **92**(5): 593-596.

Kamper, P., K. Bendix, et al. (2011). "Tumor-infiltrating macrophages correlate with adverse prognosis and Epstein-Barr virus status in classical Hodgkin's lymphoma." Haematologica **96**(2): 269-276.

Kawa, S., T. Nikaido, et al. (2002). "Growth inhibition and differentiation of pancreatic cancer cell lines by PPAR gamma ligand troglitazone." Pancreas **24**(1): 1-7.

Khasawneh, J., M. D. Schulz, et al. (2009). "Inflammation and mitochondrial fatty acid beta-oxidation link obesity to early tumor promotion." Proc Natl Acad Sci U S A **106**(9): 3354-3359.

Kim, J. S., K. J. Ahn, et al. (2008). "Role of reactive oxygen species-mediated mitochondrial dysregulation in 3-bromopyruvate induced cell death in hepatoma cells : ROS-mediated cell death by 3-BrPA." J Bioenerg Biomembr **40**(6): 607-618.

Kim, J. W. and C. V. Dang (2006). "Cancer's molecular sweet tooth and the Warburg effect." Cancer Res **66**(18): 8927-8930.

Kinzler, K. W. and B. Vogelstein (1996). "Lessons from hereditary colorectal cancer." Cell **87**(2): 159-170.

Klaunig, J. E., M. A. Babich, et al. (2003). "PPARalpha agonist-induced rodent tumors: modes of action and human relevance." Crit Rev Toxicol **33**(6): 655-780.

Klein, W. M., R. H. Hruban, et al. (2002). "Direct correlation between proliferative activity and dysplasia in pancreatic intraepithelial neoplasia (PanIN): additional evidence for a recently proposed model of progression." Mod Pathol **15**(4): 441-447.

Klimstra, D. S. and D. S. Longnecker (1994). "K-ras mutations in pancreatic ductal proliferative lesions." Am J Pathol **145**(6): 1547-1550.

Ko, Y. H., P. L. Pedersen, et al. (2001). "Glucose catabolism in the rabbit VX2 tumor model for liver cancer: characterization and targeting hexokinase." Cancer Lett **173**(1): 83-91.

Ko, Y. H., B. L. Smith, et al. (2004). "Advanced cancers: eradication in all cases using 3-bromopyruvate therapy to deplete ATP." Biochem Biophys Res Commun **324**(1): 269-275.

Ko, Y. H., H. A. Verhoeven, et al. (2012). "A translational study "case report" on the small molecule "energy blocker" 3-bromopyruvate (3BP) as a potent anticancer agent: from bench side to bedside." J Bioenerg Biomembr **44**(1): 163-170.

Kong, X. X., R. Wang, et al. (2009). "Function of SIRT1 in physiology." Biochemistry (Mosc) **74**(7): 703-708.

Kostadinova, R., W. Wahli, et al. (2005). "PPARs in diseases: control mechanisms of inflammation." Curr Med Chem **12**(25): 2995-3009.

Krejs, G. J. (2010). "Pancreatic cancer: epidemiology and risk factors." Dig Dis **28**(2): 355-358.

Kristiansen, G., J. Jacob, et al. (2006). "Peroxisome proliferator-activated receptor gamma is highly expressed in pancreatic cancer and is associated with shorter overall survival times." Clin Cancer Res **12**(21): 6444-6451.

Kurahara, H., H. Shinchi, et al. (2011). "Significance of M2-polarized tumor-associated macrophage in pancreatic cancer." J Surg Res **167**(2): e211-219.

Kurokawa, T., Y. Shimomura, et al. (2011). "Peroxisome proliferator-activated receptor alpha (PPARalpha) mRNA expression in human hepatocellular carcinoma tissue and non-cancerous liver tissue." World J Surg Oncol **9**: 167.

Lacy-Hulbert, A. and K. J. Moore (2006). "Designer macrophages: oxidative metabolism fuels inflammation repair." Cell Metab **4**(1): 7-8.

Lee, S. S., T. Pineau, et al. (1995). "Targeted disruption of the alpha isoform of the peroxisome proliferator-activated receptor gene in mice results in abolishment of the pleiotropic effects of peroxisome proliferators." Mol Cell Biol **15**(6): 3012-3022.

Leek, R. D., C. E. Lewis, et al. (1996). "Association of macrophage infiltration with angiogenesis and prognosis in invasive breast carcinoma." Cancer Res **56**(20): 4625-4629.

Lefebvre, A. M., I. Chen, et al. (1998). "Activation of the peroxisome proliferator-activated receptor gamma promotes the development of colon tumors in C57BL/6J-APCMin/+ mice." Nat Med **4**(9): 1053-1057.

Levens, D. L. (2003). "Reconstructing MYC." Genes Dev **17**(9): 1071-1077.

Levine, A. J. and A. M. Puzio-Kuter (2010). "The control of the metabolic switch in cancers by oncogenes and tumor suppressor genes." Science **330**(6009): 1340-1344.

Levy, A. G., P. E. Zage, et al. (2012). "The combination of the novel glycolysis inhibitor 3-BrOP and rapamycin is effective against neuroblastoma." Invest New Drugs **30**(1): 191-199.

Lewis, B. C., H. Shim, et al. (1997). "Identification of putative c-Myc-responsive genes: characterization of rcl, a novel growth-related gene." Mol Cell Biol **17**(9): 4967-4978.

Li, D., K. Xie, et al. (2004). "Pancreatic cancer." Lancet **363**(9414): 1049-1057.

Li, H., G. K. Rajendran, et al. (2007). "SirT1 modulates the estrogen-insulin-like growth factor-1 signaling for postnatal development of mammary gland in mice." Breast Cancer Res **9**(1): R1.

Liang, F., S. Kume, et al. (2009). "SIRT1 and insulin resistance." Nat Rev Endocrinol **5**(7): 367-373.

Liu, Y. (2006). "Fatty acid oxidation is a dominant bioenergetic pathway in prostate cancer." Prostate Cancer Prostatic Dis **9**(3): 230-234.

Liu, Y. C., F. Li, et al. (2008). "Global regulation of nucleotide biosynthetic genes by c-Myc." PLoS One **3**(7): e2722.

Lohr, M., P. Maisonneuve, et al. (2000). "K-Ras mutations and benign pancreatic disease." Int J Pancreatol **27**(2): 93-103.

Lopez-Lazaro, M. (2008). "The warburg effect: why and how do cancer cells activate glycolysis in the presence of oxygen?" Anticancer Agents Med Chem **8**(3): 305-312.

Lowenfels, A. B. and P. Maisonneuve (2006). "Epidemiology and risk factors for pancreatic cancer." Best Pract Res Clin Gastroenterol **20**(2): 197-209.

Lowenfels, A. B., P. Maisonneuve, et al. (1993). "Pancreatitis and the risk of pancreatic cancer. International Pancreatitis Study Group." N Engl J Med **328**(20): 1433-1437.

Lowenfels, A. B., P. Maisonneuve, et al. (1997). "Hereditary pancreatitis and the risk of pancreatic cancer. International Hereditary Pancreatitis Study Group." J Natl Cancer Inst **89**(6): 442-446.

Maisonneuve, P. and A. B. Lowenfels (2002). "Chronic pancreatitis and pancreatic cancer." Dig Dis **20**(1): 32-37.

Maisonneuve, P. and A. B. Lowenfels (2010). "Epidemiology of pancreatic cancer: an update." Dig Dis **28**(4-5): 645-656.

Mandard, S., M. Muller, et al. (2004). "Peroxisome proliferator-activated receptor alpha target genes." Cell Mol Life Sci **61**(4): 393-416.

Mannava, S., V. Grachtchouk, et al. (2008). "Direct role of nucleotide metabolism in C-MYC-dependent proliferation of melanoma cells." Cell Cycle **7**(15): 2392-2400.

References

Mantovani, A., A. Sica, et al. (2005). "Macrophage polarization comes of age." Immunity **23**(4): 344-346.

Mantovani, A., A. Sica, et al. (2007). "New vistas on macrophage differentiation and activation." Eur J Immunol **37**(1): 14-16.

Mantovani, A., A. Sica, et al. (2004). "The chemokine system in diverse forms of macrophage activation and polarization." Trends Immunol **25**(12): 677-686.

Marie, S. K. and S. M. Shinjo (2011). "Metabolism and brain cancer." Clinics (Sao Paulo) **66 Suppl 1**: 33-43.

Martinez, F. O., L. Helming, et al. (2009). "Alternative activation of macrophages: an immunologic functional perspective." Annu Rev Immunol **27**: 451-483.

Mathupala, S. P., Y. H. Ko, et al. (2009). "Hexokinase-2 bound to mitochondria: cancer's stygian link to the "Warburg Effect" and a pivotal target for effective therapy." Semin Cancer Biol **19**(1): 17-24.

Michalik, L., J. Auwerx, et al. (2006). "International Union of Pharmacology. LXI. Peroxisome proliferator-activated receptors." Pharmacol Rev **58**(4): 726-741.

Michalik, L., B. Desvergne, et al. (2004). "Peroxisome-proliferator-activated receptors and cancers: complex stories." Nat Rev Cancer **4**(1): 61-70.

Michaud, D. S., E. Giovannucci, et al. (2001). "Physical activity, obesity, height, and the risk of pancreatic cancer." Jama **286**(8): 921-929.

Milane, L., Z. Duan, et al. (2011). "Role of hypoxia and glycolysis in the development of multi-drug resistance in human tumor cells and the establishment of an orthotopic multi-drug resistant tumor model in nude mice using hypoxic pre-conditioning." Cancer Cell Int **11**: 3.

Milne, J. C., P. D. Lambert, et al. (2007). "Small molecule activators of SIRT1 as therapeutics for the treatment of type 2 diabetes." Nature **450**(7170): 712-716.

Mochiki, E., H. Kuwano, et al. (2004). "Evaluation of 18F-2-deoxy-2-fluoro-D-glucose positron emission tomography for gastric cancer." World J Surg **28**(3): 247-253.

Moreno-Sanchez, R., S. Rodriguez-Enriquez, et al. (2007). "Energy metabolism in tumor cells." FEBS J **274**(6): 1393-1418.

Motomura, W., T. Okumura, et al. (2000). "Activation of peroxisome proliferator-activated receptor gamma by troglitazone inhibits cell growth through the increase of p27KiP1 in human. Pancreatic carcinoma cells." Cancer Res **60**(19): 5558-5564.

Murdoch, C. and C. E. Lewis (2005). "Macrophage migration and gene expression in response to tumor hypoxia." Int J Cancer **117**(5): 701-708.

Murphy, K. M., K. A. Brune, et al. (2002). "Evaluation of candidate genes MAP2K4, MADH4, ACVR1B, and BRCA2 in familial pancreatic cancer: deleterious BRCA2 mutations in 17%." Cancer Res **62**(13): 3789-3793.

Mussig, K., H. Staiger, et al. (2011). "Type 2 diabetes mellitus and risk of malignancy: is there a strategy to identify a subphenotype of patients with increased susceptibility to endogenous and exogenous hyperinsulinism?" Diabet Med **28**(3): 276-286.

Must, A., J. Spadano, et al. (1999). "The disease burden associated with overweight and obesity." JAMA **282**(16): 1523-1529.

Nakano, A., H. Miki, et al. (2012). "Up-regulation of hexokinaseII in myeloma cells: targeting myeloma cells with 3-bromopyruvate." J Bioenerg Biomembr **44**(1): 31-38.

<div align="center">**References**</div>

Nakhai, H., S. Sel, et al. (2007). "Ptf1a is essential for the differentiation of GABAergic and glycinergic amacrine cells and horizontal cells in the mouse retina." Development **134**(6): 1151-1160.

Nemoto, S., M. M. Fergusson, et al. (2004). "Nutrient availability regulates SIRT1 through a forkhead-dependent pathway." Science **306**(5704): 2105-2108.

Panasyuk, G., C. Espeillac, et al. (2012). "PPARgamma contributes to PKM2 and HK2 expression in fatty liver." Nat Commun **3**: 672.

Pandol, S., A. Gukovskaya, et al. (2012). "Epidemiology, risk factors, and the promotion of pancreatic cancer: role of the stellate cell." J Gastroenterol Hepatol **27 Suppl 2**: 127-134.

Panigrahy, D., A. Kaipainen, et al. (2008). "PPARalpha agonist fenofibrate suppresses tumor growth through direct and indirect angiogenesis inhibition." Proc Natl Acad Sci U S A **105**(3): 985-990.

Park, B. H., B. Vogelstein, et al. (2001). "Genetic disruption of PPARdelta decreases the tumorigenicity of human colon cancer cells." Proc Natl Acad Sci U S A **98**(5): 2598-2603.

Pastorino, J. G., N. Shulga, et al. (2002). "Mitochondrial binding of hexokinase II inhibits Bax-induced cytochrome c release and apoptosis." J Biol Chem **277**(9): 7610-7618.

Pavlides, S., D. Whitaker-Menezes, et al. (2009). "The reverse Warburg effect: aerobic glycolysis in cancer associated fibroblasts and the tumor stroma." Cell Cycle **8**(23): 3984-4001.

Pedchenko, T. V., A. L. Gonzalez, et al. (2008). "Peroxisome proliferator-activated receptor beta/delta expression and activation in lung cancer." Am J Respir Cell Mol Biol **39**(6): 689-696.

Pedersen, P. L. (2007). "The cancer cell's "power plants" as promising therapeutic targets: an overview." J Bioenerg Biomembr **39**(1): 1-12.

Pedersen, P. L. (2007). "Warburg, me and Hexokinase 2: Multiple discoveries of key molecular events underlying one of cancers' most common phenotypes, the "Warburg Effect", i.e., elevated glycolysis in the presence of oxygen." J Bioenerg Biomembr **39**(3): 211-222.

Pelicano, H., D. Carney, et al. (2004). "ROS stress in cancer cells and therapeutic implications." Drug Resist Updat **7**(2): 97-110.

Pelicano, H., D. S. Martin, et al. (2006). "Glycolysis inhibition for anticancer treatment." Oncogene **25**(34): 4633-4646.

Pereira da Silva, A. P., T. El-Bacha, et al. (2009). "Inhibition of energy-producing pathways of HepG2 cells by 3-bromopyruvate." Biochem J **417**(3): 717-726.

Peters, J. M., T. Aoyama, et al. (1998). "Role of peroxisome proliferator-activated receptor alpha in altered cell cycle regulation in mouse liver." Carcinogenesis **19**(11): 1989-1994.

Peters, J. M., R. C. Cattley, et al. (1997). "Role of PPAR alpha in the mechanism of action of the nongenotoxic carcinogen and peroxisome proliferator Wy-14,643." Carcinogenesis **18**(11): 2029-2033.

Peters, J. M., C. Cheung, et al. (2005). "Peroxisome proliferator-activated receptor-alpha and liver cancer: where do we stand?" J Mol Med (Berl) **83**(10): 774-785.

Pfeiffer, T., S. Schuster, et al. (2001). "Cooperation and competition in the evolution of ATP-producing pathways." Science **292**(5516): 504-507.

References

Pham, N. A., J. Schwock, et al. (2008). "Immunohistochemical analysis of changes in signaling pathway activation downstream of growth factor receptors in pancreatic duct cell carcinogenesis." <u>BMC Cancer</u> **8**: 43.

Piatkiewicz, P. and A. Czech (2011). "Glucose metabolism disorders and the risk of cancer." <u>Arch Immunol Ther Exp (Warsz)</u> **59**(3): 215-230.

Pike, L. S., A. L. Smift, et al. (2010). "Inhibition of fatty acid oxidation by etomoxir impairs NADPH production and increases reactive oxygen species resulting in ATP depletion and cell death in human glioblastoma cells." <u>Biochim Biophys Acta</u>.

Pike, L. S., A. L. Smift, et al. (2011). "Inhibition of fatty acid oxidation by etomoxir impairs NADPH production and increases reactive oxygen species resulting in ATP depletion and cell death in human glioblastoma cells." <u>Biochim Biophys Acta</u> **1807**(6): 726-734.

Postovit, L. M., M. A. Adams, et al. (2002). "Oxygen-mediated regulation of tumor cell invasiveness. Involvement of a nitric oxide signaling pathway." <u>J Biol Chem</u> **277**(38): 35730-35737.

Pour, P. M., K. K. Pandey, et al. (2003). "What is the origin of pancreatic adenocarcinoma?" <u>Mol Cancer</u> **2**: 13.

Poynter, M. E. and R. A. Daynes (1998). "Peroxisome proliferator-activated receptor alpha activation modulates cellular redox status, represses nuclear factor-kappaB signaling, and reduces inflammatory cytokine production in aging." <u>J Biol Chem</u> **273**(49): 32833-32841.

Prenen, H., S. Tejpar, et al. (2010). "New strategies for treatment of KRAS mutant metastatic colorectal cancer." <u>Clin Cancer Res</u> **16**(11): 2921-2926.

Pyper, S. R., N. Viswakarma, et al. (2010). "PPARalpha: energy combustion, hypolipidemia, inflammation and cancer." <u>Nucl Recept Signal</u> **8**: e002.

Racker, E., R. J. Resnick, et al. (1985). "Glycolysis and methylaminoisobutyrate uptake in rat-1 cells transfected with ras or myc oncogenes." <u>Proc Natl Acad Sci U S A</u> **82**(11): 3535-3538.

Raimondi, S., P. Maisonneuve, et al. (2009). "Epidemiology of pancreatic cancer: an overview." <u>Nat Rev Gastroenterol Hepatol</u> **6**(12): 699-708.

Ramanathan, A., C. Wang, et al. (2005). "Perturbational profiling of a cell-line model of tumorigenesis by using metabolic measurements." <u>Proc Natl Acad Sci U S A</u> **102**(17): 5992-5997.

Rasheed, Z. A., W. Matsui, et al. (2012). "Pathology of pancreatic stroma in PDAC."

Rempel, A., S. P. Mathupala, et al. (1996). "Glucose catabolism in cancer cells: amplification of the gene encoding type II hexokinase." <u>Cancer Res</u> **56**(11): 2468-2471.

Riccardi, L., E. Mazzon, et al. (2009). "Peroxisome proliferator-activated receptor-alpha modulates the anti-inflammatory effect of glucocorticoids in a model of inflammatory bowel disease in mice." <u>Shock</u> **31**(3): 308-316.

Robey, R. B. and N. Hay (2005). "Mitochondrial hexokinases: guardians of the mitochondria." <u>Cell Cycle</u> **4**(5): 654-658.

Rozenblum, E., M. Schutte, et al. (1997). "Tumor-suppressive pathways in pancreatic carcinoma." <u>Cancer Res</u> **57**(9): 1731-1734.

Saez, E., P. Tontonoz, et al. (1998). "Activators of the nuclear receptor PPARgamma enhance colon polyp formation." <u>Nat Med</u> **4**(9): 1058-1061.

Saidi, S. A., C. M. Holland, et al. (2006). "In vitro and in vivo effects of the PPAR-alpha agonists fenofibrate and retinoic acid in endometrial cancer." <u>Mol Cancer</u> **5**: 13.

References

Saltiel, A. R. and C. R. Kahn (2001). "Insulin signalling and the regulation of glucose and lipid metabolism." Nature **414**(6865): 799-806.

Sarraf, P., E. Mueller, et al. (1998). "Differentiation and reversal of malignant changes in colon cancer through PPARgamma." Nat Med **4**(9): 1046-1052.

Sawai, H., J. Liu, et al. (2006). "Activation of peroxisome proliferator-activated receptor-gamma decreases pancreatic cancer cell invasion through modulation of the plasminogen activator system." Mol Cancer Res **4**(3): 159-167.

Schek, N., B. L. Hall, et al. (1988). "Increased glyceraldehyde-3-phosphate dehydrogenase gene expression in human pancreatic adenocarcinoma." Cancer Res **48**(22): 6354-6359.

Schenk, M., A. G. Schwartz, et al. (2001). "Familial risk of pancreatic cancer." J Natl Cancer Inst **93**(8): 640-644.

Semenza, G. L. (2009). "Regulation of cancer cell metabolism by hypoxia-inducible factor 1." Semin Cancer Biol **19**(1): 12-16.

Shao, J., H. Sheng, et al. (2002). "Peroxisome proliferator-activated receptors modulate K-Ras-mediated transformation of intestinal epithelial cells." Cancer Res **62**(11): 3282-3288.

Shaw, R. J., R. M. Evans, et al. (2010). "Metabolism and cancer in La Jolla." Cancer Res **70**(10): 3864-3869.

Shim, H., C. Dolde, et al. (1997). "c-Myc transactivation of LDH-A: implications for tumor metabolism and growth." Proc Natl Acad Sci U S A **94**(13): 6658-6663.

Silverman, D. T., J. A. Dunn, et al. (1994). "Cigarette smoking and pancreas cancer: a case-control study based on direct interviews." J Natl Cancer Inst **86**(20): 1510-1516.

Silverman, D. T., C. A. Swanson, et al. (1998). "Dietary and nutritional factors and pancreatic cancer: a case-control study based on direct interviews." J Natl Cancer Inst **90**(22): 1710-1719.

Simon, M. C. (2006). "Coming up for air: HIF-1 and mitochondrial oxygen consumption." Cell Metab **3**(3): 150-151.

Singh, K. K. and M. Kulawiec (2009). "Mitochondrial DNA polymorphism and risk of cancer." Methods Mol Biol **471**: 291-303.

Solinas, G., G. Germano, et al. (2009). "Tumor-associated macrophages (TAM) as major players of the cancer-related inflammation." J Leukoc Biol **86**(5): 1065-1073.

Sommer, M., N. Poliak, et al. (2006). "DeltaNp63alpha overexpression induces downregulation of Sirt1 and an accelerated aging phenotype in the mouse." Cell Cycle **5**(17): 2005-2011.

Stock, D., C. Gibbons, et al. (2000). "The rotary mechanism of ATP synthase." Curr Opin Struct Biol **10**(6): 672-679.

Stolzenberg-Solomon, R. Z., P. Pietinen, et al. (2002). "A prospective study of medical conditions, anthropometry, physical activity, and pancreatic cancer in male smokers (Finland)." Cancer Causes Control **13**(5): 417-426.

Stunkel, W., B. K. Peh, et al. (2007). "Function of the SIRT1 protein deacetylase in cancer." Biotechnol J **2**(11): 1360-1368.

Suchanek, K. M., F. J. May, et al. (2002). "Peroxisome proliferator-activated receptor alpha in the human breast cancer cell lines MCF-7 and MDA-MB-231." Mol Carcinog **34**(4): 165-171.

Sun, C., F. Zhang, et al. (2007). "SIRT1 improves insulin sensitivity under insulin-resistant conditions by repressing PTP1B." Cell Metab **6**(4): 307-319.

Sun, H. C., Z. J. Qiu, et al. (2007). "Expression of hypoxia-inducible factor-1 alpha and associated proteins in pancreatic ductal adenocarcinoma and their impact on prognosis." Int J Oncol **30**(6): 1359-1367.

Tachibana, K., D. Yamasaki, et al. (2008). "The Role of PPARs in Cancer." PPAR Res **2008**: 102737.

Talbot, D. A., N. Hanuise, et al. (2003). "Superoxide activates a GDP-sensitive proton conductance in skeletal muscle mitochondria from king penguin (Aptenodytes patagonicus)." Biochem Biophys Res Commun **312**(4): 983-988.

Tang, Q., Y. Chen, et al. (2011). "A comprehensive view of nuclear receptor cancer cistromes." Cancer Res **71**(22): 6940-6947.

Tang, Z., S. Yuan, et al. (2012). "Over-expression of GAPDH in human colorectal carcinoma as a preferred target of 3-bromopyruvate propyl ester." J Bioenerg Biomembr **44**(1): 117-125.

Taylor, P. R. and S. Gordon (2003). "Monocyte heterogeneity and innate immunity." Immunity **19**(1): 2-4.

Thannickal, V. J. and B. L. Fanburg (2000). "Reactive oxygen species in cell signaling." Am J Physiol Lung Cell Mol Physiol **279**(6): L1005-1028.

Thompson, D. and D. F. Easton (2002). "Cancer Incidence in BRCA1 mutation carriers." J Natl Cancer Inst **94**(18): 1358-1365.

Thuillier, P., G. J. Anchiraico, et al. (2000). "Activators of peroxisome proliferator-activated receptor-alpha partially inhibit mouse skin tumor promotion." Mol Carcinog **29**(3): 134-142.

Tisdale, M. J. (2009). "Mechanisms of cancer cachexia." Physiol Rev **89**(2): 381-410.

Tong, X., F. Zhao, et al. (2009). "The molecular determinants of de novo nucleotide biosynthesis in cancer cells." Curr Opin Genet Dev **19**(1): 32-37.

Toyoda, T., Y. Kamei, et al. (2008). "Effect of peroxisome proliferator-activated receptor-alpha ligands in the interaction between adipocytes and macrophages in obese adipose tissue." Obesity (Silver Spring) **16**(6): 1199-1207.

Trifunovic, A. and N. G. Larsson (2008). "Mitochondrial dysfunction as a cause of ageing." J Intern Med **263**(2): 167-178.

Tuveson, D. A., A. T. Shaw, et al. (2004). "Endogenous oncogenic K-ras(G12D) stimulates proliferation and widespread neoplastic and developmental defects." Cancer Cell **5**(4): 375-387.

Vander Heiden, M. G., L. C. Cantley, et al. (2009). "Understanding the Warburg effect: the metabolic requirements of cell proliferation." Science **324**(5930): 1029-1033.

Vasseur, S., S. Afzal, et al. (2009). "DJ-1/PARK7 is an important mediator of hypoxia-induced cellular responses." Proc Natl Acad Sci U S A **106**(4): 1111-1116.

Wang, R. H., K. Sengupta, et al. (2008). "Impaired DNA damage response, genome instability, and tumorigenesis in SIRT1 mutant mice." Cancer Cell **14**(4): 312-323.

Warburg, O. (1930). "Note on the metabolism of tumours." Biochemische Zeitschrift **228**: 257-258.

Warburg, O. (1956). "On respiratory impairment in cancer cells." Science **124**(3215): 269-270.

Warburg, O. (1956). "On the origin of cancer cells." Science **123**(3191): 309-314.

Warshaw, A. L. and C. Fernandez-del Castillo (1992). "Pancreatic carcinoma." N Engl J Med **326**(7): 455-465.

Weinberg, F., R. Hamanaka, et al. (2010). "Mitochondrial metabolism and ROS generation are essential for Kras-mediated tumorigenicity." Proc Natl Acad Sci U S A **107**(19): 8788-8793.

Wild, S., G. Roglic, et al. (2004). "Global prevalence of diabetes: estimates for the year 2000 and projections for 2030." Diabetes Care **27**(5): 1047-1053.

Wilentz, R. E., C. A. Iacobuzio-Donahue, et al. (2000). "Loss of expression of Dpc4 in pancreatic intraepithelial neoplasia: evidence that DPC4 inactivation occurs late in neoplastic progression." Cancer Res **60**(7): 2002-2006.

Wise, D. R. and C. B. Thompson (2010). "Glutamine addiction: a new therapeutic target in cancer." Trends Biochem Sci **35**(8): 427-433.

Wokolorczyk, D., B. Gliniewicz, et al. (2008). "A range of cancers is associated with the rs6983267 marker on chromosome 8." Cancer Res **68**(23): 9982-9986.

Wray, C. J., S. A. Ahmad, et al. (2005). "Surgery for pancreatic cancer: recent controversies and current practice." Gastroenterology **128**(6): 1626-1641.

Xu, R. H., H. Pelicano, et al. (2005). "Synergistic effect of targeting mTOR by rapamycin and depleting ATP by inhibition of glycolysis in lymphoma and leukemia cells." Leukemia **19**(12): 2153-2158.

Xu, R. H., H. Pelicano, et al. (2005). "Inhibition of glycolysis in cancer cells: a novel strategy to overcome drug resistance associated with mitochondrial respiratory defect and hypoxia." Cancer Res **65**(2): 613-621.

Xu, Z., Y. Zhang, et al. (2010). "Epidermal growth factor induces HCCR expression via PI3K/Akt/mTOR signaling in PANC-1 pancreatic cancer cells." BMC Cancer **10**: 161.

Yeo, T. P., R. H. Hruban, et al. (2002). "Pancreatic cancer." Curr Probl Cancer **26**(4): 176-275.

Yeung, S. J., J. Pan, et al. (2008). "Roles of p53, MYC and HIF-1 in regulating glycolysis - the seventh hallmark of cancer." Cell Mol Life Sci **65**(24): 3981-3999.

Ying, H., A. C. Kimmelman, et al. (2012). "Oncogenic Kras Maintains Pancreatic Tumors through Regulation of Anabolic Glucose Metabolism." Cell **149**(3): 656-670.

Yoshizaki, T., J. C. Milne, et al. (2009). "SIRT1 exerts anti-inflammatory effects and improves insulin sensitivity in adipocytes." Mol Cell Biol **29**(5): 1363-1374.

Yun, J., C. Rago, et al. (2009). "Glucose deprivation contributes to the development of KRAS pathway mutations in tumor cells." Science **325**(5947): 1555-1559.

Zhang, Z., P. E. Burch, et al. (2004). "Genomic analysis of the nuclear receptor family: new insights into structure, regulation, and evolution from the rat genome." Genome Res **14**(4): 580-590.

Zhao, G., J. Cui, et al. (2011). "SIRT1 RNAi knockdown induces apoptosis and senescence, inhibits invasion and enhances chemosensitivity in pancreatic cancer cells." Gene Ther **18**(9): 920-928.

Zimmet, P., K. G. Alberti, et al. (2001). "Global and societal implications of the diabetes epidemic." Nature **414**(6865): 782-787.

Zimmet, P. Z. (1999). "Diabetes epidemiology as a tool to trigger diabetes research and care." Diabetologia **42**(5): 499-518.

WHO (http://www.who.int/mediacentre/factsheets/fs311/en/index.html, 07.06.2010)

Danksagung